Upgrading of Liquid Products from Estonian Kukersite Oil Shale by Catalytic Hydrogenation

JULIA KRASULINA

TUT
PRESS

TALLINN UNIVERSITY OF TECHNOLOGY
Faculty of Chemical and Materials Technology
Department of Polymer Materials
Laboratory of Oil Shale and Renewables Research

This dissertation was accepted for the defense of the degree of Doctor of Philosophy in Chemistry and Materials Technology on 17 April, 2015

Supervisor: Dr. (chem) Hans Luik, Laboratory of Oil Shale and Renewables Research, Department of Polymer Materials, Tallinn University of Technology

Opponents: Dr. Antero Moilanen, Tampere University of Technology, Finland

Dr. Indrek Aarna, Eesti Energia AS, Estonia

Defense of the thesis: 21 May, 2015, at 12.30 Lecture hall: U06A-229
Tallinn University of Technology, Ehitajate tee 5, Tallinn

Declaration:

Hereby I declare that this doctoral thesis, my original investigation and achievement, submitted for the doctoral degree at Tallinn University of Technology, has not previously been submitted for doctoral or equivalent academic degree.

Julia Krasulina

European Union
European Social Fund

Investing in your future

Kukersiitpõlevkivi vedelproduktide vääristamine katalüütilise hüdrogeenimise meetodil

JULIA KRASULINA

CONTENTS

LIST OF PUBLICATIONS

Article I:

Krasulina, J., Luik, H., Palu, V., Tamvelius, H. Thermochemical co-liquefaction of Estonian kukersite oil shale with peat and pine bark. – *Oil Shale*, 2012, vol. 29, no. 3, pp. 222-236.

Article II:

Sokolova, J. (Krasulina, J.), Tiikma, L., Bityukov, M., Johannes, I. Ageing of kukersite thermobitumen. – *Oil Shale*, 2011, vol. 28, no. 1, pp. 4-18.

Article III:

Tiikma, L., **Sokolova, J. (Krasulina, J.)**, Vink, N. Effect of the concentration of organic matter on the yield of thermal bitumen from the Baltic oil shale kukersite. – *Solid Fuel Chemistry*, 2010, vol. 44, no. 2, pp. 89-93.

Article IV:

Luik, H., Luik, L., Johannes, I., Tiikma, L., Vink, N., Palu, V., Bitjukov, M., Tamvelius, H., **Krasulina, J.**, Kruusement, K., Nechaev, I. Upgrading of Estonian shale oil heavy residuum bituminous fraction by catalytic hydroconversion. – *Fuel Processing Technology*, 2014, vol. 124, pp. 115-122.

Article V:

Johannes, I., Tiikma, L., **Sokolova, J. (Krasulina, J.).** Dissolution rate of oil shale thermobitumen in different solvents. – *Oil Shale*, 2009, vol. 26, no. 3, pp. 399–414.

Article VI:

Johannes, I., Tiikma, L., Luik, H., Tamvelius, H., **Krasulina, J.** Catalytic thermal liquefaction of oil shale in tetralin. – *International Scholary Research Netrwoek (ISRN), Chemical Engineering*, 2012, pp. 1-11, (ID 617363).

Article "Upgrading of Estonian shale oil heavy residuum bituminous fraction by catalytic hydroconversion" was identified by Target Selection Team at *Advances in Engineering* as a Key Scientific Article contributing to excellence in engineering, scientific and industrial research (www.advanceseng.com).

Copies of these publications are included in APPENDIX A.

In addition, results of this thesis have been presented at different scientific conferences:

Krasulina, J., Bitjukov, M., Vink, N., Gregor, A., Luik, L., Luik, H. (2013). Termobituumeni katalüütiline hüdrogeenimine. – In: *XXXIII Eesti Keemiapäevad. Teaduskonverentsi teesid*: XXXIII Eesti Keemiapäevad. Tallinn, 11. oktoober 2013, p. 35.

Krasulina, J., Bitjukov, M., Vink, N., Gregor, A., Luik, L., Luik, H. (2013). Catalytic hydrogenation of thermobitumen. – In: *Oil Shale Symposium, Tallinn 2013*: International Oil Shale Symposium, Tallinn, Estonia, June 10-13, 2013, pp. 56-57.

Luik, H., Luik, L., **Krasulina, J.**, Riisalu, H. (2012). Upgrading of Estonian shale oil bituminous fractions. – *In: Proceedings of the 32nd Oil Shale Symposium*: The 32nd Oil Shale Symposium, Colorado School of Mines, Golden, Colorado, October 15-19, 2012, 17.1.

Luik, H., Luik, L., Sharayeva, G., **Krasulina, J**., Johannes, I., Kruusement, K. (2014). Fundamentals of Oil Shale Upgrading. – In*: Abstracts Book of 34th Oil Shale Symposium:* 34th Oil Shale Symposium, Colorado School of Mines, Golden, Colorado, October 13-17, 2014. Golden, Colorado, 45.

Sokolova, J. (Krasulina, J), Palu, V., Luik, H. (2009). Copyrolysis of Estonian oil shale and peat. – In*: Book of abstracts: International Oil Shale Symposium,* Tallinn, Estonia, 8-11 June 2009, 75.

Other publications:

Yanik, J., Secim, P., Karakaya, S., Tiikma, L., Luik, H., **Krasulina, J.**, Raik, P., Palu, V. Low-temperature pyrolysis and co-pyrolysis of Göynük oil shale and terebinth berries (Turkey) in an autoclave. – *Oil Shale*, 2011, vol. 28, no. 4, pp. 469-486.

Тийкма Л., **Соколова Ю.**, Винк Н. Влияние содержания органического вещества на выход термобитума из прибалтийского сланца-кукерсита. – *Химия твердого топлива*, 2010, № 2, стр. 25-30, 2010.

Luik, H., Palu, V., Luik, L., **Sokolova, J.** Peat semicoking and hydrocracking. – *Journal of Analytical and Applied Pyrolysis*, 2009, vol. 85, no. 1-2, pp. 497-501.

THE AUTHOR'S CONTRIBUTION

I   The author carried out the experiments, interpretated the results and wrote the manuscript.

II   The author carried out the experiments, participated in the interpretation of the results and wrote the manuscript.

III   The author participated in the experimental part, interpretation and discussion of the results.

IV   The author participated in carrying out the experiments, the calculation and interpretation of the results.

V   The author participated in carrying out the experiments

VI   The author participated in carrying out experiments, discussions and data processing.

LIST OF ABBREVIATIONS

AlHC	Aliphatic hydrocarbons
FT-IR	Fourier Transform Infrared Spectroscopy
GC-MS	Gas chromatography-mass spectrometry
HC	Hydrocarbons
Het	Heteroatomic compounds
HPHet	High-polar heteroatomic compounds
HO	Heavy oil fraction 360 °C+
K-90	Kukersite kerogen concentrate with 90.1% content of organic matter
LPHet	Low-polar heteroatomic compounds
MAHC	Monoaromatic hydrocarbons
MM	Mineral matter
OM	Organic matter
PAHC	Polyaromatic hydrocarbons
TB	Thermobitumen
TBO	Mixture of thermobitumen and oil
TLC	Thin-layer chromatography
W^a	Analytical moisture

INTRODUCTION

Worldwide total dependence on natural petroleum is obvious in 21st century. Demand for petroleum products increases everywhere in the world. At the same time the reserves of petroleum are finite and rapidly being depleted. Fluctuating price and depleting force petroleum-importing countries to find alternative petroleum-substitutes in order to ensure their energy security.

The origin of petroleum in the Earth's crust is observed as a result of catagenesis of the sedimented and fossilized organic matter (OM) in oil shale – kerogen, during millions of years in geothermal conditions (elevated temperatures, pressure and presence of minerals, water etc.). Using pyrolysis, hydrogenation and thermal dissolution methods it is possible to create thermochemical conditions for the technological production of synthetic petroleum within some hours or less.

Oil shales become more and more important as an alternative source for production of liquid fuels. Deposits of oil shale occur in many parts of the world. Oil shales of different deposits considerably differ by the content of OM and chemical composition of both kerogen and mineral matter (MM) [1].

Total world reserves of shale oil are estimated by World Energy Council Report, 2013 conservatively at 4.8 trillion barrels that surpassing several times the amount of petroleum [2]. Only a few deposits of oil shale are currently being exploited – in Brazil, China, Estonia, and from recent time there is an interest to their exploitation in Jordan, USA, Morocco, and Iran. The Estonian deposits were first developed in 1920s and up to now it is the main industry in Estonia. With an increasing interest towards oil shale liquefaction, an interest to effective opportunities using oil shale as a feedstock in production of unconventional petroleum increases also.

The yield of oil depends on the initial oil shale composition and on the method applied for thermochemical liquefaction and its conditions. For production of shale oil in Estonia from domestic kukersite oil shale modifications of slow pyrolysis have been used by heating the oil shale up to 500ºC in special retorts without solvent. The mechanism of Estonian kukersite thermal decomposition is schematically represented as follows [3]:
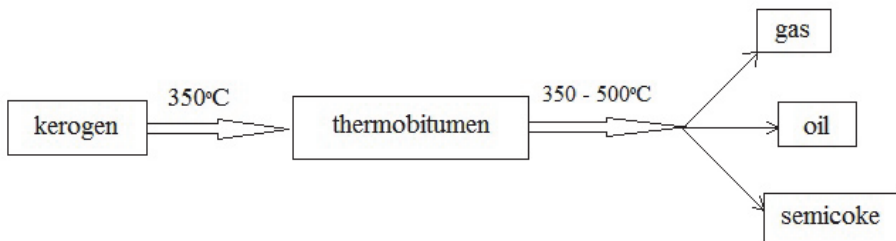
Upon heating oil shale in retorts the kerogen is initially converted to high-molecular thermobitumen (TB), soluble in organic solvents. Oil, gas and semicoke as final products are formed as a result of thermal decomposition of TB. Several other oil shales are described by the similar scheme [4-7].

In Estonia there are two types of industrial retorts in use for shale oil production: gas heated vertical retorts and horizontal solid heat carrier retorts. Despite retort oil is observed as a type of unconventional petroleum, its yield in industrial retorts is not high. Maximum attainable oil yield in retorting, determined in laboratory Fischer Assay amounts approximately to 66% on OM basis. Industrial retorting yields about 1 barrel shale oil per 1 tonne kukersite oil shale depending on the retort configuration and on the content of OM and moisture of the shale. So, less than a half of valuable kerogen is converted into liquid phase. The rest is transformed into carbonaceous semicoke and low calorific gas. The semicoke from vertical retorts represents a hazardous waste and is sent to the landfills. In more progressive solid heat carrier retorts the formed semicoke is combusted for heat production. As a result, CO_2 in large quantities is emitted into the atmosphere. It is known that there are reduction targets validated for the emission of CO_2 (Kyoto Conference of World Climate Changes). That is why fundamentals of a new technology were investigated as a possibility for replacement of the oil shale retorting by more effective and sustainable liquefaction technologies enhancing oil yield and diminishing amounts of low calorific by-products polluting atmosphere.

A specific feature of the kukersite oil shale and kukersite shale oil is their high content of O. The compounds, which are not typical to petroleum crude such as phenols, alkenes and neutral oxygen compounds, are dominating. The possibilities of shale oil utilization without upgrading are limited. Today it is used as fuel oil and a source of chemicals. The compounds boiling above 350 °C make up to 50% of total retort oil obtained in vertical retorts. Kukersite shale oil is characterized as an unstable, unsaturated complex mixture of compounds.

So, initial shale oil and its distillation fractions are unsuitable for exploitation as a feedstock for motor fuels without stabilization, heteroatoms removal and visbreaking of the compounds boiling above 350 °C. That is why recent advances in the production of high quality transportation fuels have been focused on the upgrading technologies of high boiling fractions of shale oils and residues by hydrogenation. Upgrading is necessary to obtain from oil shale liquids at least so-called synthetic petroleum.

Hydrogenation techniques are the most perspective, enabling to remove heteroelements, to elevate hydrogen-to-carbon ratio, to saturate the unsaturated bonds, to correct the boiling range and group composition of synthetic petroleum, so bringing its properties closer to the properties of natural petroleum and its distillation products.

The aim of this thesis was to work out conditions for production from kukersite oil shale OM the maximum possible quantum of the upgraded shale oil

(later raffinate) rich in hydrocarbons (HC) being a synthetic analogue to the natural petroleum.

For this purpose the experiments of hydrogenation at varied experimental conditions of kukersite oil shale and industrial shale oil fractions obtained in vertical retort were carried out. The influence of presence of catalysts and H-donor compounds on raffinate yield and its fractional and elemental composition was studied. Both qualitative and quantitative alterations in raffinate compounds groups were determined.

It was demonstrated that hydrogenation of retort oil and its fractions resulted in high yield of raffinate on the basis of the feed but the result on the basis of OM was not efficient due to the low oil yield (45% of OM in retorting). That is why a new upgrading scheme for kukersite oil shale was proposed.

For accomplishing the new scheme in the first stage kukersite oil shale was thermochemically dissolved with different solvents under various temperatures and durations to find out the most effective conditions for producing a liquid product – the mix of thermobitumen and oil (TBO). As a result, 86-91% yields of TBO on the basis of OM were achieved. In the second stage TBO obtained was subjected to the catalytic hydrogenation, also varying experimental conditions to optimize raffinate yield and composition. High yield of hydrocarbon rich oil was obtained.

A new effective technology for producing a synthetic analogue to the natural petroleum from kukersite oil shale was suggested.

1. LITERATURE REVIEW

1.1   Oil shale

Oil shales are fine-grained, layered sedimentary rocks containing MM and OM, from which oil can be obtained by destructive distillation. The major component of OM is kerogen – cross-linked macromolecular OM insoluble in solvents at usual conditions. Another part of OM is bitumen, which is soluble in solvents. Oil shales from different deposits vary in the content of kerogen and its chemical composition. Urov and Sumberg have represented characteristic data for hundred known oil shale deposits and outcrops [1]. Few of those found already industrial exploitation are characterized in Table 1.

Table 1. Elemental composition of oil shales and their Fischer Assay oil yields, % [1]

	Kukersite (Estonia)	Nebi Musa (Jordan)	Green River (USA)	Irati (Brazil)	Fushun (China)
OM	35.5	22.0	20.6	34.0	21.2
O	10.8	7.6	5.6	16.3	11.0
N	0.4		2.6	1.6	3.0
S	1.7	7.0	1.5	3.7	2.4
C	77.3	75.4	80.2	68.1	73.7
H	9.8	10.0	10.1	10.3	9.9
H/C	1.52	1.59	1.51	1.81	1.61
Fischer Assay yields, % per OM					
Oil	65.6	54.7	66.5	40.9	36.8
Water	5.4	5.6	33.5	9.8	16.0
Gas	10.7	18.1		15.2	19.4
Semicoke	18.3	21.6		34.1	27.8

In Table 2 the elemental compositions of retort oil from those selected oil shales are represented.

Table 2. Elemental composition of shale oils, % [1]

	Kukersite (Estonia)	Nebi Musa (Jordan)	Green River (USA)	Irati (Brazil)	Fushun (China)
H	9.9	9.7	11.5	10.2	12.2
S	1.1	8.5	0.7	0.5	0.6
N	0.1	3.2	1.8	0.7	1.3
O	5.9		1.6	1.2	0.5
C	83.0	78.6	84.4	87.4	85.4
H/C	1.43	1.48	1.64	1.4	1.71

One can see that OM of kukersite is rich in O and yields also rich in O oil. However, the OM of Irati and Fushun oil shales is characterized as rich in O as

well, but O content in oils is low. In case of other heteroelements it seems that OM of oil shales rich in N or S rather yields oil rich in N or S.

Kukersite is outstanding among other oil shales by its high kerogen content – 35-50% depending on the depth of layer, and by low content of nitrogen (0.4% only). The mineral part of oil shale prevails over the OM. The typical mineralogical composition of inorganic part of kukersite oil shale is – carbonates 65.9%, argillaceous minerals 5.0%, quarts 8.5%, feldspars 8.5%, sulphates 0.8% and pyrite 3.1% [8]. Kukersite contains only 0.17% of natural soluble bitumens. The chemical composition of kukersite kerogen is stable in all its deposits [3].

1.2. Thermochemical methods of oil shale liquefaction

Thermochemical methods of oil shale liquefaction are divided into:

- Pyrolysis
- Thermochemical dissolution
- Hydrogenation

1.2.1. Pyrolysis

Pyrolysis is a basic method of thermochemical decomposition of OM of solid fuels in the absence of oxygen. It can be accomplished under largely varied thermal and chemical conditions. The yield and composition of pyrolysis products depend on material pyrolyzed and pyrolysis conditions – temperature and heating rate, the content of gaseous atmosphere and its pressure, process duration. Depending on the operation conditions, the pyrolysis process can be subdivided into conventional pyrolysis, fast pyrolysis and flash pyrolysis. Conventional pyrolysis (slow pyrolysis, retorting in Fischer Assay) takes from 10 minutes to several hours to complete. In flash pyrolysis the material is heated for less than 0.5 second with heating rate more than 1000 K/s. The heating time of fast pyrolysis is 0.5-10 seconds [8].

Pyrolysis of oil shale can produce oil fractions that have a similar calorific value, density and viscosity to petroleum. However, the fractions also have properties which make them less attractive than petroleum, including their high heteroatomic content.

Khisin [10] has described that decomposition of kukersite begins at 170-180 °C, when the change becomes visible but not a lot of vapor and gas products are vented. During thermal decomposition of kukersite firstly water is formed at 270-290 °C, then gas at 325-350 °C and oil at the same temperature but with a lag of time. In that temperature range the softening of OM takes place and TB is formed.

Kask and Aarna [11, 12] studied the yield and composition of products depending on pyrolysis conditions in laboratory retort. Obtained data are given in Table 3.

Table 3. Yield and elemental composition of oil obtained from kukersite

Conditions	Oil yield, % OM	Elemental composition, %				H/C
		C	H	S	O+N	
Kerogen concentrate		82.1	10.63	0.75	6.5	1.55
275 °C, 456 h	17.9	83.0	10.1	0.50	6.7	1.46
300 °C, 387 h	69.8	85.1	8.77	0.32	5.8	1.24
340 °C, 12 h	59.8	83.8	9.78	0.52	5.9	1.40
360 °C, 4 h	63.8	83.6	9.56	0.50	6.3	1.37
380 °C, 4 h	29.1	85.3	8.85	0.53	5.3	1.25

One can see that to obtain oil in maximum 69.8% the process takes several weeks and under temperature not lower than 300 °C.

The laboratory retorting in standard conditions called Fischer Assay test [13] is widely used for evalution of oil potential of solid fuel.

A number of experimental studies on the decomposition process of kukersite oil shale have been carried out. Experiments by Kogerman [14] and Karavayev [15] were carried out in the autoclaves with different heating time and temperature of pyrolysis in order to study the influence of these conditions on the yield and chemical composition of oil. It was shown that more than 80% of bituminous oil rather like TB than oil was yielded.

1.2.2. Thermochemical dissolution

The pyrolysis in autoclaves allows alteration of pyrolysis conditions by the addition of solvent (and/or hydrogen) accompanied by the modification of products yield and composition [16-19].

By thermochemical dissolution of oil shale - pyrolysis in the presence of solvents in their sub- or supercritical conditions, it is possible to liquefy also this part of kerogen forming hazardous semicoke in retorting. Secondary reactions of decomposition and condensation of formed products are depressed, if the processing temperature is low and chemically inert solvent has a high ability for dissolution [19].

It is known that solvents can promote the thermal destruction of high-molecular weight OM, having the most destructive ability under their supercritical conditions. So, supercritical extraction of OM from kukersite represents an alternative to the traditional retorting and can be carried out at milder temperature than retorting, resulting in less degradation and charring [17].

At the same time, some factors, including the type of solvent, the process conditions and initial oil shale composition influence on the extraction process.

Luik and Klesment [17, 19] have submitted the kerogen concentrate of kukersite with OM 90.1% (K-90) to liquefaction in a microautoclave (20 cm^3) at

temperatures 330-370 °C in the presence of various supercritical solvents: hexane, cyclohexane, toluene, benzene, methanol and water. Pure hydrocarbon solvents liquefied comparable amounts of OM (25-28%); methanol and water as the sources of hydrogen revealed a higher destructive activity. When the half of the solvent was replaced by water, the oil yield increased by 5-9%, and even by 17% when using benzene.

Further investigations by Luik et al. [18] were carried out in 500 cm^3 autoclave in the presence of benzene, diethyl ether, ethanol, *n*-hexane, dimethyl ketone and water as solvents. The liquefaction temperature was 360 °C and residence time of 4 h. The yield of liquid product, 70% and more on basis of OM, depended strongly on the solvent type and its portion of incorporation. For example, ethanol yielded 146% of liquid because it was decomposed forming chemically active fragments, which began to react with kerogen and incorporated into extract composition.

Upon traditional retorting (450-550 °C), the process of separation of oil from the solid residue occurs only after decomposition of the primary bitumen accompanied by the formation of coke, gas and oil. Under sufficient oil vapour pressure oil is evacuated in the vapour phase. Differently, in thermochemical dissolution, the total solvent-soluble product consisting of the highmolecular intermediate product TBO is dissolved and separated from the solid residue in its original form before coke formation. That is why retorting yields less oil and more solid residue than dissolution at optimum conditions.

1.2.3. Hydrogenation

Hydrogenation is the main technique which is practised in upgrading both solid fuels and liquid products derived from petroleum, bitumens, coal and oil shale. As a result of hydrogenation the chemical composition and qualities of the syncrude obtained will be closer to those of the light natural petroleum.

Because of the oil obtained from kukersite oil shale, its distillation fractions and particulary TBO significantly differ from natural petroleum and are unsuitable for exploitation as a feedstock for motor fuels without upgrading – their visbreaking, stabilization and removing of the heteroatoms via hydrogenation method is inevitable. About 80 years ago Kogerman concluded that deep conversion of OM of Estonian shale into liquid products can be achieved in principle by hydrogenation [20].

For syncrude, crude distillates and heavy crude oil residues upgrading by catalytic cracking, fluid catalytic cracking, coking, deasphalting and mostly catalytic hydrocracking and hydropurification processes are used. Hydrocracking is practised in modern petroleum refineries for converting higher boiling ranges into more valuable low-boiling products such as gasoline, diesel and jet fuel. Hydrocracking is a highly flexible petroleum refining process. Applications of this process include upgrading of petrochemical feedstock, improvement of either diesel fuel cetane number or gasoline octane number, and

production of high quality lubricants removing heteroatoms. Its result, heavy HC feedstock is upgraded by increasing overall hydrogen-to-carbon ratio in original feedstock and decreasing its average relative molecular mass. The operation conditions and catalysts for hydroprocessing may vary, depending upon requirements to the end products.

1.2.3.1. Hydrogenation catalysts

The type of the used catalysts varies with hydrogenation process and the feedstock being hydrogenated.

Development of hydrogenation catalysts is a separate field of science. A lot of research in this area is made by special catalyst manufacturing companies like Haldor Topsoe, Abermarle, Chevron Lummus, Akzo Nobel, Shell, etc. Know-how generated by these companies is very strictly protected and not publicly available.

A dispersed-phase water soluble catalysts as ammonium molybdate were demonstrated to have advantages over supported catalysts due those can be recovered and recycled [21]. $Co-Mo/Al_2O_3$ has been widely used for hydrocracking of heavy feedstocks such as residual raffinate, solvent deasphalted residual oil and vacuum residue. The catalysts activity decreases and the selectivity changes with ageing. More gas than naphtha is produced as the temperature of catalytic hydrogenation is raised to maintain the conversion. Tian et al. [22] have made a comparison between dispersed and supported catalysts. Hydrodenitrogenation of residue over dispersed water soluble Ni-Mo-catalyst was compatible with that of commercial presulphided $Co-Mo/Al_2O_3$ catalysts.

Ni-Mo, Ni-W and Ni-Co have been used as hydrocracking catalysts. Mo-Ni/SiO_2-Al_2O_3 catalysts have been used for hydrocracking of vacuum distillates from coal liquefaction [23]. The effect of distribution and dispersion of Mo ions in NiO-CoO-MoO_3/Al_2O_3 catalysts has been reported; more highly dispersed Mo ions gave higher hydrogenation activity whereas agglomeration of Mo ions resulted in a higher hydrocracking activity [24].

Dufresne et al. [25] have presented the pilot plant data of two-stage high conversion hydrogenation using supported by zeolite hydrocracking catalysts. Ni-Mo-zeolite catalyst has been recommended for maximizing gasoline production and Ni-W-zeolite catalysts for maximum gas oil manufacture.

Sasaki et al. [26, 27] prepared the catalysts from heavy oil, known as ash catalysts, which had high vanadium content, and used it for hydrocracking of heavy oils. Although the activity of this catalyst was lower than that of $Co-Mo/Al_2O_3$, it produced the same level of liquid products. The coke formation decreased, whereas metal removal increased, with an increase in the amount of ash catalysts.

Suspended Fe-catalysts on coke were used in earlier works to upgrade shale oil fractions [28].

In this thesis the special catalysts delivered for kukersite oil hydrogenation from Akzo Nobel, Shell and OAO AZKiOS (Russia) were tested.

1.2.3.2. Hydroprocessing of petroleum residuums

About 50% of kukersite retort oil boils above 350 °C and its upgrading can have parallels with hydroprocessing of petroleum residuums.

Heavy petroleum fractions can be originated from both technological and natural processes. Despite of their origin petroleum pitches, residual fractions from atmospheric and vacuum distillation, tar sand bitumens and others are characterized as high-boiling and rich in heteroatoms, but representing large reserve of available feedstock for producing liquid fuels. Different methods for upgrading heavy bituminous fractions have been developed basing mostly on hydroprocessing, but differing by process severities, catalyst type and technological solutions.

By Dolbear et al. [29] detailed chemical composition data were obtained for five atmospheric residues and products prepared in a continuous pilot plant by residual oil hydrotreating process. The results showed that the reactivities for removal of sulphur, nickel, vanadium and coke precursors cannot be predicted from simple physical or chemical properties. In particular, sulphur and metals removal reactivities are not proportional to feed sulphur or metal levels. There was a correlation of metals removal reactivities with the fraction of total feed metals found in the resin fractions. The oils studied were Heavy Arabian, Hondo (from California), Maya (from Mexico) and a blend of West Coast refinery feed-stocks.

Guan et al. [30] have investigated the two-stage hydrocracking of petroleum residue in a batch autoclave consisting of hydrogenation at 416 °C and 436 °C. Compared with one-stage reaction, two-stage reaction had the following advantages: lower coke formation, higher cracking and higher removal of heteroelements. Anthracene had been regarded as the model compound of coke precursor. After two-stage hydrocracking about 51% of anthracene was hydrogenated at 416 °C and about 10% of the hydrogenated compound released the activated hydrogen, which could prevent the residue from coke formation and removed the heteroatoms at 436 °C. Comparison of two kinds of reactions showed that two-stage reaction was more effective than the one-stage reaction and 72.1% of liquid conversion product was yielded from the feed instead of 66.1%, coke yields being, respectively, 0.71 and 0.91%. $FeSO_4 \cdot 7H_2O$ and $(NH_4)_6Mo_7O_{24} \cdot 4H_2O$ as catalysts were used.

Ancheyta et al. [31] have reported the experimental information about the hydroprocessing of Maya heavy crude oil (from Mexico) using two reaction stages. Experiments were performed in a high-pressure fixed-bed pilot plant. Hydroprocessing reactions were carried out at a constant pressure (7 MPa) and temperature range 360-400 °C. The first reaction stage used a Ni-Mo/Al_2O_3, while the second stage employed a Co-Mo/Al_2O_3 catalyst. Experimental and

characterisation results showed that Maya crude oil quality can be substantially improved by hydroprocessing in two reaction stage.

Ovalles et al. [32] have studied the upgrading of extra-heavy crude oil (Hamaca oil field, Venezuela) in batch reactor at 420 °C with a residence time of 1 h using methane at 11 MPa as source of hydrogen. In the presence of $Fe_3(CO)_{12}$ as catalyst, the reaction of Hamaca extra-heavy crude oil led to 14% reduction in sulphur content and 41% conversion of the 300 °C+ fraction in the upgrading product with respect to the original crude.

Chen et al. [33] have described a mild cracking solvent deasphalting – for upgrading of heavy oil. Continuous bench experiments were carried out on Shengli and Gudao (China) vacuum residues. The effect of cracking temperature and time on the yield and properties of raffinate asphalt were examined. The deasphalted oil obtained was high yielded and qualify to that from solvent deasphalted alone. At the same yield of deasphalted oil, the softening point of the raffinate asphalt was lower and the penetration and the ductility were greater than those for the solvent deasphalting process.

Due to different materials need special hydrogenation conditions, the effective upgrading of Estonian oil shale and its liquid transformations requires special investigations.

1.3. Hydrogenation of oil shale, shale oil and its fractions

1.3.1. Direct hydrogenation of OM in oil shale

A deficiency of hydrogen relative to carbon in oil shale reduces the amount of kerogen that can be converted to hydrocarbon products by conventional retorting methods. A new approach to oil recovery from low grade oil shales has been developed jointly by the Mineral Resources Institute of The University of Alabama and the Hycrude Corporation. The approach is based on the HYTORT process, which utilized hydrogen gas during the retorting process to enhance oil yields from many types of oil shales [34].

Hydroretorting studies were conducted [35] on several oil shale samples using a Hydroretorting Assay unit designed to evaluate the hydroretorting characteristics of oil shale samples. A 100 gram sample of material was reacted with hydrogen gas under the following conditions, represented in Table 4:

Table 4. Conditions for hydroretorting [35]

Parameter	Value
H_2 pressure, atm	70
Temperature, °C	538
Duration, min	30

Results of Hydrotreating Assay tests on the raw shale samples are given in Table 5.

Table 5. Yields from hydroretorting of different oil shales samples [35]

Oil shale sample	Oil yield (gal/ton)		
	Fischer Assay	Hydroretorting Assay	Increasing times
Sweden – Billingen	3.8	17.5	4.6
Sweden – Naerke	10.9	32.3	3.0
Sicily	4.4	12.2	2.8
Indiana – New Albany	12.5	28.2	2.3
Montana – Heath Formation	16.2	33.6	2.1
Canada – Kittle	10.0	21.1	2.1
Jordan – El Lajjun	32.8	57.0	1.7
Brazil – Lower Irati	19.4	32.7	1.7

The results indicate that the HYTORT process can produce oil yields of over 400% of those obtained by conventional, thermal retorting in at least one instance, with a number of samples showing oil yields of more than 150% of Fischer Assay. In some instances, these results mean that oil yields over 30 gallons per ton can be produced from oil shale resources which would normally be considered too lean for commercial exploitation by conventional retorting processes.

1. 3. 2. Direct hydrogenation of OM of kukersite oil shale

Direct destructive hydrogenation of kukersite shale flotated kerogen concentrate K-90 in an autoclave at 320-420 °C and 25 atm H_2 pressure using ammonium molybdate as a catalyst was carried out by Klesment et al. [36]. The results of products yields are represented it Table 6.

Table 6. The yields of products from hydrogenation of kukersite kerogen concentrate, elemental composition and group composition of liquids obtained, %

Product	Hydrogenation temperature, °C				
	320	360	380	400	420
Liquid product	45.3	44.0	39.0	36.7	36.2
Solid residue	35.8	27.1	29.7	32.8	43.1
Water + gas	18.9	28.9	31.3	30.5	29.7
Elemental composition, %					
Carbon	84.9	85.0	84.4	86.5	88.0
Hydrogen	10.6	10.4	10.8	11.3	9.9
Heteroatoms	4.5	4.6	4.8	3.2	2.1
Group composition, %					
AlHC	17	24	19	20.4	12
MAHC	18	14	13	17.5	12
PAHC	19	21	22	20.1	40
LPHet	42.1	38.4	43.8	39.9	34
Phenols	3.9	2.6	2.2	2.1	2.0

One can see in Table 6 that only 36.2-45.3% on OM basis liquid products was produced. In addition to low yield of the liquid product, the content of HC was also not high. The content of heteroatoms was reduced down to 2.1 at 420 °C as compared with 6.9 in retort oil. Phenols yield in raffinate was only 2.0-3.9%, but the yield of aromatic compounds was considerably higher than in retort oil (21%).

Hydrogenation of kukersite kerogen concentrate with 76% of OM in autoclave at 420-480 °C and 3.5-7.0 MPa H_2 during 0.5 or 1.5 h resulted in high kerogen conversion degree, but in low liquid yield (up to 47.0) [37]. Lots of gases were formed (more than 40%). Gorlov et al. [38] have investigated the petroleum tar H-donor effect on kukersite oil shale hydrocracking and an increase in both gasoline and diesel fraction yields and significant decrease in H_2 was noted.

The yield of liquid products was lower than oil yield in direct pyrolysis because a part of oxygen was removed as CO_2 and H_2O, and additional gas and coke were formed.

1.3.3. Hydrogenation of total and dephenolated kukersite retort oil

Luik et al. [39-47] investigated upgrading of Estonian kukersite shale oil submitting total shale oil, dephenolated shale oil, phenols, diesel fraction, light and heavy mazute to the catalytic hydrogenation in 500 cm^3 batch autoclave at various reaction conditions. The shale oil distillate fractions were industrial products obtained from AS Kiviter.

Moderate conditions and Co-Mo/Al_2O_3 catalysts were used for hydrogenation of kukersite total and dephenolated retort oil [39, 40]. Conditions of experiments are represented in Table 7, and results of hydrogenation in Tables 8 and 9.

Table 7. Hydrogenation parameters

Parameter	Value
Ratio catalyst/shale oil, g/g	0.1
Temperature, °C	370
Initial pressure of hydrogen, atm	97-103
Duration, h	2

Table 8. Products obtained on hydrogenation and their yields

Material of hydrogenation	Product, mass %			
	Raffinate	Water	Gas	Coke
Total retort oil	93.1	4.2	2.1	0.6
Dephenolated retort oil	80.2	3.1	16.1	0.6

Considerably more gas was formed on hydrogenation of dephenolated oil than from the initial oil - 16.1 and 2.1%, respectively, the coke yield being the

same. It can be supposed that during alkali-acidic dephenolation some bonds in condensed molecules decomposed enhancing gas formation.

Table 9. Chemical group composition of compounds present in initial and hydrogenated oils.

Compounds	Retort oil, %			
	Initial	**Dephenolated**	**Hydrogenated**	**Dephenolated, then hydrogenated**
AlHC	11.1	15.0	32.7	35.7
MAHC	5.4	7.3	1.7	2.1
PAHC	23.1	31.2	41.1	40.9
LPHet	16.7	22.6	12.5	8.7
HPHet	17.7	23.9	10.4	11.9
Phenols	26.0	0	1.6	0.7

As a result of hydrogenation, the content of heterocompounds significantly decreased. At the same time the content of HC in raffinates increased. This increase was especially significant in case of the aliphatic hydrocarbons (AlHC), 2-3 times (Table 9).

1.3.4. Hydrogenation of phenols

Hydrogenation of phenols [41] was performed in conditions given in Table 7.

The yield of products removed from autoclave after 2 h hydrogenation and chemical group composition are represented in Table 10 and Table 11. As compared with the results of hydrogenation of dephenolated and total retort oil, phenols yielded as much neutral oil as dephenolated oil on hydrogenation at the same conditions, but no coke.

At the same time total retort oil yielded more raffinate and 0.6% coke, but markedly less gas and water. Therefore, just the phenols give the lion's share of gas and water on the retort oil hydrogenation at the conditions used while neutral oil yielded some coke.

Table 10. The yield of hydrogenation products of phenols, %

Product	Yield, wt.%
Raffinate	81.6
Gas	12.8
Water	5.6
Coke	0

Table 11. Chemical group composition of compounds formed on hydrogenation of phenols, wt.%

Compounds	Wt.%
AlHC	15.1
MAHC	3.6
PAHC	40.9
LPHet	17.8
HPHet	17.0
Phenols	5.6

The compound groups similar to those present in the initial retort oil were formed. The proportions between different compound classes were also the same, only raffinate contained markedly less phenols and more polyaromatic hydrocarbons (PAHC) as compared with the initial retort oil. As a result, the phenol raffinate is aromatic by its nature, with up to 45% total aromatic compounds (PAHC + MAHC). Low-polar heteroatomic compounds (LPHet), which composition was similar to that in primary retort oil established by gas chromatographic analysis, were formed in amounts equal to the amount of high-polar heteroatomic compounds (HPHet) – both 17%. The most interesting compound classes formed on hydrogenation were AlHC and phenols of secondary origin.

1.3.5. Hydrogenation of retort oil industrial fraction 180-240 °C

Retort oil fraction 180-240 °C called "diesel fraction" by AS Kiviter was submitted to hydrogenation [42, 43]. Experimental conditions applied for "diesel fraction" hydrogenation are represented in Table 12.

Table 12. Experimental conditions

Parameter	Value
Initial pressure of hydrogen, atm	50
Temperature, °C	370
Time of hydrogenation, h	2
Catalyst Co-Mo/Al$_2$O$_3$, %	5

The yield of hydrogenation products is represented in Table 13.

Table 13. The yield of hydrogenation products of the "diesel fraction"

Product	Yield, wt.%
Raffinate	94.9
Gas	3.8
Water	1.3
Coke	0

It can be seen that the yield of raffinate was high and that of water and gas low. No coke was formed.

Judging by the group composition of compounds (Table 14), "diesel fraction" did not contain much heteroelements; HPHet and LPHet as the main source of heteroelements constituted only one fifth of total fraction. The industrial "diesel fraction" consists mainly of HC and their content was increased from 55 to 69% as a result of hydrogenation.

Table 14. Chemical group composition of "diesel fraction", mass %

Compounds	"diesel fraction"		
	Initial	Dephenolated	Dephenolated then hydrogenated
AlHC	52	55	69
Aromatic hydrocarbons	23	25	28
Among them: MAHC	16	17	2
PAHC	7	8	26
LPHet	7	7	1
HPHet	12	13	2
Phenols	6	0	0

Hydrogenation of the "diesel fraction" changed essentially its group composition; raffinate contained 6-7 times less HPHet and LPHet and 8 times less MAHC, but 3 times more PAHC.

The main reactions occurring on hydrogenation of the "diesel fraction" was saturation of unsaturated bonds and removal of heteroelements. HPHet and LPHet, the latter consisting of *n*-alkanones and *n*-2-alkanones, gave an additional amount of aromatic and AlHC after the removal of heteroelements. At the same time MAHC have been submitted to hydrogenation yielding cyclohexane derivatives.

Also the effect of different hydrogen pressure (50, 85, 100 atm) on the yield and composition of "diesel fraction" hydrogenation products was studied. It was concluded that the higher the initial pressure of hydrogen the lower the yield of raffinate and the higher the yields of water and gas.

Two-step hydrogenation of "diesel fraction" was carried out. It was concluded that at hydrogenation of the already hydrogenated "diesel fraction" practically no typical final products of hydrogenation – gas and water – were formed and the main difference in its composition was the increased content of MAHC and decreased content of PAHC.

1.3.6. Hydrogenation of retort oil industrial fraction 240-320 °C

Retort oil fraction 240-320 °C called "light mazute" by AS Kiviter was submitted to hydrogenation [44, 45]. Experimental conditions for hydrogenation are represented in Table 15, and results in Tables 16 and 17.

Table 15. Experimental conditions

Parameter	Value
Initial pressure of hydrogen, atm	80
Temperature, °C	370
Time of hydrogenation, h	2
Catalyst Co-Mo/Al_2O_3, %	5

Table 16. The yield of "light mazute" hydrogenation products

Product	Yield, wt.%
Raffinate	89.0
Gas	2.9
Water	2.0
Coke	6.1

Hydrogenation resulted in a high yield of raffinate, but also some amount of coke was formed.

Table 17. Chemical composition of "light mazute", wt. %

Compounds	"Light mazute"		
	Initial	Dephenolated	Dephenolated then hydrogenated
AlHC	21	31.2	50.8
Aromatic hydrocarbons	25.7	38	39.6
Among them: **MAHC** **PAHC**	3.5 22.2	5.2 32.8	13 26.6
LPHet	12	17.7	3.6
HPHet	8.9	13.1	6
Phenols	32.4	0	0

The initial "light mazute" is characterized by a high content of phenols, but after dephenolation it consisted of almost equal parts of AlHC (31.2%), aromatic HC (38%) and heteroatomic compounds (30.8 %). Hydrogenation increased the total content of HC including both aliphatic and aromatic ones on account of the decrease in the content of LPHet and HPHet. The phenols were removed by dephenolation.

The effect of the hydrogen pressure (70, 80, 96 atm) on the yield and composition of "light mazute" hydrogenation products was studied. It was concluded that the higher the initial pressure of hydrogen the lower the yield of raffinate and the higher the yield of coke. The increase of the hydrogen pressure leaded to an increase in the content of AlHC and decrease in the content of aromatic HC, LPHet and HPHet.

Three-step hydrogenation of "light mazute" was carried out. During the last two phases of hydrogenation the loss in oil weight was only 2% and it was concluded that the influence of hydrogen on the products yield was very small.

1.3.7. Hydrogenation of retort oil industrial fraction boiling over 320 °C

The most viscous and boiling over 320 °C retort oil fraction called "heavy mazute" by AS Kiviter was submitted to hydrogenation [46, 47]. Hydrogenation was carried out at 370 °C during 2 hours, at the initial pressure of H_2 100 atm using Co-Mo and Ni catalysts. The results are represented in Table 18.

Table 18. Yields of "heavy mazute" hydrogenation products

Product	Yield, wt.%	
	Co-Mo catalyst	Ni catalyst
Raffinate	90.2	91.1
Gas	1.3	3.4
Water	4.9	3.4
Coke	3.6	2.1

Hydrogenation of "heavy mazute" resulted in its high recovery (90%), while coke, gas and water make less than 10% of reaction products. More gas, but less water and coke were formed, when Ni catalyst was used. The group composition of compounds obtained using Co-Mo catalyst is represented in Table 19.

Table 19. Chemical group composition of " heavy mazute"

Compounds	"Heavy mazute"		
	Initial	Dephenolated	Dephenolated then hydrogenated
AlHC	6.6	10.4	21.3
Aromatic hydrocarbons	27.3	43.0	53.8
Among them: **MAHC** **PAHC**	2.7 24.6	4.3 38.7	6.1 47.7
LPHet	14.4	22.6	10.5
HPHet	15.2	24.0	14.4
Phenols	36.5	0.0	0.0

As compared with "diesel fraction" and "light mazute", „heavy mazute" contains 3-5 times less AlHC and twice more LPHet and HPHet.

To investigate the effect of time and hydrogen pressure on the yield and composition of hydrogenation products the consecutive three-step hydrogenation of „heavy mazute" was carried out. The yield of raffinates was 93.9% and, despite of significant consumption of hydrogen, it did not change much during the 2nd and 3rd steps of hydrogenation.

2. EXPERIMENTAL

2.1. Samples, thermochemical methods and conditions

2.1.1. Samples

Materials submitted to hydrogenation are represented in Table 20.

Table 20. Materials hydrogenated

Solid samples	Liquid samples
Kukersite with 35.8% OM[1], W^a = 1.3%	Flash pyrolysis oil
40.2% OM[1], W^a = 1.4%	Heavy oil fraction 360 °C+ (HO)
50.5% OM[1], W^a = 1.5%	
Kukersite concentrate (90.1% OM[1], W^a = 1.9%)	Thermobitumen + oil (TBO)
	Maltenes of TBO
	Asphaltenes of TBO

[1] OM content was determined on the basis of ash at 825 °C (A^d_{825}) and pyritic sulphur, (S_p), as follows: OM = 100 - A^d_{825} - $0.625S_p$

2.1.2. Thermochemical methods and conditions

Thermochemical dissolution of the solid samples before hydrogenation was carried out varying parameters as solvent, duration, experimental temperature and oil shale-to-solvent ratio. Conditions for thermochemical dissolution are represented in Table 21.

Table 21. Conditions for thermochemical dissolution

Solvent	Benzene, ethanol, water, water + benzene
Duration, h	1-4
Temperature, °C	360-400
Oil shale-to-solvent ratio	1:2; 1:3

Thermochemical dissolution of kukersite was carried out in 500 cm^3 batch autoclave with thermocouple (Figure 1). Kukersite samples were charged into autoclave with addition of applied solvent. Autoclave was placed and fixed into electric heater, connected to the electric engine, so that the system rocked. The heating time from ambient temperature to reaction temperature was 1 hour.

Some of experiments were carried out in 100 cm^3 autoclaves, which were placed into electrical oven, heated to the nominal temperature and after the duration prescribed after the end of the process the autoclave was left at ambient temperature for cooling and opened on the next day.

Majority hydrogenation experiments were carried out in the 500 cm^3 batch autoclave as in the case of thermochemical dissolution. The autoclave was filled with sample and hydrogen to nominal pressure and then heated. The heating time from ambient to hydrogenation temperature was 1 hour. The hydrogenation

time was measured since the nominal temperature was achieved. After the end of the process the autoclave was cooled and opened.

Figure 1. Batch rocking autoclave

Hydrogenation was performed at following conditions (Table 22):

Table 22. Conditions for hydrogenation

Autoclave volume, cm^3	100, 500	
Mass of sample, g	10-100	
H$_2$ initial pressure, atm	50-88	
Duration	40 min - 4 hours	
Temperature, °C	340-470	
Catalyst content, % of feed	0-15	
Catalyst	Producer	Purpose
KGU-950	OAO AZKiOS, Irkutsk, Russia	Hydropurification
GO-30-7	OAO AZKiOS, Irkutsk, Russia	Hydrocracking
DN-3100 TL	Shell Chemicals LP, US	Universal
KF-848	Akzo Nobel, Netherlands	Hydropurification
KF-1015	Akzo Nobel, Netherlands	Hydrocracking
KC-3210	Akzo Nobel, Netherlands	Hydrocracking

2.1.3. Separation methods

Liquids, solids and gases. Liquids and solids were removed from autoclave by a benzene wash to the filter; as a result liquid and solid phases were separated. Benzene was evaporated from liquids under the vacuum. Solid residues were dried for solvent removal and then weighted; liquids were weighted after benzene evaporation. For 500 cm^3 autoclave gas yield was found by formula as difference

$$Gas = 100 - (Liquid + Solid) \qquad\qquad (1)$$

For 100 cm^3 autoclaves the mass of gas formed was determined by the difference in weights of closed and opened autoclave.

Maltenes and asphaltenes. Sample of TBO was dissolved in benzene (TBO-to-benzene ratio 1:10) and hexane was added in a 1:50 benzene solution-to-hexane ratio and stirred. Asphaltenes, being insoluble in hexane, were estimated by weight after 12 hours of precipitation and their filtration. Maltenes, soluble in hexane, were estimated by the weight after solvent evaporation.

Dephenolation. The total phenols were extracted with 5% NaOH (1:5) from the oils diluted with benzene (1:1), and thereafter re-extracted from the acidified water phase with diethyl ether.

2.2. Analytical methods

The products obtained were analyzed by thin-layer chromatography (TLC), Fourier transform infrared spectroscopy (FT-IR), gas chromatography-mass spectrometry (GC-MS), fractional and elemental analysis.

2.2.1. Thin-layer chromatography

Shale oil consists in thousands of compounds. TLC is a simple and quick technique giving shale oil group composition. A TLC plate is a sheet of glass, metal or plastic, which is coated with a thin layer of a solid absorbent, usually silica gel. About 0.5 g of the sample is spotted on the starting line of the plate. Then the bottom edge of TLC plate is introduced with the eluating solvent in the chamber. Solvent slowly rises up to the plate by capillary action eluating the sample. When the solvent achieves the top of plate, the plate is removed from chamber and after drying the separated components of sample are visualized. Usually the components are colorless and UV lamp is used for visualization the plate.

In this work glass plate with size 24×24 cm coated with 2 mm layer of silica gel and n-hexane as eluation solvent was used. Five groups of compounds were separated and washed out from silica gel with using diethyl ether:

- Aliphatic hydrocarbons (AlHC)
- Monoaromatic hydrocarbons (MAHC)
- Polyaromatic hydrocarbons (PAHC)

- Low-polar heteroatomic compounds (LPHet)
- High-polar heteroatomic compounds (HPHet)

Yields of the respective compound groups were determined by weigh-analysis after evaporation of diethyl ether.

2.2.2. Infrared spectroscopy

Infrared spectroscopy is the measurement of the wavelength and intensity of the absorption of mid-infrared light by a sample. Mid-infrared is energetic enough to excite molecular vibrations to higher energy levels. The wavelength of infrared absorption bands is characteristic of specific types of chemical bonds, and infrared spectroscopy finds its greatest utility for identification of organic and organometallic molecules.

The high selectivity of the method makes the estimation of an analyte in a complex matrix possible. This method involves examination of the twisting, bending, rotating and vibrational motions of atoms in a molecule.

An infrared spectrophotometer passes infrared light through an organic molecule and produces a spectrum that contains a plot of the amount of light transmitted on the vertical axis against the wavelength of infrared radiation on the horizontal axis. In infrared spectra the absorption peaks point downward because the vertical axis is the percentage transmittance of the radiation through the sample. Absorption of radiation lowers the percentage transmittance value. Since all bonds in an organic molecule interact with infrared radiation, IR spectra provide a considerable amount of structural data.

In this work Fourier transform infrared (FT-IR) spectroscopic method was used. FT-IR spectra are represented and interpreted as visual (qualitative), calculated (quantitative) and graphic modes.

1. Visual mode. Visual mode represents itself as an original FT-IR spectrum. It contains a row of absorption bands, by which location and relative intensity it is possible to characterize the studied sample.

2. Calculated mode. The comparison of FT-IR absorption maxima with that at 1460 cm^{-1}, representing long aliphatic chains in each spectrum, enables quantitative characterization. The absorbance is measured as a peak height ratio. For this the height of each visible peak of studied sample is divided to the absorption maximum of the peak of studied sample at 1460 cm^{-1}. As a result, the relative concentration of certain functional group in the sample is obtained [48].

3. Graphic mode. For graphic construction and comparison of functional groups calculated data from spectra of liquids obtained at different conditions were used.

In this work infrared spectra were taken on an Interspec 2020 FT-IR-spectrometer.

2.2.3. Gas chromatography-mass spectroscopy

Gas chromatography-mass spectrometry (GC-MS) method is gas chromatography with mass spectrometer detector.

In this work GCMS – Shimadzu QP 2010 Plus gas chromatograph-mass-spectrometer was used.

2.2.4. Elemental analysis

Content of carbon, hydrogen, sulphur, nitrogen and oxygen was determined by "Elementar Vario EL"analyzer.

2.2.5. Fractional composition of raffinates

The boiling curves of the raffinates were obtained according to ASTM D86-72 standart "Test Method for Distillation of Petroleum Products at Atmospheric Pressure".

3. RESULTS AND DISCUSSION

3.1. Direct hydrogenation of the kukersite oil shale with molecular H_2

Experiments were carried out in 500 cm^3 autoclave using kukersite with 35.8% of OM. Conditions of the experiments are represented in Table 23.

Table 23. Experimental conditions

Parameter	Value
Mass of sample, g	100
Time, h	4
H_2 initial pressure, atm	50
Temperature, °C	340-430

No catalyst was added like in HYTORT process applied earlier for hydroretorting of oil shales from several countries [34, 35].

The yield of the products from kukersite with 35.8% of OM hydrogenation is shown in Table 24.

Table 24. The yield of products from direct hydrogenation of kukersite, % OM

Temperature, °C	Raffinate	Solid residue	Gas
340	49.0	25.0	26.0
350	45.9	26.6	27.5
390	27.8	34.1	38.1
430	26.0	29.4	44.6

As it can be seen the yield of raffinate decreases with the increasing of temperature, while the yield of gas increases significantly.

To determine the efficiency of the process, obtained results were compared with results obtained by Klesment et al.[36] in direct hydrogenation of kukersite concentrate K-90. All the experiments were carried out at different temperature. Duration of hydrogenation, 8 hours, and initial pressure of H_2, 25 atm, were kept constant. $(NH_4)_2MoO_4$ was used as catalyst. The results obtained in [36] have been represented in Table 6.

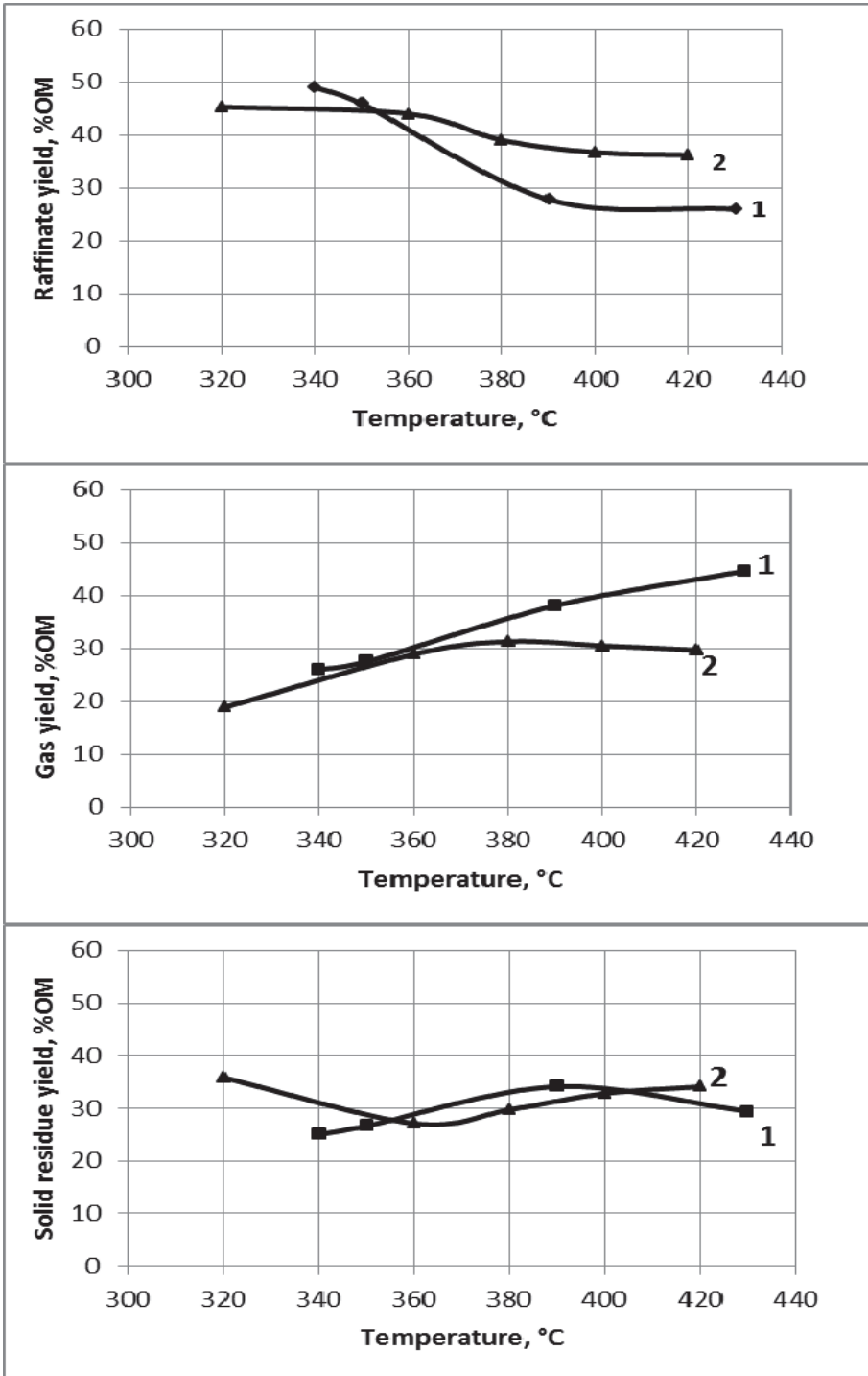Figure 2 shows the comparison of the yields of obtained products.

Figure 2. The comparison of results from hydrogenation of kukersite with 35.8% OM (curve 1) and K-90 with catalyst (curve 2 [36])

The decreasing yield of raffinates with increasing temperature was noticed because about one third of OM was transformed into gas and one third into coke. So, contrary to HYTORT process of several oil shales [34, 35], the direct hydrogenation of kukersite oil shale without catalysts did not give high yield of raffinate. The same was found also in case of kukersite OM concentrate [36].

The group composition of raffinates from hydrogenation of kukersite and K-90 were also compared by TLC. The results are depicted in Figure 3 (without catalyst) and Figure 4 (with catalyst).
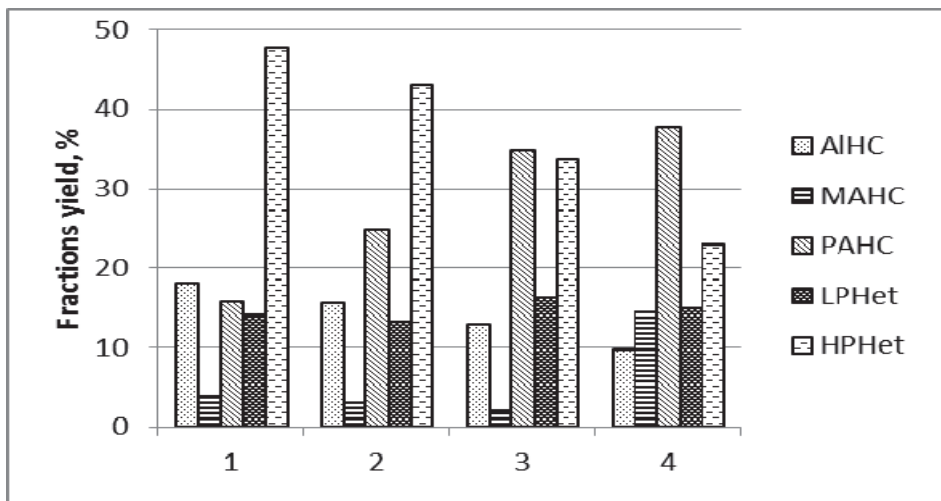

Figure 3. The group composition of hydrogenated kukersite with 35.8% OM (1 – 340°C, 2 – 350°C, 3 – 390°C and 4 – 430°C)
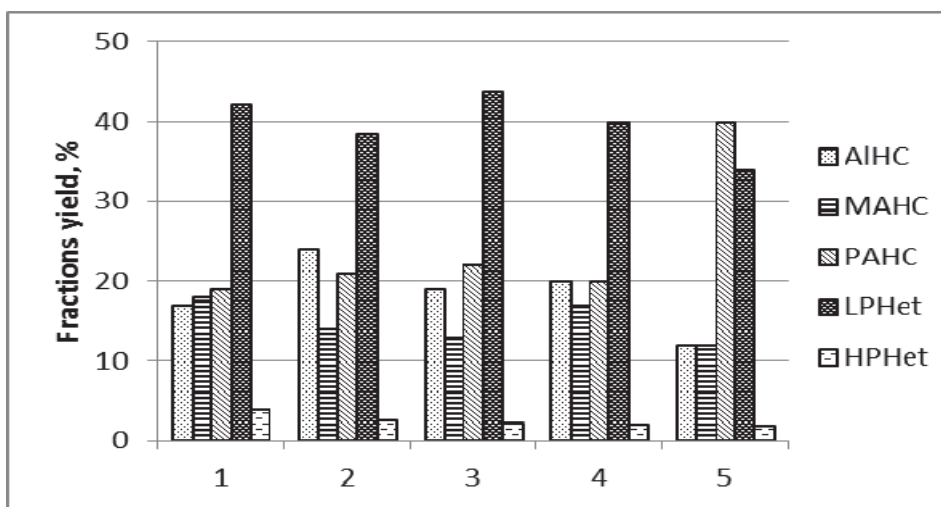

Figure 4. The group composition of hydrogenated K-90 (1 – 320 °C, 2 – 360 °C, 3 – 380 °C, 4 – 400 °C, 5 – 420 °C)

It can be seen, there is a significant difference in yield of HPHet. In case of oil shale with 35.8% of OM hydrotreated without addition of any catalyst, the amount of HPHet is determined in range 23-47%, while in case of K-90 with using of catalyst the amount was 2-4% only depending on temperature. It was demonstrated that the presence of catalyst influenced mainly the distribution of heteroatoms between HPHet and LPHet. The raffinate yield was less influenced.

The results above confirm that direct hydrogenation of kukersite oil shale and its concentrate with H_2 resulted in small yield of oil and also in small yield of HC, and high yield of gas and coke. So, the method of direct hydrogenation with molecular hydrogen cannot be suggested for upgrading of Estonian kukersite oil shale.

3.2. Direct hydrogenation of the kukersite oil shale with H-donor (tetralin)

Experiments were carried out in 100 cm^3 batch autoclaves filled with kukersite (40.2% OM). The weight of the initial oil shale charged into the autoclave was 10 gram. Conditions of hydrogenation are represented in Table 25.

Table 25. Experimental conditions

Parameter	Value
Time, h	1, 1.5, 2, 3
Tetralin:OM	1:1
Temperature, °C	360-400
Catalysts	DN-3100, KF-848, KF-1015
Catalyst-to-OM ratio	1:10

The effect of time on the yield of the products in "dry" pyrolysis, in the environment of tetralin without any catalyst, and adding the hydropurification catalyst KF-848 is depicted in (see Figure 1, Article VI).

It was found that the main advantage of the addition of tetralin occurs in an increase in the maximum yield of total extract to 86%, and in decrease in the minimum percentage of OM remaining in solid residue to 5.2%. At that, formation of the target product, maltenes is higher in the "dry" experiment than in tetralin. Addition of the catalyst KF-848 in tetralin environment moderates the decomposition rate of the initial shale and formation of the total extract.

The influence of temperature on the thermal treatment of oil shale in tetralin without catalyst and with the catalyst KF-848 is depicted in (see Figure 2, Article VI).

The results suggest that under the conditions studied, the addition of the catalyst KF-848 being the best in hydrogenation of heavy shale oil with molecular hydrogen (see Figure 9) rather decreases the yield of total extract in comparison with the test without any catalyst. The maximum extract yield under

two hours duration is at temperature 380 °C without any catalyst, and at 400 °C with the catalyst. But at that, the addition of the catalyst amplifies the effect of temperature on the increase in the yield of the target product, maltenes, and decreases the yield of organic solid residue at 360 °C.

As a result addition of tetralin as a hydrogen-donor in thermal decomposition of oil shale increases the raffinate yield and suppresses coke formation. In hydrogenation of the unstable TB about one third of tetralin per OM of oil shale, g/g, is expended and transformed into naphthalene. Addition of tetralin avoids the secondary decomposition and condensation of hexane soluble fraction, maltenes.

The main disadvantage of the tetralin addition is in the circumstances that tetralin and naphtalene formed incorporate into the raffinate and cannot be regenerated.

3.3. Hydrogenation of oil from flash pyrolysis

Flash pyrolysis of kukersite (50.1% OM) was carried out in a bench-scale fluidised bed unit at Technical Research Center of Finland (VTT). As a result of pyrolysis at 550 and 600 °C in the alumina sand bed with fluidising velocity 90 cm/s the maximum yield of oil obtained was 70% per OM.

Flash pyrolysis oil differs significantly from slow pyrolysis oil in Fischer Assay by high content of HPHet (63%) and by low content of AlHC. Flash pyrolysis oil is also characterized by high viscosity and density .

Three hydrogenation experiments of flash pyrolysis oil were carried out. Conditions of experiments and yields of the products are discribed in Tables 26 and 27.

Table 26. Experimental conditions

Parameter	Value
Time, h	2
H_2 initial pressure, atm	70
Temperature, °C	390-410
Catalyst	KF-848, KGU-950
Catalyst, % of oil	10

Table 27. The yield of flash pyrolysis oil hydrogenation products

Exp no.	Catalyst	Temperature, °C	Raffinate	Coke	Gas
1	KF848	390	56.3	12.4	31.3
2	KGU-950	390	50.3	19.6	30.1
3	KGU-950	410	42.4	26.7	30.9

The maximum yield of raffinate was achieved at 390 °C, 2 h, and initial pressure of H_2 70 atm with KF-848 catalyst and amounted 56.3% of the initial oil, and only 39.4% of kukersite OM.

The efficiency of hydrogenation of kukersite oil shale primary liquids was estimated by the yield of raffinate and, additionally by the ratio of HC (AlHC + MAHC + PAHC) to the heteroatomic compounds remained (LPHet + HPHet).

The group composition of raffinates is represented in Table 28.

Table 28. Chemical group composition of hydrogenated flash pyrolysis oil

	KF-848, 390 °C	**KGU-950, 390 °C**	**KGU-950, 410 °C**
HPHet	43.1	37.6	32.6
LPHet	19.5	21.3	22.6
PAHC	22.7	24.5	24.6
MAHC	4.3	5.8	8.7
AlHC	10.4	10.8	11.5
HC/Het	0.6	0.7	0.8

The maximum ratio HC/Het was 0.8 at 410 °C with KGU-950 catalyst.

If to compare the results obtained with results of retort oil hydrogenation, presented in Tables 8 and 9, it can be concluded that the yield of raffinate from retort oil surpasses that of raffinate from flash pyrolysis oil in two times calculated on OM basis. Besides the low yield, raffinate from flash pyrolysis oil was characterized by low content of HC and high that of heteroatomic compounds.

3.4. Hydrogenation of kukersite HO

Kukersite heavy oil fraction 360 °C+ (HO) was an industrial fraction produced at VKG (Viru Keemia Grupp), which makes about 50% of vertical retort oil.

The single- and two-step hydroprocessing was performed in a 500 cm^3 autoclave under the ranges of temperature 340-420 °C, duration 40-240 minutes, and the hydrogen initial pressure 62-88 atm. Catalysts, presented in Table 22, were added in the quantity of 10% per HO. About 50 grams of the initial or dephenolated HO were charged. The efficiency of the treatment was evaluated by yields of oil, gas, coke and water, by true boiling point curves, elemental composition, and group composition of the hydrogenated oil and by composition of the gases formed.

3.4.1. Phenolic compounds

The results concerning dephenolation of the diluted oil are represented in Tables 29 and 30.

Table 29. Extraction of total phenols from initial HO

HO dilution		Extraction with NaOH aqueous solution			
Solvent	HO:solvent (g/g)	NaOH solution:HO(g/g)	NaOH (%)	Yield of phenols (% from HO)
Diethyl ether	1:1	2:1	10	0[a]
Diethyl ether	1:1	4:1; 4:1; 4:1	2.5; 5; 10	17.0[b]
Gasoline	1:2	2:1; 1:1; 1:1	2.5; 5; 10	16.4[b]
Toluene	1:4	4:1; 4:1; 4:1	2.5; 5; 10	26.8[b] (25.98, 0.739 and 0.113)[c]
Benzene	1:4	5:1; 5:1; 5:1	2.5; 5; 10	26.9[b]

[a] Phases did not separate. [b] Total yield. [c] Yield in the subsequent steps.

Table 30. Extraction of the water soluble phenols

HO dilution		Extraction with water (W)	
Solvent	HO:solvent (g/g)	Water:HO (g/g)	Yield of phenols (% from HO)
None	–	3:1, three times	0.18
None	–	10:1, once	0.196
Benzene	1:4	10:1, once	0.11

The data obtained evident that the yield of total phenols extracted depends on the solvent applied for dilution. The two phases were not separated when diethyl ether was added. The yield of phenols reaches 17% at higher ratios of the alkali solution using diethyl ether or the light fraction of shale oil, called gasoline. When benzene or toluene was used the yield reached 26.9%. Probably, hydrogen bonding arises between the molecules of oxygen containing solvents and HO. So, distribution of the phenols is declined to the organic solutions, and only the anionic phenolates with shorter alkyl radicals can be extracted into the alkali water solution.

3.4.2. Hydroprocessing of initial and dephenolated HO

The hydroprocessing conditions tested and the yields of the products are given in Table 31.

Table 31. Hydroprocessing conditions and yields of the products

Test no.	HO	Catalyst	T, °C	Time, min	H$_2$ pressure (MPa)			Yields (% from the material)			
					Initial	Working	Residual	Raffinate	Gas	Coke	Water
1	Dephenolated	GO-30-7	400	60	7.7	17.3	5.0	75.8	17.4	3.2	3.6
2	Dephenolated	GO-30-7	430	60	8.8	22.5	6.2	46.4	36.6	15.1	1.9
3	Dephenolated	GO-30-7	380	60	7.0	16.0	5.5	75.0	19.8	5.2	below sensitivity
4	Dephenolated	GO-30-7	400	240	6.4	16.0	4.5	58.9	29.8	10.0	1.3
5	Dephenolated	DN-3100TL	400	60	6.5	16.5	5.4	60.2	25.7	12.8	1.3
6-I	Initial	DN-3100TL	380	120	6.3	13.2	3.5	90.5	6.1	1.2	2.2
6-II	Raffinate and solid products from 6-I	DN-3100TL + GO-30-7	400	60	7.5	17.0	4.8	93.8	3.5	0.9	1.8
6I+II								84.9[a]	9.3[a]	2.0[a]	3.8[a]
7-I	Dephenolated	KGU-950	360	60	6.2	13.3		89.5	7.6	1.5	1.4
7-II	Raffinate from 7-I	GO-30-7	420	60	6.4	14.6	4.6	91.6	4.8	1.4	2.2
7-I+II								82.0[a]	11.9[a]	2.7[a]	3.4[a]
8-I	Initial	DN-3100TL	360	60	6.4	13.3	4.6	n. d.	n. d.	n. d.	n. d.
8-I+II	Raffinate and solid products from 8-I	DN-3100TL GO-30-7	400	40	6.5	15.0	4.7	83.9[a]	10.4[a]	1.6[a]	4.1[a]
9-I	Initial	KGU-950 GO-30-7	360	60	6.4	13.3	4.6	n. d.	n. d.	n. d.	n. d.
9-I+II	Raffinate and solid products	KGU-950 GO-30-7	400	40	6.5	15.4	4.6	n. d.	n. d.	n. d.	n. d.

	from 9-I									
9-I+II+III	Raffinate and solid products from 9-II	KGU-950 GO-30-7	340	60	6.5	15.6	6.0	86.5[a]	9.8[a]	1.3[a]	2.4[a]
10	Initial + gasoline fraction (1:1)	DN-3100TL	380	120	6.3	13.5	3.1	90.6	6.8	0.9	1.7
11-I	Initial	DN-3100TL +GO-30-7	340	40	7.1	15.5	–	n. d.	n. d.	n. d.	n. d.
11-I+II	Raffinate and solid from 11-I	DN-3100TL GO-30-7	380	40	7.1	14.9	5.4	95.7[a]	2.6[a]	0.9[a]	0.8[a]
13	Initial	No	400	120	0	5.5	0.9	34.5	25.0	39.3	1.2
14-I	Initial	KF-848	380	60	7.0	14.8	4.5	90.0	7.9	0.7	1.4
14-II	Raffinate 14-I	KF-1015	400	60	6.5	13.9	4.8	83.6	12.9	1.9	1.6
14 I+II								75.2[a]	19.6[a]	2.4[a]	2.8[a]
15-I	Initial	KF-848	380	60	7.3	15.0	4.8	90.8	7.3	0.5	1.4
15-II	Raffinate from 15-I	KC 3210	380	40	6.3	13.3	5.6	92.8	5.3	1.9	traces
15 I+II								84.3[a]	12.1[a]	2.2[a]	1.4[a]
16	Initial	No	420	90	7.5	20.6	6.8	54.0	28.9	16.5	0.6

[a] total yield of the product from the initial HO in the step I; n. d. – not determined because the temperature was regulated without opening of the autoclave

41

According to Table 31, the highest total yield of raffinate (95.7%) was obtained in the two stage experiment 11-I+II where the mix of universal catalyst DN-3100TL and the hydrocracking catalyst GO-30-7 was used in the first stage at 340 °C, and in the second stage the temperature was increased to 380 °C. In the both stages the duration was 40 minutes and the initial hydrogen pressure 7.1 MPa. The total raffinate yield was also high in the second stage of the experiments 6-II, 15-II, and 7-II (93.8, 92.8 and 91.6% from the first stage oil) loosing 3.5-8.4% as gas, coke and water.

The test numbers and according conditions are applied for characterization of the raffinates obtained in parts 3.4.3-3.4.6.

3.4.3. Fractional composition of raffinates

Fractional composition of the raffinates obtained under various conditions of the hydroprocessing is depicted in Figure 5.
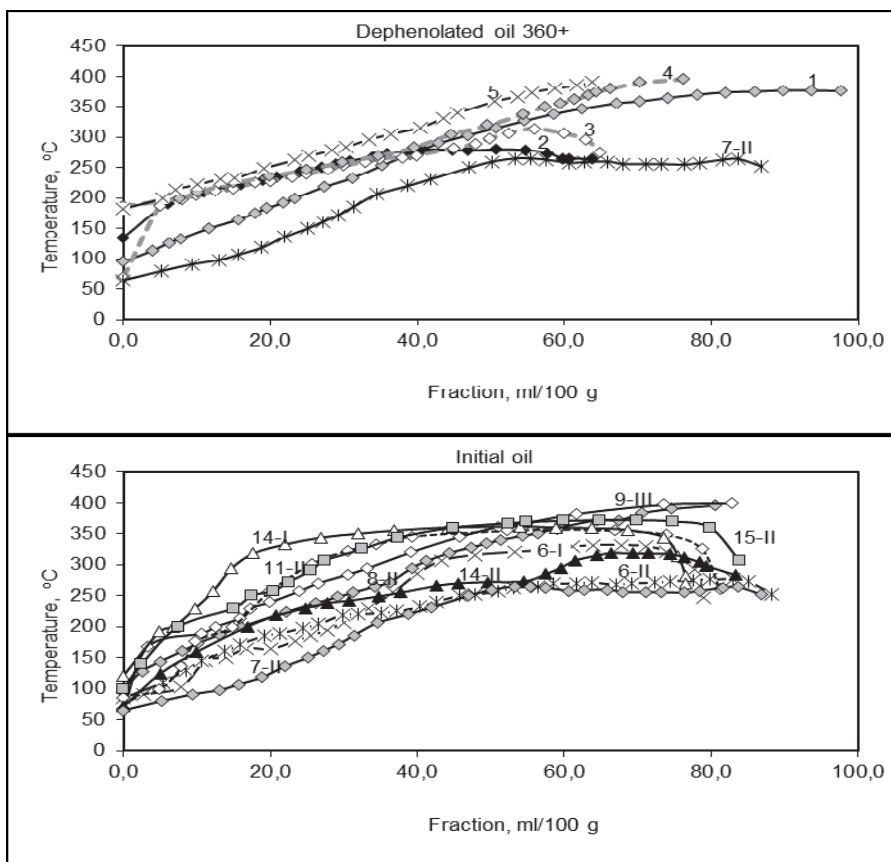
Figure 5. Fractional composition of the raffinates obtained at hydroprocessing of the dephenolated and initial HO under conditions given in Table 29

42

The distillation curves show principal similarity when the dephenolated and initial HO were used as feedstocks. As it can be expected, the cracking catalysts GO-30-7 (experiments 4, 6-II, 7-II, and 11-II) and KF-1015 (experiment 14-II) obviously enhanced the formation of the lower boiling fractions in comparison with the hydropurification catalysts applied in the first stage (I). The results obtained revealed that in the distillation most of the raffinates decline to secondary thermal decomposition, especially in the cases without dephenolation (Figure 5).

The distribution of the raffinates between the fractions with boiling range 200 °C-, 200-275 °C and 275-360 °C is depicted in Figure 6.
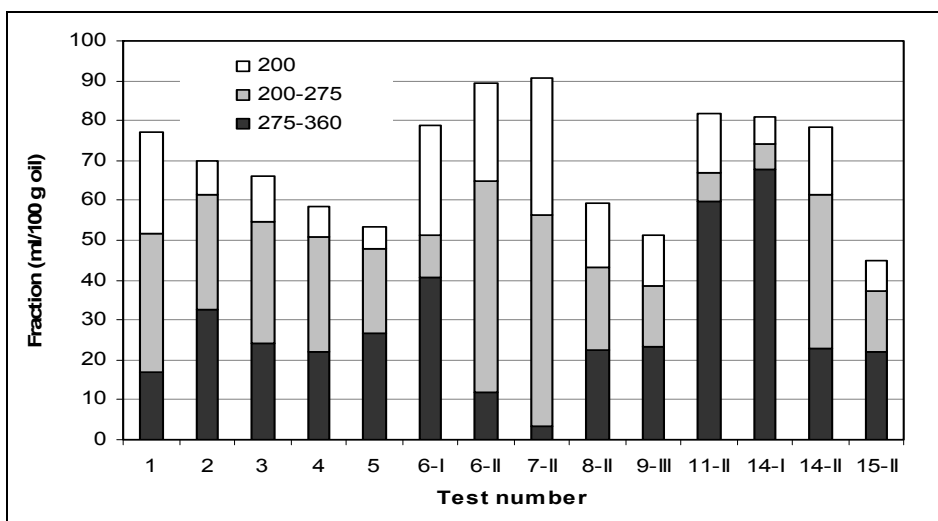
Figure 6. Distribution of the raffinates between boiling fractions under conditions given in Table 29.

Yields of the main fractions of the raffinates from the dephenolated and initial HO, and the iodine numbers are presented in Table 32.

According to Figures 5 and 6 and Table 32, the most wanted raffinate fraction, kerosene (200-275 °C), prevails (53%) in the raffinates 6-II and 7-II where the secondary decomposition of the raffinates at fractional distillation has already begun near 250 °C. The highest share of the heavier fraction, 275-360 °C, was obtained in the tests 14-I and 11-II where the secondary cracking was delayed close to 360 °C. According to Table 32, the highest share of the fraction 200-360 °C was formed in the experiments 14-I and 14-II, 11-II and 6-II (72.7 and 64.6, 59.7 and 62.6 g/100g) where the hydropurification catalyst KF-848 and the mix of catalysts consisting of the universal catalyst DN-3100TL and the hydrocracking catalyst GO-30-7 were applied.

Table 32. *Yield of distillation fractions and iodine number of the raffinates (g/100 g initial HO)*

Test No	Yield					Iodine number
	200 °C–	200-360 °C	360 °C–	360 °C+	Gas	
1	21.2	49.7	70.9	25.0	4.1	9.7
2	7.0	59.3	66.3	30.7	3.0	n. d.
3	10.3	55.0	65.3	29.6	5.1	n. d.
4	6.1	49.4	55.5	41.5	3.0	n. d.
5	4.4	46.3	50.7	46.8	2.5	n. d.
6-I	22.8	49.4	72.2	25.4	2.4	21.6
6-II	20.1	62.6	82.7	16.0	1.3	5.6
7-II	27.9	54.5	82.4	15.0	2.6	18.7
8-II	13.2	41.8	55.0	42.8	2.2	18.3
9-III	10.3	37.2	47.5	48.4	4.1	21.5
10	37.2	46.9	84.1	9.9	6.0	23.3
11-II	20.5	59.7	80.2	15.3	4.5	35.4
14-I	5.7	72.7	78.4	16.1	5.5	34.3
14-II	13.8	64.6	78.4	18.3	3.3	14.3
15-II	5.3	33.5	38.8	56.5	4.7	23.4

3.4.4. Group composition of raffinates

The results of the TLC of the representative raffinates are represented in Table 33.

Table 33. *Group composition of the raffinates, %*

Compound group	Initial HO	6-II	9-III	11-II	14-I	14-II
AlHC	1.8	16.1	13.2	7.4	3.9	12.7
MAHC	2.9	11.2	10.4	4.5	5.2	7.0
PAHC	14.5	35.6	35.9	21.0	21.8	33.1
LPHet	46.8	24.3	22.8	35.8	37.5	25.3
HPHet	34.0	12.8	17.7	31.3	31.6	21.9
HC/Het	0.23	1.70	1.47	0.49	0.45	1.12

The data explain that under the best conditions (6-II) hydroprocessing can increase the content of AlHC from 1.8 to 16.1% whereas the total content of HC is increased from 19.2 to 62.9%, and the content of undesirable LPHet and

HPHet being 46.8 and 34.0% in the initial HO decrease to 24.3 and 12.8% in raffinate. The ratio of HC/Het is increased from 0.23 to 1.70.

3.4.5. Secondary phenols and asphaltenes in raffinates

The total phenols after hydroprocessing of the dephenolated and initial HO were extracted with 5% NaOH (1:5) from the raffinates diluted with benzene (1:1), and thereafter re-extracted from the acidified water phase with diethyl ether. The results are represented in Table 34.

Table 34. Total phenols in raffinates, %

Test number	1	6-II	7-II	8-II	8-II (360+)[a]	11-II	14-I	14-II	15-I
Phenols in the initial HO (%)	0	26.8							
Phenols in the raffinate (%)	6.73	3.88	3.57	3.23	9.06	24.8	29.6	7.61	31.7
Hydrogenation temperature (°C)	400	400	420	400	360	380	380	400	380

[a]– Distillate fraction 360 °C+ of oil 8-II

The data in Table 34 evident that hydroprocessing can increase the content of phenols, as it occurred in the test 1 with the dephenolated initial HO and in the first stages of the tests 14 and 15 where the hydropurification catalyst KF-848 was applied at 380 °C. The content of phenols is significantly decreased during the next stage of the experiments 6, 7, and 8 where the universal catalyst DN-3100TL (8-I) or the hydrocracking catalyst GO-30-7 (7-II) were used at temperatures 400–420 °C. Noteworthy is that more than 90% of the initial phenols were not decomposed at hydrogenation in the presence of the mix of the latter catalysts at 380 °C (11-II). The results obtained suggest an essential role of temperature on the decomposition of phenols.

According to Table 30, the content of water soluble phenols in the initial HO was between 0.11-0.20%, depending on their isolation conditions. As shown in Table 35, the content of water soluble phenols extracted three times with water in ratio 1:10 is increased for some scores of times in the stage of hydropurification (14-I and 15-I) whereas in the cracking stage (7-II, 8-II, 11-II) decomposition of the newly formed phenols takes place.

Table 35. Water soluble phenols in raffinates, %

Test number	7-II	8-II	11-II	14-I	15-I
Water soluble phenols	0.26	0.16	0.57	4.90	4.17

Dephenolation before hydroprocessing, common for the shale oil lower fractions, cannot be suggested for HO, because a lot of HC would be wasted as side chains of the high molecular alkylphenols not having any marketable value yet.

3.4.6. Ultimate analysis of HO and raffinates

The results of the ultimate analysis of HO and selected raffinates are represented in Table 36.

Table 36. Elemental composition, wt.%

Oil sample	C	H	N	O	S
HO	84.11	8.16	0.20	6.80	0.73
Dephenolated HO (after separation of 27% as phenols)	83.66	8.42	0.21	7.07	0.64
Dephenolated HO (after separation of 17% as phenols)	82.74	8.14	0.21	8.31	0.60
8-I	86.02	8.70	0.18	4.85	0.25
8-II	89.28	8.74	0.19	1.66	0.13
9-III	86.68	9.07	0.21	3.96	0.08
14-I	86.36	8.84	0.14	4.33	0.33
14-II	88.35	8.78	0.11	2.57	0.19

The data in Table 36 evident that dephenolation of HO increases a little the atomic ratio of H/C (from 1.16 to 1.21 or 1.18), but the contents of oxygen and nitrogen increase either, and the sulfur content decreases from 0.73 to 0.64 and 0.60%.

Hydrogenation of the initial HO reveals that the most effective removal of the heteroatoms has taken place in the experiment 8-II, where the mix of universal catalyst DN-3100TL and the hydrocracking catalyst GO-30-7 were applied at 400 °C. At that, the content of sulphur has decreased by 82%, the content of oxygen by 76%, but the content of nitrogen only by 5%. The highest removal of sulphur, by 89%, was obtained in the experiment 9-III using the mix of KGU-950 and GO-30-7.

It has been found that more than 70% of HO boiling above 360 °C can be transformed into raffinates boiling below 360 °C by two-stage (360 and 400-420 °C) hydroprocessing (H_2 64-75 atm) in the presence of various Mo–Co and/or –Ni catalysts: KGU-950, GO-30-7, DN-3100TL, KF-848, KF-1015 and KC-3210. Characteristics of the hydrogenated products depend on the co-effects of the pyrolysis conditions, temperature, time and catalysts.

3.5. Kukersite thermochemical dissolution followed by catalytic hydrogenation

3.5.1. Thermochemical dissolution method as an alternative to traditional retorting

3.5.1.1. The effect of solvent type on the yield of the primary liquid product

A variety of experiments of kukersite thermochemical dissolution was carried out to find out the most effective solvent for kerogen transformation into primary liquid product. Table 37 represents the results of thermochemical dissolution of kukersite (35.8% OM) in autoclave using different solvents under different conditions. Kukersite-to-solvent ratio was 1:3.

Table 37. Yield of products at different conditions

Solvent	Temperature, °C	Time, h	Yield, % OM		
			Liquid	Solid	Gas
Ethanol	360	1	80.3	11.7	8.0
Ethanol	360	3	97.9	10.2	n. d.
Benzene	360	3	78.9	13.6	7.5
Water + benzene	360	3	80.9	6.9	12.2
Benzene	360	2	75.3	20.1	4.6
Benzene	380	2	58.8	14.2	27
Benzene	400	2	50.8	16.1	33.1
Water	390	4	65.8	29.2	5.0-

High liquid yield in case of ethanol is a result of ethanol decomposition fragments incorporation into products composition. Excluding ethanol, the maximum yields were achieved using benzene or benzene + water as solvents.

FT-IR spectra of liquids obtained from kukersite thermochemical dissolution using different solvents (benzene, ethanol, water and benzene + water) are represented in Figure 7.

In general, FT-IR spectra of liquids obtained in the medium of different solvents are relatively similar and do not have particular differences. All spectra have common absorption bands at 2380, 1460, 2850, 2930 and 2960 cm^{-1}, and at 840 and 1600 cm^{-1} belonging to CH_3, CH_2 and CH groups in aliphatic chains and aromatic ring systems of different degree of condensation and substitution. Absorption bands with a maximum at 3450 cm^{-1} indicate OH groups. And it is more intensive in case of water + benzene as a solvent. Absorption at 1700-1720 cm^{-1} refers to C=O group. In the case of ethanol liquid one can notice an increase in absorptions at 2930 and 2960 cm^{-1} and appearance of narrow absorption at nearby 1740 cm^{-1}, the former absorptions belonging to methylene and terminal methyl groups in mainly cycloalkanes and aliphatic heterocompounds, and the latter being a result of the incorporation of acetaldehyde into liquid composition.
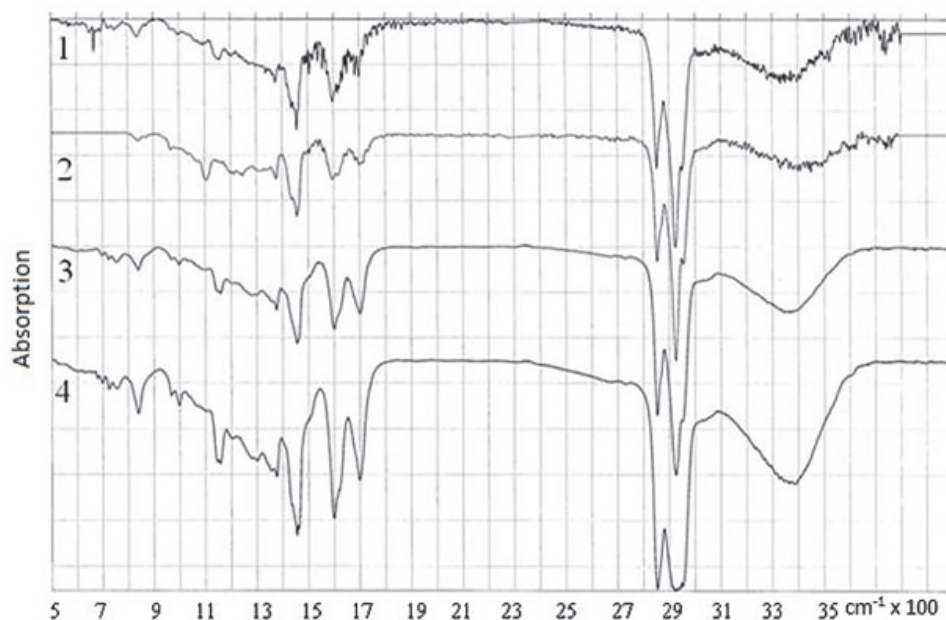
Figure 7. FT-IR spectra of liquids obtained from kukersite as a result of thermochemical dissolution with using water+benzene (4), water (3), ethanol (2) and benzene (1) as a solvent

So, it can be proposed that the liquid product obtained represents partially decomposed TB, a mixture of thermobitumen and oil (TBO).

3.5.1.2. The effect of temperature on the yield of TBO

Table 38 represents the results of thermochemical dissolution of K-90 in autoclave with water + benzene (1:1) as a solvent during 1 hour. Oil shale-to-solvent ratio was 1:2.

Table 38. Yield of products from K-90+water+benzene at different temperatures

Products, % OM	370 °C	380 °C	390 °C	400 °C
TBO	78.1	82.5	91.1	90.2
Solid	17.8	13.4	3.2	3.3
Gas	4.1	4.1	5.7	6.5

It is seen that the maximum yield of TBO was obtained at 390 °C (duration 1 h).

Table 39 represents the results of thermochemical dissolution of kukersite with 50.5% of OM content in autoclave at different temperatures using benzene as a solvent during 3 hours. Oil shale-to-solvent ratio was 1:3.

Table 39. Yield of products from kukersite+benzene at different temperatures

Products, % OM	340 °C	360 °C	390 °C	420 °C
TBO	48.6	91	81.3	42.8
Solid	48.2	4.4	13.5	49.5
Gas	3.2	4.6	5.2	7.7

For benzene as a solvent the maximum yield of TBO (91.0% on OM basis) was achieved at 360 °C (duration 3 h).

Table 40 represents the results of thermochemical dissolution of kukersite with 50.5% OM in autoclave at different temperatures using water as a solvent (duration 3 h). Oil shale-to-solvent ratio was 1:3.

Table 40. Yield of products from kukersite+water at different temperatures

Products, % OM	340 °C	360 °C	390 °C	420 °C
TBO	43.5	50.2	72.4	41
Solid	52.4	45	22.2	50.9
Gas	4.1	4.8	5.4	8.1

The maximum TBO yield using water as a solvent was achieved at 390 °C, but if to compare with benzene and benzene+water solvents, it can be seen that the maximum TBO yield in water is lower.

3.5.1.3. The effect of time on the yield of TBO

Table 41 represents the results of thermochemical dissolution of K-90 in the autoclave at 360 °C with benzene as a solvent. Oil shale-to-benzene ratio was 1:3.

Table 41. Yield of products

Duration, h	Yield, % OM		
	TBO	Solid	Gas
2.5	81.1	12.3	6.6
3	85.6	12.5	1.9
3.5	81.5	12.0	6.5
3.25	81.4	13.6	5.0

One can see that the maximum yield of TBO was obtained during 3 hours at 360 °C using benzene as solvent.

3.5.1.4. The influence of OM content on the yield of TBO

Figure 8 shows the results of thermochemical dissolution of kukersite with different OM content using benzene as a solvent (1:3, 360 °C, 3 h).
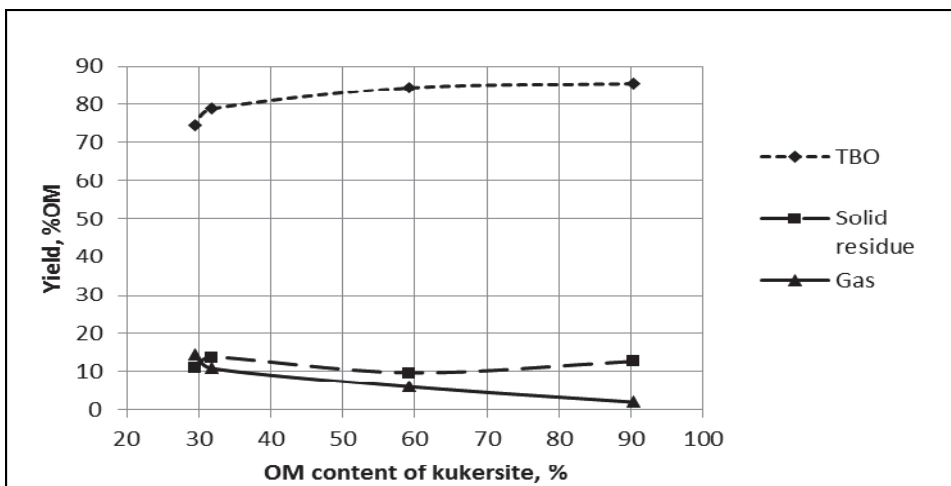
Figure 8. Yield of products from kukersite with different OM content

It can be seen that the higher the content of OM, the higher the yield of TBO.

It was shown that as a result of thermochemical dissolution of kukersite oil shale containing different contents of OM, more than 80% of kerogen can be transformed into TBO.

3.5.1.5. Changes in composition of TBO during storage

Varying kukersite samples thermochemical dissolution conditions (solvent type, temperature, duration) enables to obtain TBO in yields 86-91% on OM basis. The maximum yield of TBO using benzene as a solvent was achieved at 360 °C during 3 hours with oil shale-to-solvent ratio 1:3, and using benzene+water as a solvent at 390 °C during 1 hour with oil shale-to-solvent ratio 1:2.

Changes in TBO chemical composition during storage were studied.

In all the experiments 4.0 g of kukersite, containing 40.2% OM was put into a 20 cm^3 micro-autoclave and submitted to the thermobitumenization without any solvent. The solid residue was not removed from TBO to avoid any loss of the lighter fractions during evaporation of the organic solvents applied. The samples were weighted in open and closed tubes kept at room temperature and in a refrigerator. After different durations of the storage, the solid pyrolyzed product was extracted exhaustively in Soxhlet extractor successively with hexane, benzene and tetrahydrofurane. The mass of the corresponding extracts – maltenes, asphaltenes and pre-asphaltenes, was found from the decrease in the sample mass at the extraction after drying of the corresponding residue.

Distribution of the pyrolysis products between the three phases: gas, TBO and organic solid residue are depicted in (see Figure 1, article II). It can be seen that the experimental results obtained in different series fluctuate. Nevertheless,

a continuous increase in the yields of volatiles and solid residue on account of the target product, TBO, is evident at ageing. The mass of pyrolysates consisting of TBO and solid residue decreased at ageing.

The results obtained extracting the pyrolysates after different storage duration in Soxhlet apparatus subsequently with hexane (maltenes), benzene (asphaltenes) and tetrahydrofurane (pre-asphaltenes) are represented in (see Figure 4, article II). The experimental points in the figure show again diffusive clouds of the extract yields, probably because the pyrolysates from different series were applied for extraction. Yet, the results prove that the decrease in TBO yield described above by curve 1 in previous figure is compiled from decreases in the yield of both maltenes and asphaltenes, and the yield of solid residue increases due to the increase in the yield of preasphaltenes. It can be concluded that a condensation of the both TBO fragments, maltenes and asphaltenes, takes place at ageing.

The experimental results above have revealed that at ageing of the pyrolysate obtained at low temperature pyrolysis of kukersite in an autoclave an aggregation of the compounds takes place that shifts maltenes and asphaltenes to the preceding adjacent class – pre-asphaltenes and solid residue, and the content of AlHC, MAHC and PAHC soluble in hexane decreases and those soluble in benzene increases.

3.5.2. Hydrogenation of TBO

Obtained TBO was submitted to hydrogenation using the three catalysts (Table 22) found the most effective in hydrogenation of HO in part 3.4. Different TBO-to-catalyst ratio was tested in order to observe how catalyst and its content influence on the yield of raffinate and HC content. Results of experiments conducted at 390 °C and 40 min are represented in Figure 9.
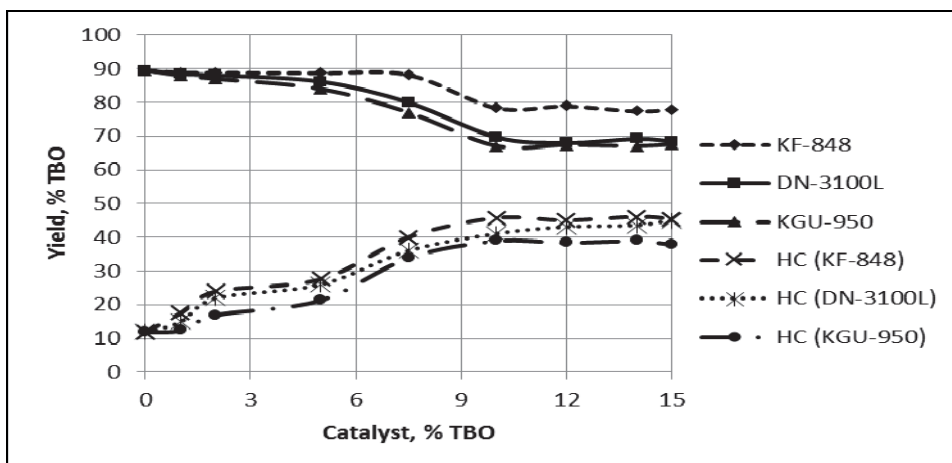

Figure 9. Dependence between concentration of various catalysts, and the yield of raffinates of TBO and HC content in raffinates

Understandable, that both replacement of heteroatoms with hydrogen in hydropurification and gas formation in hydrocracking should result in decrease of the yield of raffinate. Figure 9 shows that the yield of raffinate decreases from 3% of catalyst content and attains a steady state at 10%. The maximum HC content is obtained in the presence of 10% catalyst also. It is the minimal amount of catalyst, when the content of HC does not decrease.

The influence of time on the raffinate yield was studied in the presence of 10% of KF-848 catalyst. The results are depicted in Figure 10.
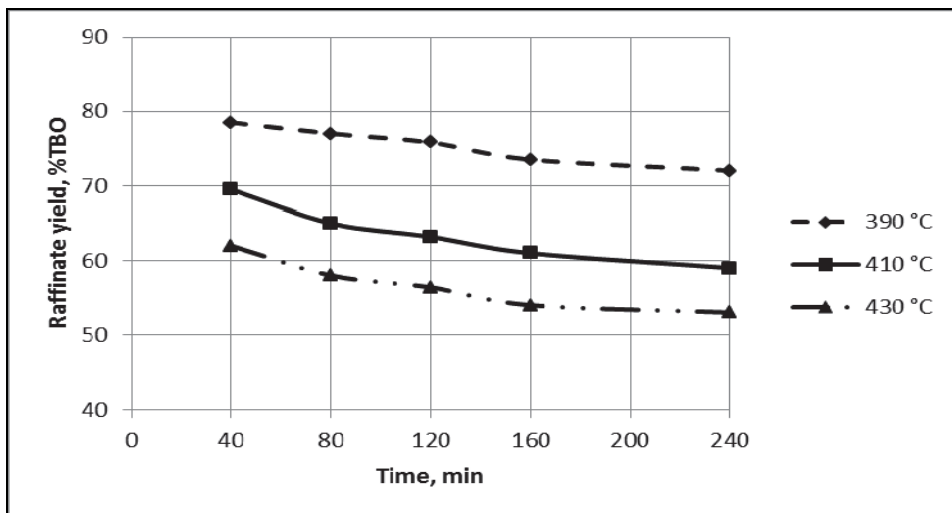
Figure 10. The effect of hydrogenation time on raffinate yield at various temperatures

With increase in time and temperature the decrease in raffinate yield was observed.

Figure 11 shows the influence of hydrogenation temperature on the yield of raffinate and HC content. It can be seen that the rise of temperature decreases the yield of raffinate, but at the same time increases the content of HC. Increase in time has insignificant influence on the yield of raffinate and increases HC content.
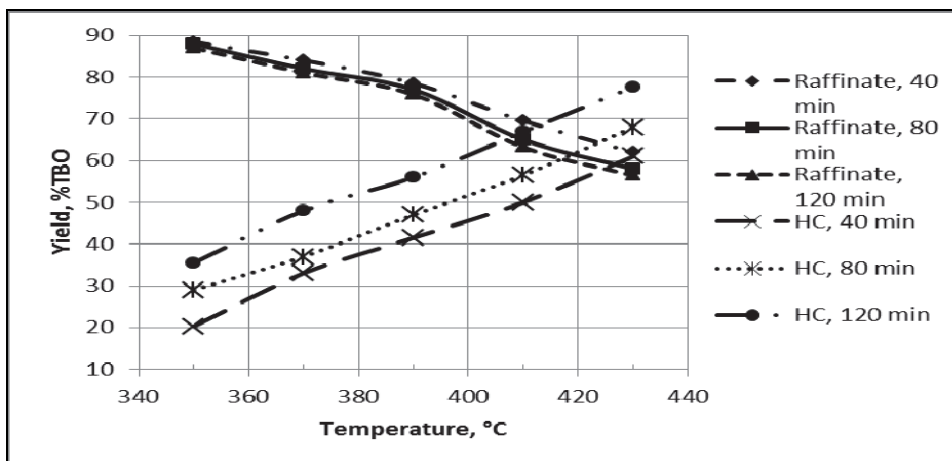
Figure 11. The effect of temperature on raffinate yield and HC content in raffinate at varied time of hydrogenation

The characterization of changes in the composition of functional groups of raffinate obtained from hydrogenation at various temperatures was issued from calculated interpretation of infrared spectra and represented in Table 42.

It can be followed that hydrogenation decreases the absorption intensities at 1600 and 1700 cm^{-1} and with elevating the initial temperature of hydrogenation the content of polar carbonyl and carboxyl groups decreases.

Table 42. Characterization absorption intensities of raffinates at different temperatures by FT-IR spectra (duration 40 min, H$_2$ pressure 40 atm)

Frequency (cm^{-1}) and corrresponding functional group	340 °C	360 °C	380 °C	400 °C
720 (CH$_2$)$_n$	0.12	0.16	0.15	0.20
745 (CH$_{ar}$)	0.35	0.32	0.33	0.36
815 (CH$_{ar}$)	0.30	0.24	0.25	0.27
880 (CH$_{ar}$)	0.26	0.20	0.17	0.20
1380 (CH$_3$)	0.65	0.63	0.58	0.61
1600 (C=C)$_{ar}$	0.75	0.71	0.58	0.56
1700 (C=O)	0.40	0.39	0.22	0.20
2930 (CH$_2$)	1.28	1.55	2.06	2.09
2960 (CH$_3$)	1.16	1.27	1.78	1.84
3020 (CH$_{ar}$)	0.37	0.33	0.39	0.45
3055 (CH$_{ar}$)	0.39	0.35	0.39	0.43
3400 (OH)	0.40	0.41	0.42	0.40
2930/2960	1.11	1.23	1.16	1.04
3050/2930	0.30	0.22	0.19	0.26
1160 (C–O)	0.47	0.43	0.33	0.39
2850 (C-O-C)	1.05	1.14	1.47	1.43

Heteroelemental composition of initial kerogen, intermediate TBO and raffinate are compared in Figure 12.
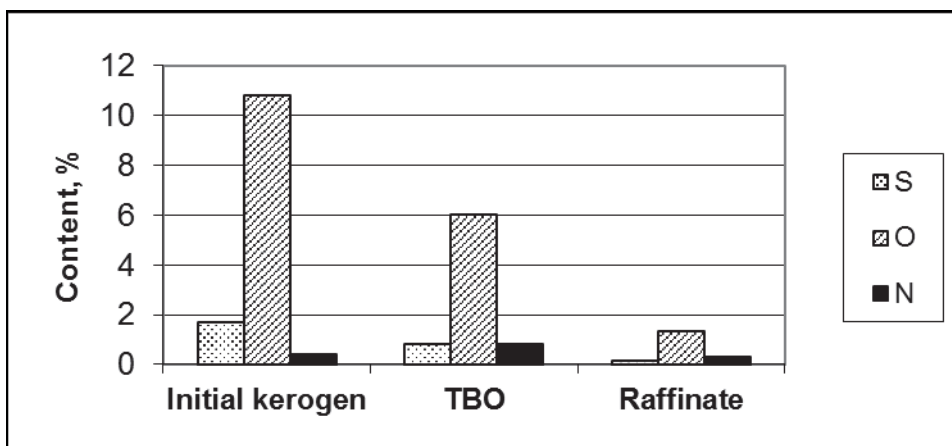

Figure 12. Comparison of heteroelemental composition of initial kerogen, TBO and raffinate

Significant decrease in O, S and N content can be observed in raffinate. Hydrogenation of TBO resulted in 59.2% removal of heteroelements. The decrease of oxygen content amounts to 77.5%, that of sulphur to 81% and that of nitrogen to 62.5% compared with their content in TBO.

The individual composition of raffinates was analyzed by GC-MS. Table 43 contains the compounds identified in the fraction of MAHC, and Table 44 those of AlHC.

Table 43. Compounds in raffinate MAHC fraction (see chromatogram in Appendix A, Figure 1). Reliability not lower than 80%

Peak	Name	Area %
1	Ethylbenzene	0.3
2	m-Xylene	0.2
3	p-Xylene	0.4
4	Isopropylbenzene	0.1
5	Propylbenzene	0.6
6	p-Ethyltoluene	1.9
7	o-Ethyltoluene	3.0
8	m-Ethyltoluene	1.4
9	Trimethylbenzene	0.7
10	Indane	2.7
11	o-Propyltoluene	2.0
12	p-Propyltoluene	1.7
13	m-Propyltoluene	2.0
14	1-methylindane	5.8
15	4-Methylindane	4.2
16	5-Methylindane	7.0
17	Tetraline	11.2
18	Naphtalene	4.3
19	Dimethylindane	3.3
20	2-Ethylindane	2.9
21	Dimethylindane	3.9
22	2-Methyltetraline	2.4
23	Methyltetraline	1.9
24	1-Ethylindan	2.8
25	4,7-Dimethylindane	1.8
26	n-Hexylbenzene	1.5
27	5-Methyltetralin	6.8
28	Methylnaphtalene	10.4
29	2-Methylnaphtalene	2.3
30	6-Ethyltetralin	1.4
31	n-Heptylbenzene	1.5
32	Dimethylnaphtalene	3.9
33	Dimethylnaphtalene	0.7
34	Dimethylnaphtalene	0.5
35	6-Propyltetralin	0.4
36	1-Cyclohexylethylbenzene	0.5
37	1-Propylnaphtalene	1.1
38	Trimethylnaphtalene	0.9
		100

MAHC fraction is represented mostly as alkyl derivatives of benzene (5.2%), toluene (12%), indane (34.4%), tetralin (24.3%) and naphtalene (24.1%).

Table 44. Compounds in raffinate AlHC fraction (see chromatogram in Appendix A, Figure 2). Reliability not lower than 95%

Peak	Name	Area %
1	n-Nonane	1.3
2	n-Decane	7.9
3	n-Butylcyclohexane	0.4
4	1,4-Dimethylcyclooctane	0.8
5	3,5-Dimethyldecane	0.6
6	3,7-Dimethyldecane	0.4
7	n-Undecane	13.1
8	Pentylcyclohexane	0.6
9	Hexylcyclopentane	1.2
10	4,8-Dimethylundecane	0.4
11	3,7-Dimethylundecane	0.7
12	n-Dodecane	13.3
13	n-Hexylcyclohexane	0.6
14	1,2-Diethylcyclooctane	1.3
15	n-Tridecane	12.2
16	n-Heptylcyclohexane	0.7
17	n-Octylcyclopentane	0.9
18	n-Tetradecane	12.2
19	n-nonylcyclopentane	1.9
20	n-Pentadecane	10.5
21	n-Decyclopentane	1.1
22	n-Hexadecane	7.9
23	n-Decyclohexane	0.5
24	n-Heptadecane	4.8
25	n-Octadecane	1.6
26	n-Nonadecane	1.0
27	n-Eicosane	0.7
28	n-Heneicosane	0.5
29	n-Docosane	0.4
		100

Aliphatic and alicyclic HC were formed. In homologous series n-alkanes C_9-C_{22} (87.4%) were identified in the composition of raffinate. Alicyclic HC (12.6%) were identified as cyclopentane, cyclohexane and cyclooctane derivatives. Unsaturated HC were not found.

Table 45 shows that the elemental composition and some physical properties of the raffinate obtained agree with the corresponding data of natural petroleum.

Table 45. Elemental composition and physical properties of natural petroleum [49] and raffinate obtained

	Natural petroleum	Raffinate
Hydrocarbons, %	79-88	79
Oxygen, %	0.02-3.6	1.35
Sulphur, %	0.1-7	0.15
Nitrogen, %	0.1-1.7	0.3
Specific weight, kg/m3	730-1050	930
Kinematic viscosity, cSt, at 20 °C	10-300	11.3
Flash point, °C	35-120	118

3.5.2.1. Hydrogenation of maltenes and asphaltenes

Obtained in maximal yield TBO was divided into maltenes and asphaltenes in yields 46 and 54%, respectively and were analyzed by FT-IR spectroscopy. The spectra are represented in Figure 13.
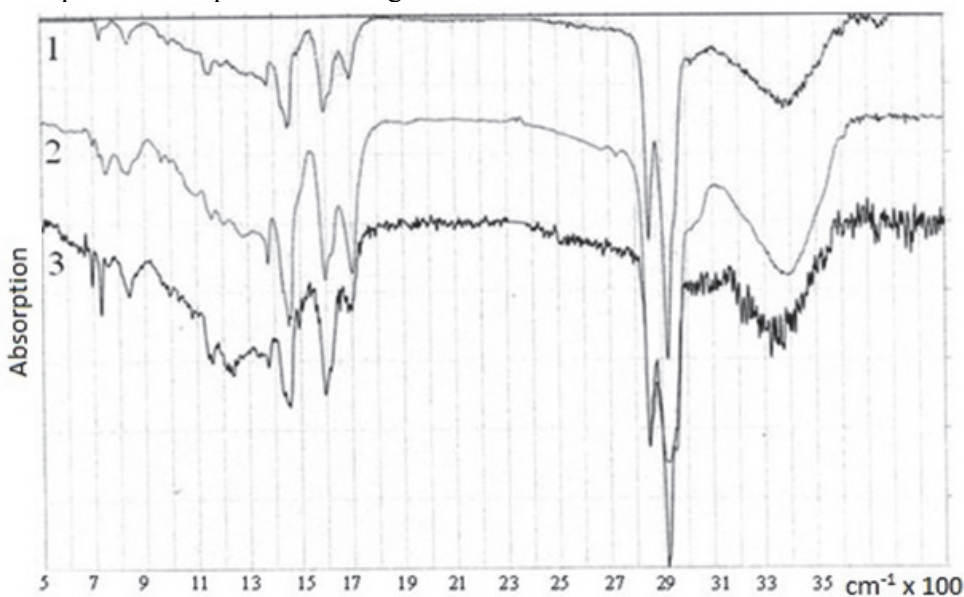
Figure 13. FT-IR spectra of TBO (3), maltenes (2) and asphaltenes (1)

Every spectrum displays absorption at 725, 1400 - 1380, 1460, 2860, 2930 and 2960 cm^{-1} caused by methyl and methylene groups in aliphatic chains, and absorptions at 850, 1080, 1600 and at nearby 3000 cm^{-1} characteristic for aromatic compounds. Absorption at 1600 cm^{-1} confirms the presence of benzene nucleus. The most part of oxygen can be found in carbonyl and hydroxyl groups. The absorptions at 1700-1720 cm^{-1} (C=O) and 3230-3500 cm^{-1} (OH) are clearly distinguishable. Besides, there is less intensive absorption at 1150 cm^{-1}, which refers to oxygen-carbon bond in the phenol molecule.

Maltenes and asphaltenes were hydrogenated separately with KF-848 catalyst (1:10) during 2 hours and initial H_2 pressure 7 MPa at different temperatures. Figure 14 and 15 show the yield of products from hydrogenation of maltenes and asphaltenes and content of HC in raffinate.
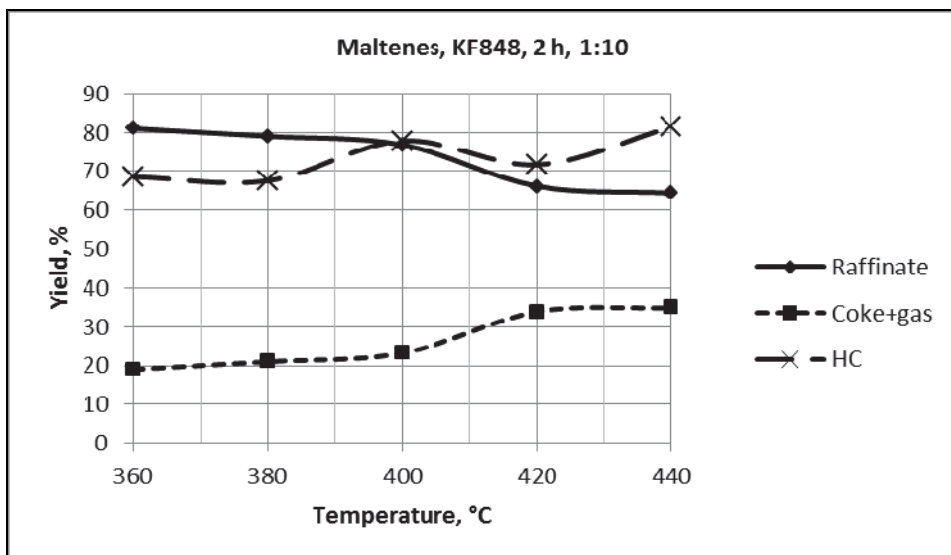
Figure 14. Yield of products from hydrogenation of maltenes and HC content in raffinate
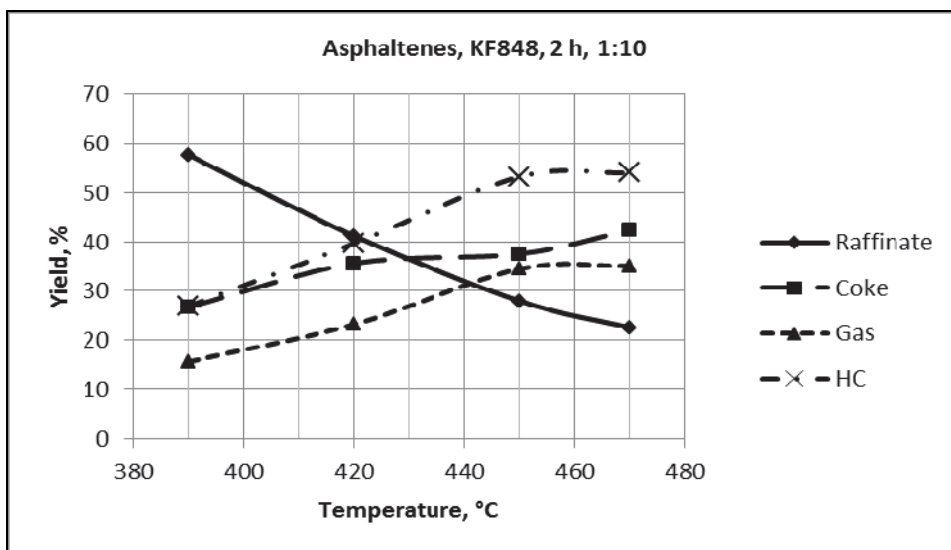

Figure 15. Yield of products from hydrogenation of asphaltenes and HC content in raffinate

As in the case of hydrogenation of initial TBO it can be seen that with the temperature increasing the yield of raffinate decreases, but the content of HC in

raffinate increases. At that, upgrading of asphaltenes of TBO was not satisfactory and needs optimization in future.

Changes in elemental composition of hydrogenated maltenes and asphaltenes depending on hydrogenation temperature are represented in Table 46.

Table 46. Heteroelemental composition of maltenes and asphaltenes raffinates

Maltenes raffinate	360 °C	380 °C	400 °C	420 °C	440 °C
Content, %					
S	0.15	0.15	0.15	0.1	0.08
O	11.55	10.65	17.65	9.6	3.42
N	0.2	0.1	0.2	0.3	0.7
S+O+N	11.9	10.9	18	10	4.2
Asphaltenes raffinate	390 °C	420 °C	450 °C	470 °C	
Content, %					
S	0.26	0.24	0.2	0.21	
O	5.34	13.16	9.3	7.49	
N	0.1	0.1	0.2	0.3	
S+O+N	5.7	13.5	9.7	8	

It can be seen that the removal of S, O and N from maltenes and asphaltenes separately occurs less effectively than from TBO as a whole. The minimum content of S+O+N is 4.2% in case of maltenes and 5.7% in case of asphaltenes compared with less than 2% in TBO raffinate.

TLC of maltenes and asphaltenes raffinates showed the following results (Table 47):

Table 47. Group composition and HC/Het ratio of raffinates from maltenes and asphaltenes

Group composition	Asphaltenes 470 °C, 2 h, KF-848	Maltenes 440 °C, 2 h, KF-848
AlHC	9.5	35.5
MAHC	12.1	20.8
PAHC	32.4	25.1
LPHet	27.0	10.6
HPHet	19.0	8.0
HC/Het	1.2	4.4

The maximum increase of HC and maximum decrease in heteroatomic compounds was observed in case of maltenes and asphaltene at different

temperatures – 440 and 470 °C respectively with using the same catalyst and 2 h duration.

Maltenes and asphaltenes raffinates were analyzed by GC-MS. Table 48 shows identified compounds in maltenes raffinate AlHC fraction.

Table 48. Compounds in maltenes raffinate AlHC fraction (see chromatogram in Appendix A, Figure 3). Reliability not lower than 95%

Peak	Name	Area %
1	n-Nonane	1.6
2	n-Decane	6.1
3	n-Pentylcyclopentane	0.4
4	n-Undecane	10.4
5	Pentylcyclopentane	0.4
6	Hexylcyclopentane	0.7
7	n-Dodecane	11.3
8	Hexylcyclohexane	0.4
9	1-Butyl-2-propylcyclopentane	0.8
10	n-Tridecane	12.1
11	Dicyclohexylmethane	1.2
12	n-Tetradecane	12.5
13	Cyclotetradecane	1.6
14	n-Pentadecane	11.8
15	n-Nonylcyclohexane	1.4
16	n-Hexadecane	11.1
17	1,3-Dicyclohexylbutane	1.0
18	n-Heptadecane	7.2
19	5-(Cyclohexylpentyl)cyclohexane	0.8
20	n-Octadecane	2.3
21	n-Nonadecane	1.6
22	n-Eicosane	1.1
23	n-Heneicosane	0.8
24	n-Docosane	0.6
25	n-Tricosane	0.5
26	n-Heptadecylcyclohexane	0.2
27	n-Pentacosane	0.1
		100

Homologeous series of n-alkanes of C_9-C_{25} were identified (93.1%) in fraction. Alicyclic HC fraction makes 6.9% of AlHC and cyclobutane, cyclopentane and cyclohexane derivatives were identified.

Table 49 shows the composition of AlHC fraction in asphaltenes raffinate.

Table 49. Compounds in asphaltenes raffinate AlHC fraction (see chromatogram in Appendix A, Figure 4). Reliability not lower than 95%

Peak	Name	Area %
1	2,4-Dimethyl-n-octane	11.8
2	n-Nonane	1.8
3	n-Decane	6.7
4	n-Undecane	11.0
5	n-Hexylcyclopentane	0.9
6	n-Dodecane	12.6
7	impurity	0.5
8	impurity	1.1
9	n-Tridecane	12.3
10	n-Tetradecane	10.9
11	n-Pentadecane	9.5
12	1,3-Dicyclohexylbutane	1.3
13	n-Hexadecane	9.0
14	n-Heptadecane	5.8
15	n-Octadecane	1.9
16	n-Nonadecane	1.4
17	n-Eicosane	1.1
18	n-Heneicosane	0.8
		100

Homologeous series of C_8-C_{21} n-alkanes were identified making 96.6% of the AlHC fraction, the rest 3.4% being reprsesented by alycyclic HC of asphaltenes raffinate.

The raffinates were also analyzed by FT-IR-spectroscopy. For graphic construction calculated data were used and the most significant functional groups were shown. The results can be seen in Figures 16 and 17.
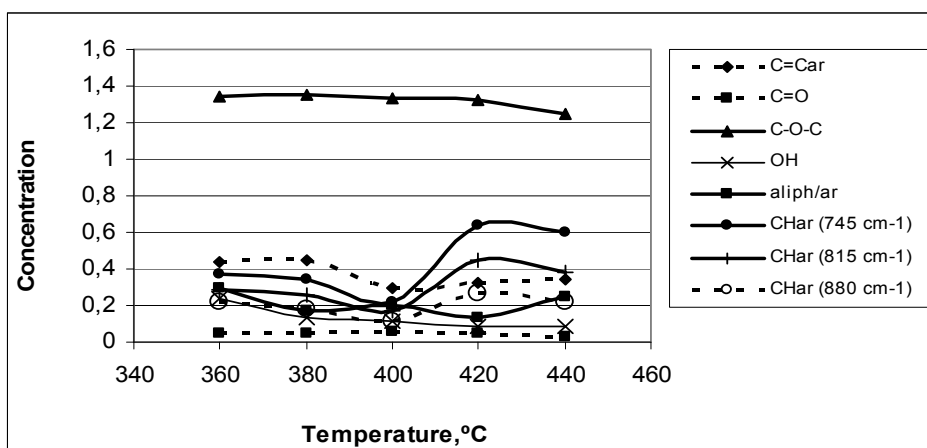
Figure 16. The effect of temperature on the maltenes raffinate functional group composition
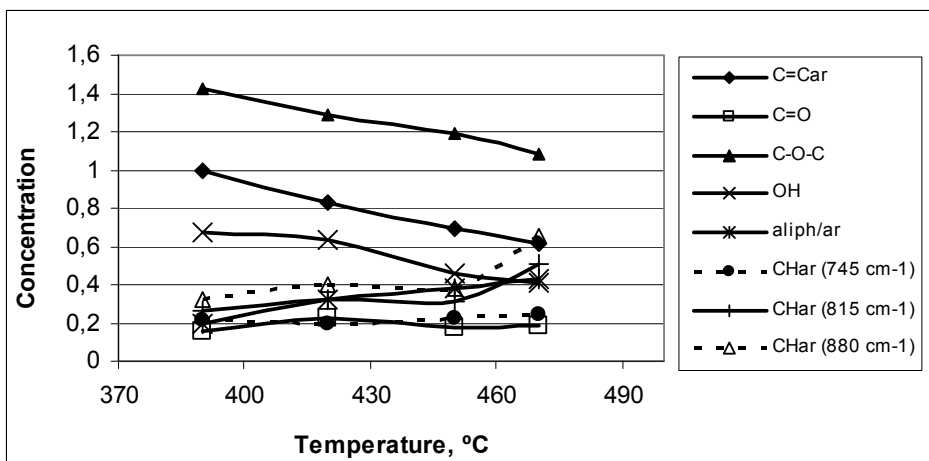
Figure 17. The effect of temperature on the asphaltenes raffinate functional group composition

As it can be seen from figures the increasing of asphaltenes hydrogenation temperature leads to decreasing of content of polar hydroxyl groups. Also the temperature rise causes the decrease in the absorption by $C=C_{ar}$ group. Some temperatures give a decrease in content of HC, but in most experiments their increasing can be observed.

3.6. Comparable table of results obtained from hydrogenation of different materials

Table 50 summarizes the results of the raffinates and HC yields from hydrogenation of different materials in this thesis and in earlier studies.

Table 50. Yields of raffinate and hydrocarbons in hydrogenation of different materials

Feed	Yield of feed samples	Yield of raffinate	Product composition			Total hydrocarbons	
			Raffinate	Coke	Water + gas	Content in raffinate	Summary yield
Basis, % of:	OM	OM	Feed	Feed	Feed	Raffinate	OM
TBO:	90	79.0	87.8	4.4	7.8	60	47.4
including							
Maltenes	46	31.8	76.8	1.9	21.3	77.8	24.7
Asphaltenes	54	28.0	57.6	16.7	25.7	26.9	7.5
Sum		59.8	66.4	14.9	23.7	54.0	32.2
Total vertical retort oil	45	41.9	93.1	0.6	6.3	75.5	31.6
1.including							
Fraction 180-240 °C [39,40]	28	12.0	94.9	0	5.1	97.0	11.6
Fraction240-320 °C [41,42]	22	8.8	89.0	6.1	4.9	90.4	8.0
Fraction320 °C+ [43,44]	50	20.5	91.1	2.1	6.8	75.1	15.4
Sum		41.3	91.7	2.4	5.9	84.6	35.0
2.including							
HO	48	18.3	84.9	2.0	13.1	62.9	11.5
Middle-light fraction	52	20.8	92.3	2.7	5.0	94.1	19.6
Sum		39.1	88.7	2.4	8.9	79.1	31.1
3.including:							
Dephenolated retort oil	74	26.7	80.2	0.6	19.2	78.7	21.0
Phenols	26	9.6	81.6	0	18.4	59.6	5.7
Sum		36.3	80.6	0.4	19.0	73.7	26.7
Flash pyrolysis oil	70	39.4	56.3	12.4	31.3	37.4	14.7
Kukersite oil shale		40.0	40.0	29.2	30.8	54.0	21.6

63

4. CONCLUSIONS

In the frames of this thesis, physical-chemical and technological fundamentals to obtain more oil of higher quality from the Estonian kukersite oil shale were worked out. The following new results were obtained.

- Resulting from direct hydrogenation of kukersite oil shale, the shale oil quality was improved by elevation of the content of hydrocarbons up to 54% but decreasing the raffinate yield up to 40% of OM compared with those (39.7% and 66%) in Fischer Assay.

- Proceeding from kukersite flash pyrolysis oil obtained in higher yield (70% of OM) compared with that in Fischer Assay, its hydrotreating results in 39.4% raffinate of OM with content of hydrocarbons 37.4% only.

- Catalytic hydrocracking of kukersite vertical retort oil 360 °C+ fraction forming about 50% of total vertical retort oil proceeded effectively, and resulted in 84.9% of raffinate yield with content of hydrocarbons being elevated in raffinate up to 62.9%. However, yield of the raffinate from the heavy oil makes only 18.3% on OM basis which together with raffinate of the lower fractions makes 39.1% of OM. So, the efforts were made to increase the degree of kerogen liquefaction by using alternative to retorting methods.

- Thermochemical dissolution method was worked out enabling to liquefy 86-91% of kerogen in the first stage already. According to this method, thermochemical liquefaction of OM before coke formation in the thermobitumenization stage gives a mix of the intermediate product thermobitumen and oil (TBO).

- Thermobitumenization conditions to maximize the yield of primary TBO were worked out as follows: using benzene as a solvent – temperature 360 °C, 3 hours, oil shale-to-solvent ratio 1:3, and using mixture of benzene with water (weight ratio 1:1) – temperature 390 °C, 1 hour, oil shale-to-solvent ratio 1:2. Thus, the proposed methods of thermal decomposition can be completed at lowered temperatures (360-390 °C) compared with standard Fischer Assay industrial retorting and coking processes used for oil shale liquefaction at 450-500 °C and bituminous fractions upgrading occurring at 850 °C.

- In the second stage the optimum conditions were found for catalytic hydrogenation of TBO resulting in raffinate yield up to 87.8% of TBO –

temperature 430 °C, duration 2 hours, initial pressure of hydrogen 7 MPa, 10% of Akzo Nobel catalyst for hydrogen activation KF-848 ($Co-Mo/Al_2O_3$).

- Upgrading of kukersite-derived liquids results in 59.2% removal of heteroelements, O, S and N, from 7.6% in TBO down to 1.8% in raffinate. Amongst hydrodesulphuration, hydrodenitrogenation and hydrodeoxygenation reactions occurred the latter was recognized as the dominating one yielding in 77.5% decrease in oxygen content.

- On the basis of this work it was found that 79% of hydrocarbon-rich raffinate similar to natural petroleum can be produced from OM of kukersite oil shale. Varying hydrogenation conditions the synthetic petroleum characterized by high content, 60-79%, of aromatic and aliphatic hydrocarbons can be obtained. Valuable (carbonaceous) oil coke with yield 4.0% of OM was formed as a hydrogenation by-product.

REFERENCES

[1] Urov, K., Sumberg, A. Characteristics of oil shales and shale-like rocks of known deposits and outcrops, Monograph. – *Oil Shale*, 1999, vol. 16, no.3, pp. 4-47.

[2] *World Energy Resources. 2013 Survey*. World Energy Council, 2013, 2.44-2.56.
http://www.worldenergy.org/wp_content/uploads/2013/09/Complete_W ER_2013_Surve y.pdf (24.03.2015).

[3] Aarna, A. Y., Lippmaa, E. T. Thermal destruction of oil shale-kukersite. – *Transactions of Tallinn Polytechnic Institute*, Series A, 1958, no. 97, pp. 3-27 [in Russian].

[4] Thakur, D. S., Nuttall, Jr. H. E. Kinetics of Moroccan oil shale by thermogravimetry. – *Ind. Eng. Chem. Res*., 1987, vol. 26, no. 7, pp. 1351-1356.

[5] Horsfield, B., Duppenbecker, S. The decomposition of Posidonia shale and Green River shale kerogens using microscale sealed vessel (MSSV) pyrolysis. – *Journal of Analytical and Applied Pyrolysis*, 1991, vol. 20, no. 7, pp. 107-123.

[6] Larsen, J. W., Kidena, K. The sudden release of oil and bitumen from Bakken shale on heating in water. – *Fuel and Energy Abstracts*, 2003, vol. 44, no. 3, p. 139.

[7] Rajeshwar, K. The kinetics of the thermal decomposition of Green River oil shale kerogen by non-isothermal thermogravimetry. – *Thermochimica Acta*, 1981, vol. 45, no. 3, pp. 253-263.

[8] Ots, A. *Oil Shale Fuel Combustion*. – Eesti Energia AS, Tallinn, 2006.

[9] Demirbas, A. Effect of initial moisture content on the yields of oily products from pyrolysis of biomass. – *Journal of Analytical and Applied Pyrolysis*, 2004, no. 71, pp. 803-815.

[10] Khisin, Ya. I. *Thermal Decomposition of Oil Shales*. Leningrad-Moscow: Gostoptekhizdat, 1948 [in Russian].

[11] Kask, K. A. About bituminizing of kerogen of oil shale-kukersite. Report I. – *Transactions of Tallinn Polytechnic Institute*, Series A, 1955, no. 63, pp. 51-64 [in Russian].

[12] Kask, K. A. About bituminizing of kerogen of oil shale-kukersite. Report II. – *Transactions of Tallinn Polytechnic Institute*, Series A, 1956, no. 73, pp. 23-40 [in Russian].

[13] Heistand, R. N. The Fischer Assay: Standard for oil shale industry. – *Energy Sources*. Part A, 1976, vol. 2, no. 4, pp. 397-405 (ISO-647-74).

[14] Kogerman, P., Luts, K., Hüsse, J., *The Chemistry of Estonian Oil Shale*. M.-L: Goskhimizdat, 1934 [in Russian]

[15]   Karavayev, N. M., Weiner, I. M. About *thermobitum of Gdov oil shale. Transactions of the Institute of Goryuchih Iskopayemyh. Academy of Sciences of USSR,* 1950, vol. 2, pp. 285-295 [in Russian].

[16]   Kramer, R., Levy, M. Extraction of oil shales under supercritical conditions. – *Fuel*, 1989, vol. 68, no. 6, pp. 702-709.

[17]   Luik, H., Klesment, I. Liquefaction of kukersite concentrate at 330-370 ºC in supercritical solvents. – *Proceedings of the Academy of Sciences of the Estonian SSR*, 1985, vol. 34, no. 4, pp. 253-262 [in Russian].

[18]   Luik, H., Palu, V., Bitykov, M., Luik, L., Kruusement, K., Tamvelius, H., Pryadka, N. Liquefaction of Estonian kukersite oil shale kerogen with selected superheated solvents in static conditions. – *Oil Shale*, 2005, vol. 22, no. 1, pp. 25-36.

[19]   Luik, H., Klesment, I. Liquefaction of kukersite concentrate at 330-370 °C in supercritical solvents. – *Oil Shale*, 1997, vol. 14, no. 3, pp. 419-432.

[20]   Kogerman, P. N., Kopwillem, J. J. Hydrogenation of Estonian oil shale and shale oil. – *Journal of the Institution of Petroleum Technologists*, 1932, vol. 18, no. 108, pp. 833-845.

[21]   Mohamed, A. R., Mathur, V. K. Hydrogenation of residual oil using an ore derived water soluble ammonium molybdate catalyst. – *Fuel*, 1991, vol. 70, no. 8, pp. 983-987.

[22]   Tian, K. P., Mohamed, A. R., Bhatia, S. Catalytic upgrading of petroleum residual oil by hydrotreating catalysts: a comparison between dispersed and supported catalysts. – *Fuel*, 1998, vol. 77, no. 11, pp. 1221-1227.

[23]   Krichko, A. A., Maloletnev, A. S., Mau, O. A., Konyashina, R. A., Lebedeva, L. N. Activity of Al-Ni-Mo catalysts in hydrogenation of coal destillates. –*Khimiya Tverdogo Topliva*, 1990, no. 6, pp. 64-70 [in Russian].

[24]   Nishiyama, A., Shimada, H., Sato, T. et al. The effect of distribution and dispersion of Mo ions in catalysts. – *Sekiyu Gakkasishi*, 1988, no. 31, p. 109.

[25]   Dufresne, P., Bigeard, P. H., Billon, A. New developments in hydrocracking: low pressure high-conversion hydrocracking. – *Catalysis Today*, 1987, vol. 1, no. 4, pp. 367-384.

[26]   Sasaki, Y., Ojima, Y., Kondo, T. et al. Hydrocracking of heavy oils from different sources. – *Sekiyu Gakknishi*, 1983, no. 26, p. 472.

[27]   Sasaki, Y., Ojima, Y., Kondo, T. et al. The activity of ash catalysts. – *Sekiyu Gakknishi*, 1983, no. 26, p. 144.

[28]   Levin, S. Z., Dinier, I. S. Obtaining of motor fuels and chemical products from Baltic oil shale by destructive hydrogenation. – *Transactions of VNIIT*, 1960, no. 9, pp. 65-90.

[29]   Dolbear, G. E., Tang, A., Moorehead, E. L. Upgrading studies with Californian, Mexican and Middle Eastern heavy oils. – *Fuel*, 1987, vol. 66, no. 2, pp. 267-270.

[30]   Guan, C., Wang, Z., Yu, S., Guo, A., Que, G. Upgrading petroleum residue by two-stage hydrocracking. – *Fuel Processing Technology*, 2004, vol. 85, no. 2, pp. 165-172.

[31] Ancheyta, J., Betancourt, G., Marroquin, G., et al. Hydroprocessing of Maya heavy crude oil in two reaction stanges. – *Applied Catalysis A: General*, 2002, vol. 233, no. 1-2, pp. 159-170.

[32] Ovalles, C., Filgueiras, E., Morales, A., et al. Use of a dispersed iron catalyst for upgrading extra-heavy crude oil using methane as source of hydrogen. – *Fuel*, 2003, vol. 82, no. 8, pp. 887-892.

[33] Chen, S.-L., Jia, S.-S., Luo, Y.-H., Zhao, S.-Q. Mild cracking solvent deasphalting: a new method for upgrading petroleum residue. – *Fuel*, 1994, vol. 73, no. 3, pp. 439-442.

[34] Tippin, B. R., Rex, R. C. Combined benefication and hydroretorting of oil shale. – *Symposium on Chemistry and Processing Supercritical Fluids*, 1985, pp. 237-246.

[35] Lynch, P. A., Janka, J. C., Lau, F. S., Feldkirchner, H. L., Dirksen, H. A. The Hydroretorting Assay – a new technique for oil shale assessment. – *Symposium on Characterization and Chemistry of Oil Shales*, 1985, pp. 71-75.

[36] Klesment, I., Nappa, L., Vink, N. Results of low-temperature destructive hydrogenation of Estonian kukersite kerogen concentrate. –*Khimiya Tverdogo Topliva*, 1979, no. 5, pp. 33-39 [in Russian].

[37] Geguchadze, R. A., Rogailin, M. I., Grebenshikova, G. V. State and perspectives of fuel producing from oil shale and coal by pyrolysis and hydropyrolysis. – *Khimiya Tverdogo Topliva*, 1982, no. 4, pp. 44-57 [in Russian].

[38] Gorlov, E. G., et al. Effect of preparation of suspension of petroleum tar with Baltic oil shale on hydrocracking. – Khimiya Tverdogo Topliva, 1997, no. 2, pp. 52-55 [in Russian].

[39] Luik, H., Vink, N., Lindaru, E. Upgrading of Estonian shale oil. 1. Effect of hydrogenation on the chemical composition of kukersite retort oil. – *Oil Shale*, 1996, vol. 13, no. 1, pp. 13-19.

[40] Luik, H., Lindaru, E., Vink, N. Upgrading of Estonian shale oil. 2. Effect of hydrogenation on the properties of kukersite retort oil. – *Oil Shale*, 1996, vol. 13, no. 3, pp. 193-196.

[41] Luik, H., Müürisepp, A.-M., Vink, N., Liiv, M. Upgrading of Estonian shale oil. 3. Hydrogenation of phenols. – *Oil Shale*, 1996, vol. 13, no. 3, pp. 197-203.

[42] Luik, H., Lindaru, E., Vink, N., Maripuu, L. Upgrading of Estonian shale oil distillation fractions. 1. Hydrogenation of „diesel fraction". – *Oil Shale*, 1999, vol. 16, no. 2, pp. 141-148.

[43] Luik, H., Vink, N., Lindaru, E., Maripuu, L. – Upgrading of Estonian shale oil distillation fractions. 2. The effect of time and hydrogen pressure on the yield and composition of "diesel fraction" hydrogenation products. – *Oil Shale*, 1999, vol.16, no. 3, pp. 249-256.

[44] Luik, H., Maripuu, L., Vink, N., Lindaru, E. Upgrading of Estonian shale oil distillation fractions. 3. Hydrogenation of the "light mazut". – *Oil Shale*, 1999, vol. 16, no. 4, pp. 331-336.

[45] Luik, H., Vink, N., Maripuu, L., Lindaru, E. Upgrading of Estonian shale oil distillation fractions. 4. The effect of time and hydrogen pressure on the yield and composition of "light mazut" hydrogenation products. – *Oil Shale*, 1999, vol. 16, no. 4, pp. 337-342.

[46] Luik, H., Vink, N., Lindaru, E., Maripuu, L. Upgrading of Estonian shale oil distillation fractions. 5. Hydrogenation of heavy mazute. – *Oil Shale*, 2000, vol. 17, no. 1, pp. 25-30.

[47] Luik, H., Vink, N., Maripuu, L., Lindaru, E. Upgrading of Estonian shale oil distillation fractions. 6. The effect of time and temperature on the yield and composition of heavy mazute hydrogenation products. – *Oil Shale*, 2000, vol. 17, no. 1, 31-36.

[48] Larina, N. K., Skripchenko, G. V., Abovyan, O. A. Characteristics of distillate fractions of hydrogenate of Irsha-Borodinski coal by IR-spectroscopyc data. – *Coal Processing into Liquid and Gaseous Fuel*, Moscow, 1982, pp. 23-31.

[49] Plotnikova, I., N. *Elementnyi Sostav Nefti i Rasseyannogo Organicheskogo Veshchestva*. Kazanski Institut Geologii i Neftegazovyh Tehnologij, 2013 [in Russian].

ACKNOWLEDGMENTS

ABSTRACT

Upgrading of liquid products from Estonian kukersite oil shale by catalytic hydrogenation

The goal of this work was to elucidate the possibilities for more effective thermochemical upgrading of Estonian kukersite oil shale in order to obtain as the main product oil with possibly high yield and high content of hydrocarbons, which would be a synthetic analogue to natural petroleum.

Firstly, hydrogenation of oils generated by traditional retorting in industrial and laboratory reactors and fractions of the oils was carried out at varied experimental conditions (temperature 350-450 °C, duration 0.5-4 hours, hydrogen initial pressure 50-88 atm) in the presence of different catalysts in a 500 cm^3 batch rocking autoclave. As a result of hydroprocessing soluble in benzene raffinate, coke and gas were obtained. The initial retort oil is characterized as rich in oxygen content. In the course of hydrodeoxygenation most part of the oxygen was transformed into water, which was separated. As a result of hydrodesulphuration most of the sulphur contained in oil was transformed into hydrogen sulphide in gas composition. The yield of products was determined and material balance was composed. The chemical composition of raffinates was studied by elemental, spectroscopic and chromatographic analysis. For the first time, the hydrocarbons belonging to diesel fraction were generated by the hydrogenation of kukersite shale oil obtained by flash pyrolysis in semi-industrial standplant and of kukersite industrial heavy oil fraction 360 °C+. Results achieved in this work are compared with earlier studies and prove the possibility to obtain high yield of raffinate rich in high content of hydrocarbons from the prime oil. If calculated on kerogen basis, the yield of raffinate is similarly low, in general about 40%, as in the case of kukersite direct hydrogenation with molecular hydrogen, due to low yield of the oil during oil shale prime liquefying.

With the task to clarify the possibilities for kerogen maximum transformation into liquid product during the prime thermochemical processing, parameters such as pyrolysis temperature, duration, solvent composition and oil shale-to-solvent weight ratio were varied. As a result, a new especially effective thermal dissolution method was worked out and optimized. Applying the new method, 86-91% of kerogen was transformed into intermediate liquid product with new composition – mixture of incompletely decomposed kerogen – thermobitumen and oil (TBO).

The investigation of TBO chemical composition during storage showed that the most effective approach is to subject it to catalytic hydrogenation directly after separation from solid residue. By varying temperature, duration, hydrogen pressure, novel Co-Mo/Al$_2$O$_3$ type catalysts and their quantity, the optimal conditions for TBO hydrogenation were found. In this case the yield of raffinate from OM was even higher (up to 79%) than the yield of prime retort oil obtained

from oil shale kerogen in Fischer Assay (up to 66%), which differes from petroleum and requires upgrading.

By implementing the innovative technology worked out in this thesis, the high yield of raffinate with high content of aliphatic and aromatic hydrocarbons and low content of heteroatomic compounds, qualifying as synthetic petroleum from Estonian kukersite oil shale, was proposed for the first time in the world.

KOKKUVÕTE

Kukersiitpõlevkivi vedelproduktide vääristamine katalüütilise hüdrogeenimise meetodil

Töö eesmärk oli võimaluste selgitamine Eesti kukersiitpõlevkivi senisest efektiivsemaks termokeemiliseks vääristamiseks, et saada põhilise lõpp-produktina võimalikult kõrge saagisega ja kõrge süsivesinikesisaldusega õli, mis oleks sünteetiline analoog looduslikule naftale.

Esmalt viidi läbi kukersiidi traditsioonilisel pürolüüsil tööstuslikes ja laboratoorsetes reaktorites genereeritud õlide ja õlifraktsioonide hüdrogeenimine varieeritud katsetingimustel (temperatuur 350—450 °C, aeg 0,5—4 tundi, vesiniku algrõhk 50—88 atm) erinevate katalüsaatorite manulusel 500 cm³ mahuga roteeritavas autoklaavis. Vesiniktöötluse tulemusena saadi benseenis lahustuv rafinaat, koks ja gaas. Pürolüüsi õlile on iseloomulik kõrge hapnikusisaldus. Hüdrodesoksüdeerimise tulemusena transformeeriti suur osa õli koostises olevast hapnikust veeks, mis eraldati. Hüdrodesulfureerimise tulemusena eraldati enamik õlis sisalduvast väävlist väävelvesinikuna gaasi koostisesse. Määrati kindlaks produktide saagis ning koostati materjalibilanss. Rafinaadi keemilist koostist uuriti elementanalüüsi, spektroskoopiliste ja kromatograafiliste meetoditega. Esmakordselt teostati kukersiidi pooltööstuslikul stendiseadmel saadud kiirpürolüüsi õli ja tööstusliku raskõli fraktsiooni 360 °C+ hüdrogeenimine diislifraktsiooni kuuluvate süsivesinike genereerimiseks. Saadud tulemusi on võrreldud varasemate töödega ja näidatud suure saagisega süsivesinike poolest rikka rafinaadi saamise võimalikkus primaarõlist. Arvestatuna kerogeeni kohta jääb rafinaadi saagis paraku sarnaselt kukersiidi otse hüdrogeenimisele molekulaarse vesinikuga madalaks, üldjuhul vaid 40% piiresse ning seda õli madala saagise tõttu põlevkivi primaarsel vedeldamisel.

Ülesandega selgitada võimalusi kerogeeni maksimaalseks transformeerimiseks vedelprodukti juba primaarsel termokeemilisel töötlemisel varieeriti pürolüüsi temperatuuri, aega, lahusti koostist ja selle kaalulist suhet põlevkivisse. Uurimistulemusena on välja töötatud ja optimeeritud uus, eriti efektiivne termilise lahustamise meetod. Uue meetodi rakendamisel transformeeriti 86–91% kerogeenist uudse koostisega intermediaarsesse vedelprodukti − mittetäielikult õliks lagunenud termobituumeni ja õli segusse (TBO).

TBO keemilise koostise muutuse uurimine säilitamisel näitas, et kõige efektiivsem on selle allutamine katalüütilisele hüdrogeenimisele vahetult pärast eraldamist tahkest jäägist. Varieerides temperatuuri, aega, vesiniku rõhku, uudseid Co-Mo/Al₂O₃ tüüpi katalüsaatoreid ja nende kogust, on esmakordselt leitud optimaalsed tingimused TBO hüdrogeenivaks vääristamiseks. Sellisel juhul saab kerogeenist isegi rohkem rafinaati (kuni 79%) kui põlevkivi

pürolüüsil Fischeri retordis primaarset, naftast erinevat ja rafineerimist vajavat poolkoksistamise õli (kuni 66%).

Antud töös väljatöötatud uue tehnoloogia järgi Eesti kukersiidist esmakordselt maailmas saadud suure saagisega rafinaat on kõrge alifaatsete ja aromaatsete süsivesinike sisaldusega ja madala heteroaatomiliste ühendite sisaldusega ning kvalifitseeritavad sünteetiliseks naftaks.
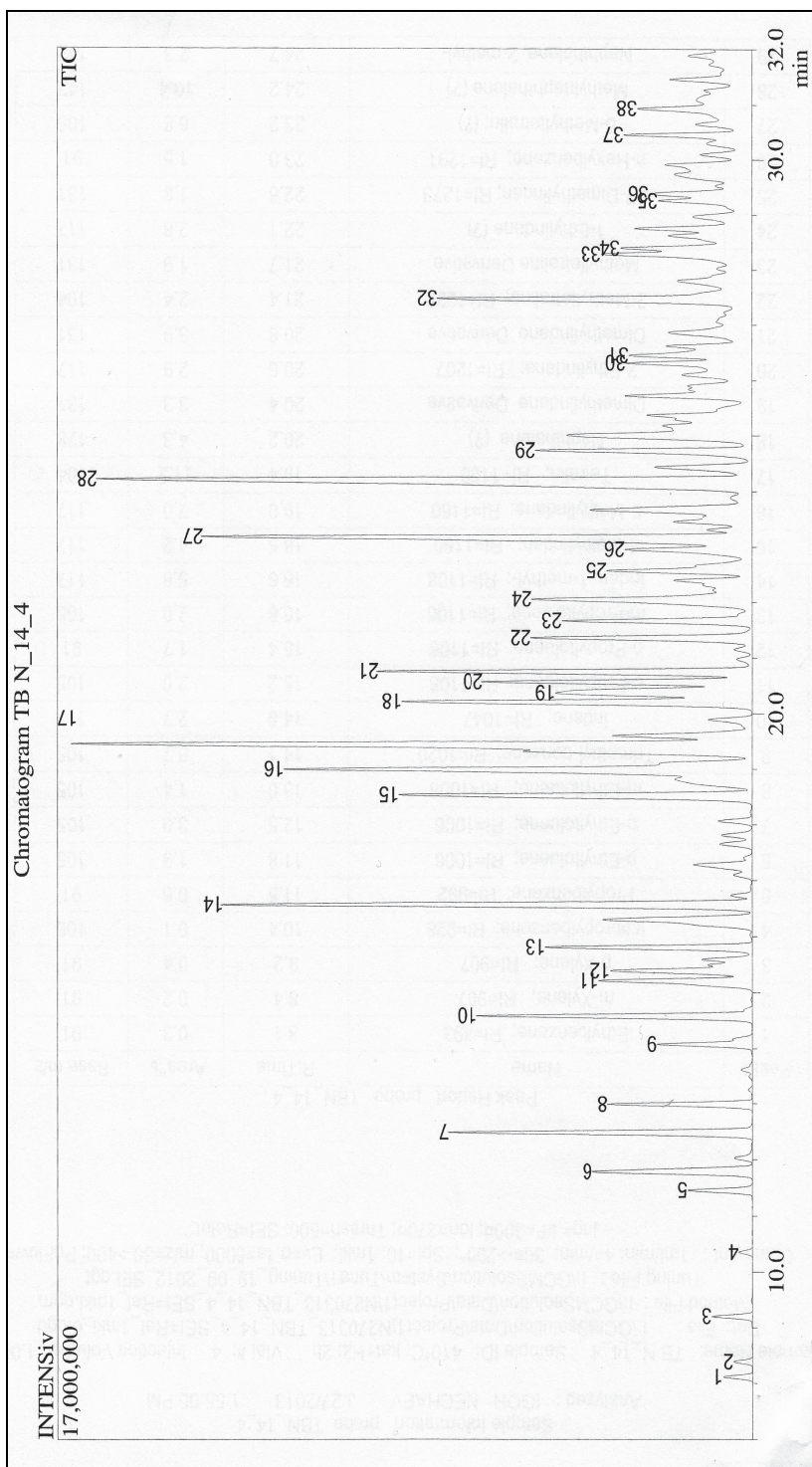
APPENDIX A: GC-MS chromatograms
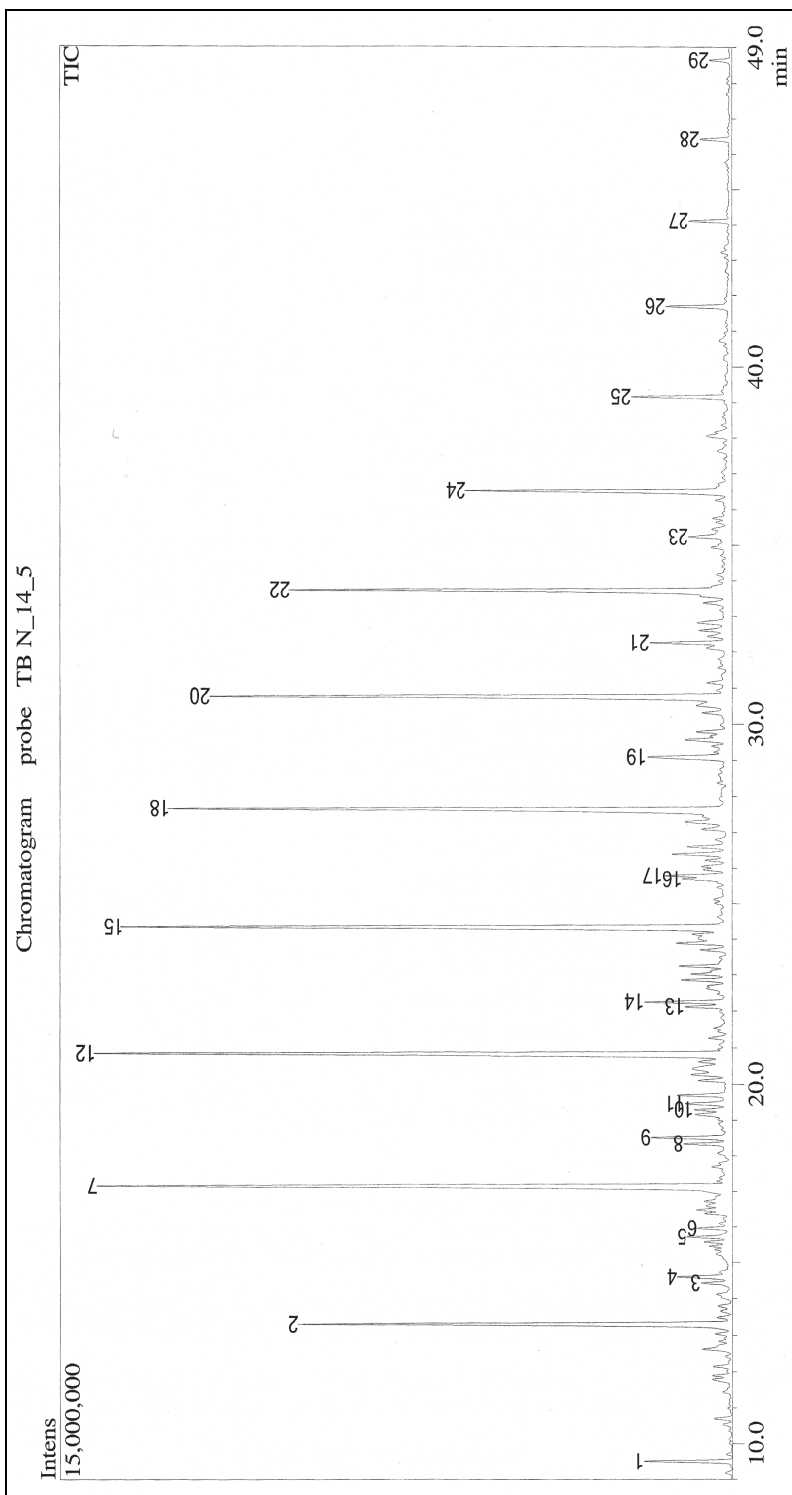
Figure 1. GC-MS chromatogram of hydrogenated TBO MAHC fraction

Figure 2. GC-MS chromatogram of hydrogenated TBO AlHC fraction
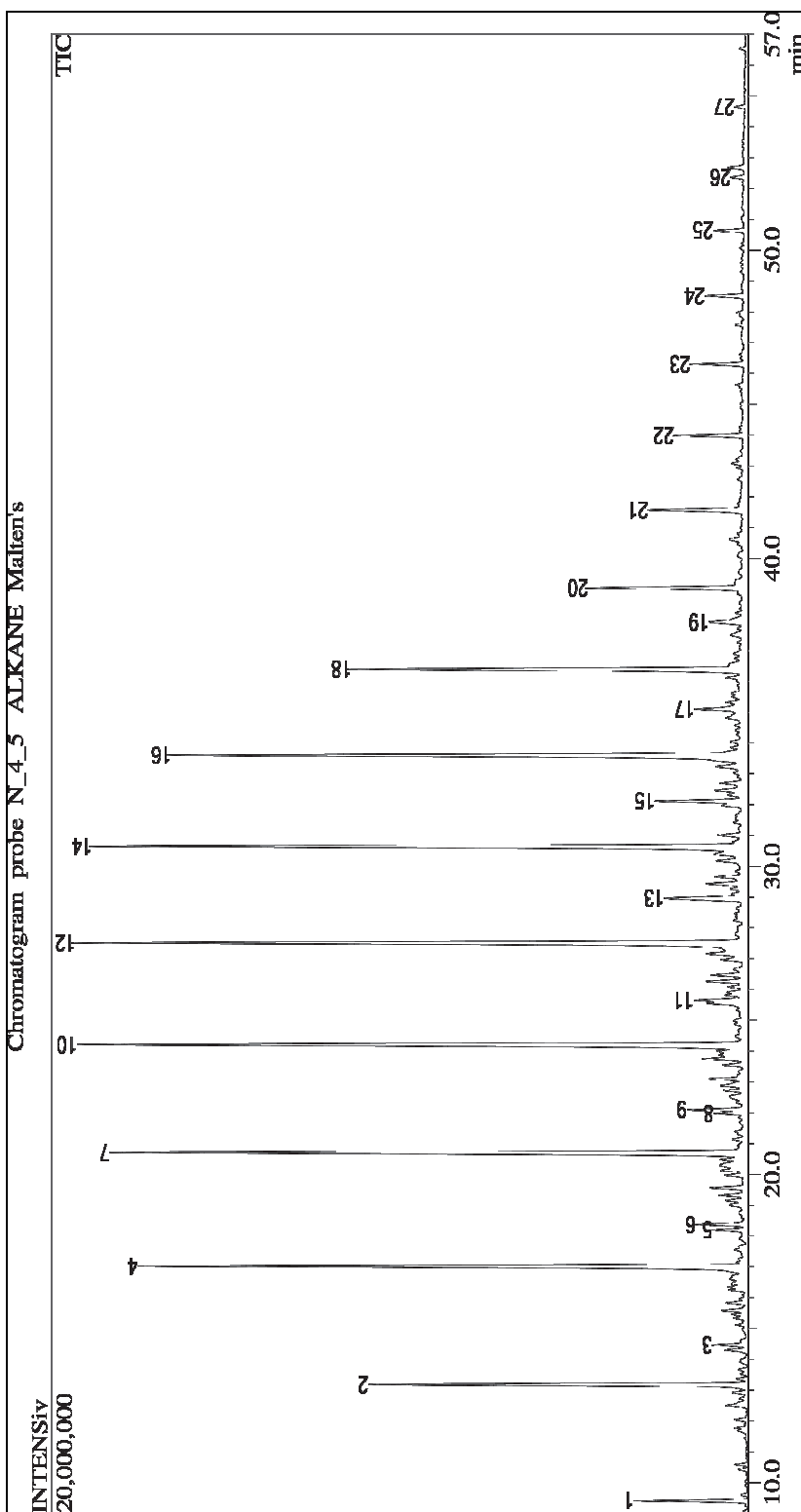
Figure 3. GC-MS chromatogram of hydrogenated maltenes AlHC fraction
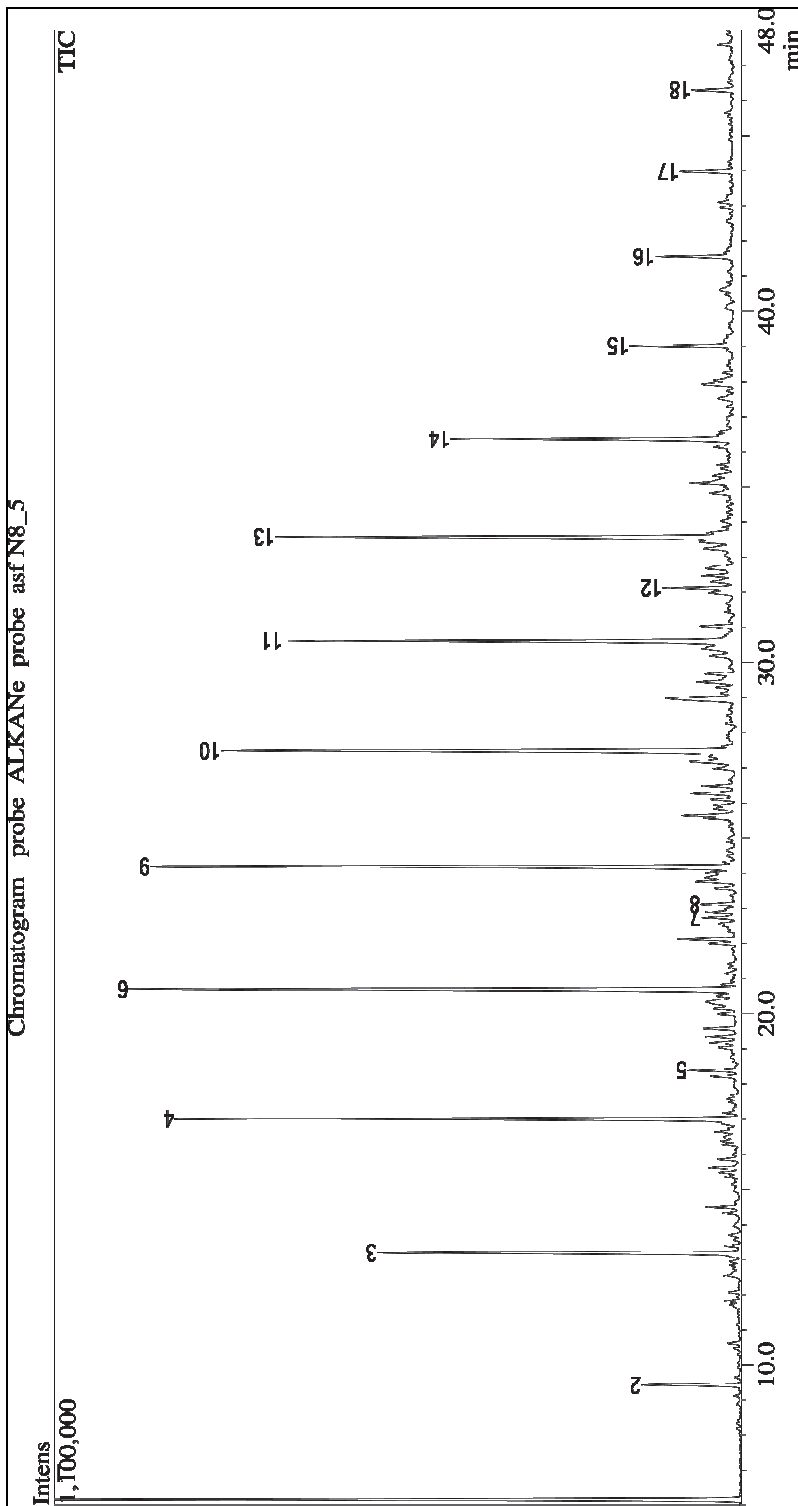
Figure 4. GC-MS chromatogram of hydrogenated asphaltenes AIHC fraction

APPENDIX B: ORIGINAL PUBLICATIONS

Article I

Krasulina, J., Luik, H., Palu, V., Tamvelius, H. Thermochemical co-liquefaction of Estonian kukersite oil shale with peat and pine bark. – *Oil Shale*, 2012, vol. 29, no. 3, pp. 222-236.

THERMOCHEMICAL CO-LIQUEFACTION OF ESTONIAN KUKERSITE OIL SHALE WITH PEAT AND PINE BARK

JULIA KRASULINA[*], HANS LUIK, VILJA PALU, HINDREK TAMVELIUS

Laboratory of Oil Shale and Renewables Research
Department of Polymer Materials
Tallinn University of Technology
Ehitajate tee 5, 19086 Tallinn, Estonia

Abstract. *Kukersite oil shale + pine bark, kukersite oil shale + peat as well as kukersite, bark and peat individually were submitted to thermochemical liquefaction in an autoclave with and without solvent for two hours at different temperatures from 340 to 420 °C. Water and benzene as solvents were used. The influence of several factors such as temperature, solvent and its type, and oil shale-to-peat or oil shale-to-biomass ratio on the yield of liquid, gaseous and solid products was investigated. The chemical composition of the goal liquid product separated as the benzene soluble oil was characterised by using FTIR-spectroscopy and ultimate analysis apparatus. Group composition of the oil was determined by using thin-layer chromatography. In co-liquefaction experiments several synergistic effects in product yields were observed. The most important synergistic effect was noticed at co-liquefaction of the mixture oil shale with peat (10 : 4 by mass of the organic matter) at 360 °C in the medium of water in which case the yield of the liquid product was 25% higher than the sum of corresponding yields obtained at liquefaction of oil shale and peat separately in the same experimental conditions. The group composition of oils shows that various polar and high-polar oxygen compounds prevail over hydrocarbon fractions. Data on the elemental and group composition demonstrate that partial substitution of biomass or peat for oil shale leads to obtaining chemically modified shale oil.*

Keywords: kukersite, peat, biomass, co-processing, synergistic effect.

1. Introduction

The demand for liquid fuels, chemicals and other products traditionally produced from natural petroleum rapidly increases in the industrialised

---
[*] Corresponding author: e-mail *julika82@mail.ru*

countries. At the same time, the reserve of fossil resources in Earth's crust is not inexhaustible. Availability and pumping of conventional petroleum become more laborious. These circumstances lead to drastic increase in prices and stimulate the search for feedstocks and technologies for production synthetic petroleum as an alternative to the natural one. Oil shales, hard and brown coals, biomass in its varieties, as well as industrial wastes of organic polymers represent an available feedstock of hydrocarbon crude, and their potential is being realised by developing advanced methods of destruction and liquefaction. Diversity in the assortment of source raw material for obtaining petroleum substitutes is a motive power impelling dynamic development of complex thermochemical co-liquefaction processes basing on pyrolysis or thermal dissolution methods. At present, studies on the potential of co-processing of varied feedstocks are highly topical on the world scale. Co-processing of biomass [1–16], plastic or rubber wastes [17–25] with fossil fuels (mainly with coal and petroleum residues) has sometimes demonstrated higher efficiency and led to chemically modified products compared with processing of aforenamed objects individually [1, 5, 9, 11–14, 19, 22, 24, 25]. The effect of kukersite oil shale co-processing with peat and biomass is the subject matter of this paper.

1.1. Kukersite oil shale – the main energy source in Estonia

The role of oil shale as feedstock has been and still is very important for Estonian industry. In fact, kukersite oil shale is the basis of the Estonian economy being used as a source of energy to produce electricity, heat, liquid fuels and lots of chemicals by combustion and liquefaction methods. Numerous chemicals have been separated from the shale oil obtained from the kukersite oil shale liquefaction by using semicoking technology in retorts of different configuration, and Estonia has historical experience on shale oil upgrading into motor fuels [26]. Shale oil produced may be considered a type of unconventional petroleum, and it has manifested itself as a marketable product meeting the demands of domestic and world market. The yield of oil is not high in industrial conditions. The main body of kukersite oil shale is transformed in vertical retorts to hazardous solid residue (semicoke) the latter having practically no prospective for further utilization. The residual carbon content of semicoke is as high as 10–14% [27, 28]. In more progressive solid heat carrier retorts the semicoke formed is combusted in the same process to produce some addition heat necessary for oil shale destruction. As a result of *in situ* combustion, large quantities of CO_2 are emitted into the atmosphere. Severe prescriptions and taxes on both CO_2 emission and disposal of hazardous wastes are established by EU Commission to limit environmental pollution. Taking into account the fact that yielding one barrel of oil from kukersite oil shale in industrial retorts is accompanied by formation of both 0.6 tons of hazardous waste and up to $250 \, m^3$ of CO_2, it is obvious that the semicoking technology should be

further improved or replaced by alternative ones to enhance oil yield and diminish the amounts of polluting by-products.

1.2. Alternative energy sources for oil shale

The most prospective substitutes for oil shale to generate synthetic petroleum in Estonia are peat, the resource of which is estimated as one of the biggest in Europe, and forest biomass. Both peat and wood have been directly used as solid fuels in Estonia to produce heat and electricity, but never being industrially liquefied. Oil shale is the strategic resource and can be economized by using these solid fuel types as components in liquefaction feedstock.

1.2.1. Peat

Peat as a regular natural organic resource in the world stratifying in wetlands is considered one of the important Estonian energy sources and the strategic reserve in the future. World's peat reserves are estimated at about 700,000 million tons [29]. Peatlands – bogs and fens – cover over 22% of the Estonian territory, peat resources exceeding 2400 million t [30]. Peat is the youngest and least-altered member of the fossil fuels, turning into brown coal with time. Coalification includes low-temperature biogeochemical processes from burial of plants to coal formation [31]. Peat as other ligno-cellulosic materials is characterized by high oxygen content. Besides humic substances formed as a result of humification, peat contains considerable amounts of lignin, cellulose and bitumens as typical constituents of ligno-cellulosics not maintained in the fossil organic matter [32]. Raw peat in the natural deposits is characterized by moisture content as high as 90%, that of ash being variable [33–35]. Thus, peat is a particularly appropriate feedstock for conversion in water needing no prior drying. The heating value of peat is close to that of wood and brown coal, but sulfur content is lower than that in petroleum or coal [36].

When peat is pyrolyzed, the volatile products consist of a condensable portion (tars and an aqueous liquid), and a noncondensable portion (pyrolysis gases) [37]. Char, a solid product formed at pyrolysis of peat, is, unlike semi-coke, not a hazardous useless waste but can be used as a chemical reducing agent, an adsorbent, and a catalyst support. It is also used, due to its electrical properties, as anode in electrochemical applications as well as a bonding agent in rubber production and in producing pigments and lubricants. Peat gas and tar can be used as fuel gas or liquid fuel, lubricant, solvent and pitch, respectively [38].

1.2.2. Biomass

Renewable biomass in its availability and variety represents a practically inexhaustible resource of feedstock for energetical and chemical needs. By its origin biomass is lignocellulosic matter consisting mainly of varying

amounts of three biopolymers – cellulose, hemicellulose, and lignin. Bio-mass is a term for all organic material that stems from plants, including trees. Biomass energy, the energy stored in plants, actually originates from solar energy through the photosynthesis process, and the energy of sunlight in plants is stored in chemical bonds [39]. In fact, oil shales are also sedimented biomass, since they are fossilized remains of higher plants and marine fauna that grew and lived hundreds of millions years ago. The chemical composi-tion of growing biomass differs from that of fossilized biomass known as kerogen by large amounts of oxygen.

In Estonia, the term biomass is most often used when referring to forestry, including all ingredients of trees. About a half of the Estonian territory (2.25 million hectares) is covered with forest. Conifers make up more than a half of the total forest resource. Processing of forest trees yields various wastes and residues. Bark usually forms up to 20% of the trunk or about 10% of the whole tree and, as disregarded so far, can be used as biomass for liquefaction. The energy enclosed in biomass can be released either by direct combustion or converted, via thermochemical upgrading, into synthetic liquid and gaseous fuels or products of higher value for the chemical industry. Pyrolysis of biomass generates three different energy-effective products in different quantities: char, gas and oil. Varying pyrolysis conditions closer to coking, gasification or liquefaction, one of these products of market value in high yield can be obtained. So, the pyrolysis of biomass can be described as direct thermal decomposition of the organic matrix in the absence of oxygen to obtain an array of solid, liquid and gaseous products. Biomass pyrolysis yield is a complex combination of the products obtained at individual pyrolysis of cellulose, hemicellulose, and lignin, each of which has its own kinetic characteristics [40]. The pyrolysis method has been used for commercial production of a wide range of fuels, solvents, chemicals and other products from biomass feedstocks. Biomass pyrolysis oils have a potential to be used as a fuel oil substitute. Combustion tests indicate that these oils burn effectively, in standard or slightly modified boilers and engines, with rates similar to those for commercial fuels [41].

1.3. Co-processing of fossil and renewable feedstocks

Oil shale, peat and biomass, being miscellaneous, by the content and chemical composition of the organic matter represent, in fact, biomass of different degree of metamorphosis, natural high-molecular matter with polymerized structure, and they can all be available sources of petroleum substitutes. Renewable lignocellulosic biomass, decaying and partly humified biomass in peat, and oil shales as kerogeneous rocks containing sedimented and fossilized biomass are, individually and in blends, con-vertible to hydrocarbon-rich light-middle oils, using analogous thermo-chemical liquefaction processes and reactors. At the same time, liquefaction regularities of blends should be investigated, as they differ significantly compared with those of individual feedstocks.

Co-processing of the kukersite oil shale with other combustible fuels to obtain petroleum substitutes is not much investigated. There are available results of kukersite co-processing with wood in supercritical water and of chlorine fixation capacity of the oil shale mineral matter in PVC and kukersite co-pyrolysis [42–48].

In this work kukersite oil shale, pine bark, peat and their mixtures were submitted to liquefaction in an autoclave with the aim to determine the effect of feedstock combination and processing conditions, including the presence of solvent, on yield and composition of the products.

2. Experimental

2.1. Initial feedstocks

Air-dried, finely powdered (less than 0.1 mm) and homogenized kukersite oil shale, peat and pine bark, characterized in Table 1, were used as the initial feedstocks. Benzene and water were used as solvents. The mixtures of kukersite with peat and kukersite with pine bark for co-pyrolysis were taken in different ratios on organic matter (OM) basis.

Table 1. Characteristics of the initial feedstocks

Proximate analysis	Kukersite	Peat	Pine bark
Moisture W^a, %	0.7	11.9	8.7
Ash content A^d, %	37.2	6.1	2.9
Carbon dioxide $(CO_2)_M^d$, %	12.8	2.0**	
Organic matter OM^d, %	50.5*	91.9***	97.1

OM content was determined on acid-treated basis

$*OM = 100 - A_{825^oC}^d - 0.625 S_p$; S_p – pyritic sulphur, %

$**(CO_2)_M^d = A_{550^oC}^d - A_{825^oC}^d$

$***OM = 100 - A_{550^oC}^d$

2.2. Liquefaction and analysis

Kukersite oil shale, peat, pine bark individually and their mixtures were submitted to the thermochemical liquefaction. Either a 4-g sample, or, in the case a solvent was used, the sample with 6 g of the solvent were charged into 20-cm³ autoclaves. The autoclaves were put into a preheated muffle oven. The liquefaction experiments were carried out at temperatures 340, 360, 390 and 420 °C with the constant residence time of two hours. The yield of liquid, gaseous and solid products obtained was determined as follows. The yield of the liquid product was calculated as a sum of benzene solubles (oil)

and reaction water. The mass of gas formed was determined by the weight loss after opening the autoclave. The share of the solid residue was determined as the mass insoluble in benzene, the latter representing the residue after filtration and containing both the mineral matter and charred input material, dried in a thermostat at 105 °C for two hours to a constant mass. The coke yield was calculated by subtracting the mass of the mineral matter from the mass of the dried solid residue.

The elemental composition of the kukersite oil shale sample, peat, pine bark and the oils generated from these individual and combined feedstocks was examined by using Elementar Vario EL analyzer.

The functional group composition of oils obtained was investigated by FTIR-spectroscopy using an Interspec 2020 FTIR-spectrometer.

The group composition of the benzene-soluble oils was determined by thin-layer chromatography using plates 24×24 cm coated with a 2-mm silica gel layer (Fluka, 40). 0.5-g oil samples were analyzed and *n*-hexane as eluent was used. Three individual groups of hydrocarbons – aliphatic, mono-aromatic and polyaromatic ones –, and two groups of oxygen compounds – neutral and high-polar oxygen compounds – were separated and their share in total oil calculated.

3. Results

3.1. Liquefaction and co-liquefaction of kukersite oil shale and peat

The yields of liquid, gaseous and solid products obtained in an autoclave after thermochemical liquefaction of oil shale, peat and their mixture without solvent are presented in Table 2.

It can be seen that gas + water yield from peat alone exceeds 5-8 times that of oil and the maximum yield of oil forms at 390 °C, a temperature 30 °C higher than the optimal conditions for oil formation from kukersite (360 °C). As for solid residue, the addition of peat to kukersite decreases its share to 30.3% at the temperature (390 °C) of maximum oil yield (35.1%), while at the same optimal temperature for oil formation from peat it amounts to 52.4%, while at the optimal temperature (360 °C) for maximum oil production from kukersite oil shale the share of solid residue is 33.4%.

Table 2. Share of pyrolysis products of oil shale, peat and their mixture without solvents, % of the total yield

	Kukersite				Peat				Kukersite + peat (OM ratio 1:1)			
Temperature, °C	340	360	390	420	340	360	390	420	340	360	390	420
Oil	15.4	56.9	51.8	38.2	6.7	7.3	9.7	5.1	12.9	15.0	35.1	16.2
Gas + water,	11.5	9.7	13.2	41.7	37.8	38.3	38.1	43.2	24.2	26.9	34.6	46.5
Solid residue	73.1	33.4	35.0	20.1	55.5	54.4	52.2	51.7	62.9	58.1	30.3	37.3

The influence of solvents on the yield of pyrolysis products from individual feedstocks and the mixture of kukersite and peat in ratio 1 : 1 on OM basis is presented in Figures 1 and 2.
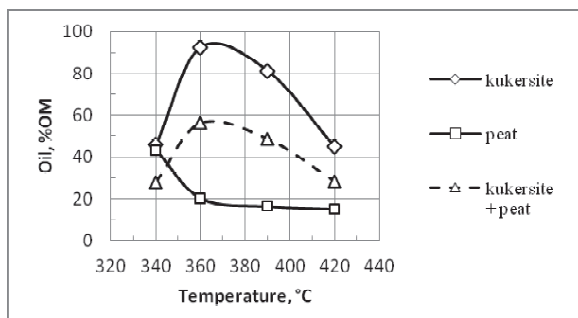

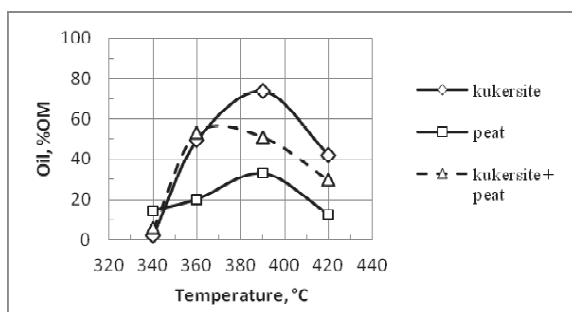Fig. 1. Oil yield *versus* temperature. Liquefaction in benzene.

Fig. 2. Oil yield *versus* temperature. Liquefaction in water.

As it can be seen from the figures, the yield of oil from peat with addition of benzene increases at 340 °C from 6.7% (Table 2) to 43.3%, but with the increasing temperature the oil yield decreases due to the presence of insoluble components in peat and formation of coke, while, as a result of using supercritical water, 33.3% of peat organic matter was transformed into an oily liquid. The addition of water to kukersite increases the oil yield in comparison with oil shale alone, but it also increases the temperature of maximum oil yield to 390 °C. The addition of benzene to kukersite has a significant influence on the oil yield giving 91%. As for the mixture, the oil yield was approximately the same at the same temperature 360 °C when

using both solvents. But due to higher price and toxity of benzene, the use of water seems to be more efficient.

Comparing different pyrolysis conditions and choosing solvent type most suitable for mixtures, it was found that addition of water at 360 °C may produce a significant synergistic effect (see Fig. 3).
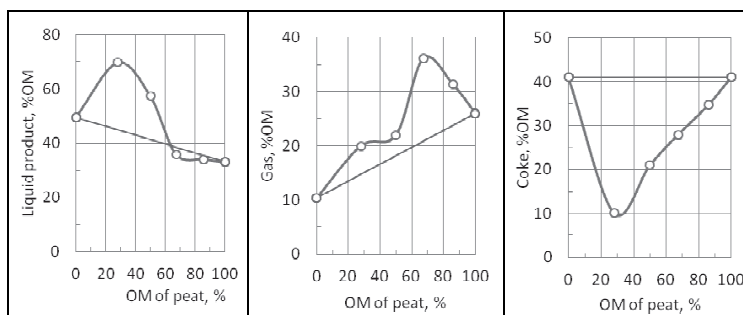

Fig. 3. The yield of liquid product, gas and coke *versus* kukersite-to-peat ratio in co-liquefaction of kukersite and peat in water medium at 360 °C.

In this case the liquid product yield from the mixture is 70% of OM, which is 24.8% more than the corresponding additive yields. The maximum gas yield obtained was 36%. Coke yield is maximum (40%) if kukersite and peat are liquefied individually. Liquefaction of the mixture decreases coke yield considerably, even four times (down to 10%).

At 340 °C a moderate synergistic effect was observed for the mixture without solvents.

3.2. Liquefaction and co-liquefaction of pine bark and kukersite oil shale

The yield of liquid, gaseous and solid products formed at thermochemical liquefaction of pine bark and oil shale + pine bark in the mixture in an autoclave without solvent are presented in Table 3.

Table 3. Share of pyrolysis products of pine bark and oil shale-pine bark mixture without solvents, % of the total yield

	Pine bark				Kukersite + pine bark (OM ratio 1:1)			
Temperature, °C	340	360	390	420	340	360	390	420
Oil	7.3	4.7	2.9	1.2	13.2	14.0	31.3	15.6
Gas + water	41.5	46.2	49.9	52.0	22.2	26.1	33.5	49.1
Solid residue	51.2	49.1	47.2	46.8	64.6	59.9	35.2	35.3

As it can be seen from the table, pine bark individually liquefied yields much more solid residue and gas + water than in oil soluble in benzene, especially at higher temperatures – the oil yield decreases from 7.3 to 1.2% with the temperature increasing from 340 to 420 °C. With the addition of oil shale the share of oil yield increases and achieves its maximum at 390 °C.

Figures 4 and 5 show the influence of added solvents on the yield of pyrolysis products from individual feedstocks and the mixture of kukersite and pine bark in ratio 1 : 1, on OM basis.
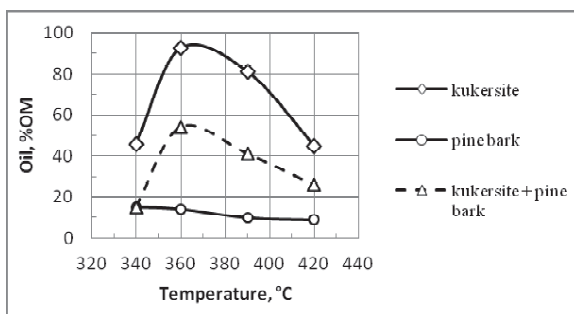

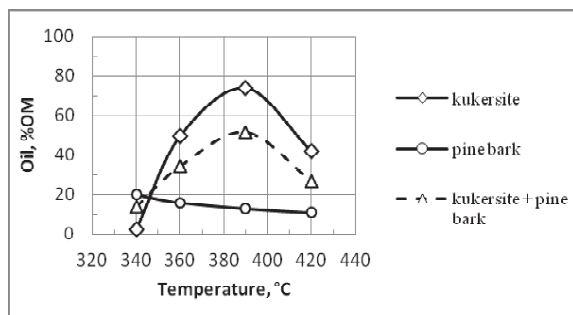Fig. 4. Oil yield *versus* temperature. Liquefaction in benzene.

Fig. 5. Oil yield *versus* temperature. Liquefaction in water.

As it can be seen, the yield of oil from pine bark is increased in the presence of solvents, benzene or water, but analogously to pine bark lique-faction alone, the quantity of oil decreases with the increasing temperature. At liquefaction of kukersite + pine bark in benzene the oil yield was increased to 52% at 360 °C, and thereafter, with increasing the temperature to 420 °C, decreased to 25%. Comparing the liquefaction of kukersite and

pine bark mixture in water and in benzene, one can see that the maximum oil yield recorded was 50%, but when using water as solvent, the maximum was achieved not at 360, but at 390 °C (see Fig. 5).
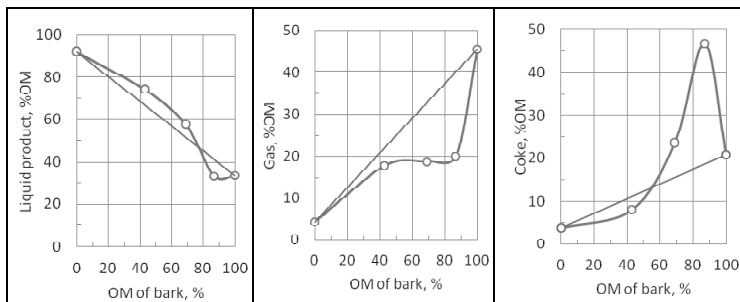

Fig. 6. The yield of liquid product, gas and coke *versus* kukersite-to-pine bark ratio at co-liquefaction of kukersite and pine bark in water medium at 390 °C.

One can see that synergism in the liquid product yield becomes evident when bark content of its mixture with kukersite is less than 80%. Gas yield at liquefaction of kukersite + pine bark was in all mixture ratios lower than that obtained at liquefaction of kukersite or bark individually. Also, it is clearly seen that the coke yield increases abruptly when bark content in the mixture exceeds 50%.

3.3. Liquefaction and co-liquefaction of kukersite oil shale, peat and pine bark: chemical composition of the products

3.3.1. Elemental composition

The results of the ultimate analysis of the initial feesdtocks and oils obtained are given in Table 4.

Table 4. Elemental analysis of the initial feedstocks and oils generated from the initial and combined feedstocks, % of organic matter

Element	Initial feedstock			Oil				
	Kuker-site	Peat	Pine bark	Kuker-site	Peat	Pine bark	Kukersite + peat (1:1)	Kukersite + pine bark (1:1)
C	78.4	57.1	52.3	82.4	75.0	76.2	78.4	78.6
H	9.3	7.2	6.3	10.1	7.3	9.0	8.7	8.8
N	0.1	2.6	0.5	0.2	0.5	0.4	1.3	0.7
S	1.3	2.6	−	0.7	0.3	0.1	1.0	1.0
O	10.9	33.1	40.9	6.6	16.9	14.3	10.6	10.9
H/C	1.426	1.514	1.449	1.472	1.169	1.419	1.333	1.345
O/C	0.104	0.435	0.590	0.060	0.169	0.141	0.101	0.104

One can see that the chemical composition of peat and pine bark biomass significantly differs from that of kukersite oil shale by lower content of carbon and hydrogen, as building blocks of hydrocarbons, and by much higher, (even 3–4 times) content of oxygen. Nevertheless, oxygen content of benzene-soluble oils is noticeably decreased amounting to 14.3–16.9% compared with 33.1–41.0% in the initial feedstocks. The most of oxygen has been transferred into gas and water.

3.4. Group composition of oils

FTIR-spectroscopic analysis was accomplished to determine the functional groups present in the benzene-soluble liquid fraction obtained at autoclaving of the following feedstocks: kukersite oil shale, kukersite oil shale blended with peat, and kukersite oil shale blended with bark.

Figure 7 shows that each of the three spectra displays absorptions at 725, 750, 1380, 1460, 2860, 2930, and 2960 cm^{-1} caused by methyl and methylene groups in aliphatic chains, and complex absorption bands at 750, 820, 880, 1020, 1080, 1600 and near 3000 cm^{-1} characteristic of aromatic compounds. Absorption at 1720 cm^{-1} refers to carbonyl groups and that at 3400 cm^{-1} is characteristic of hydroxyl groups. Absorptions in the region 1100–1250 and at 1600 cm^{-1} refer to ether groups and benzene derivatives, respectively. Also, one can see in Fig. 7 that oils obtained at thermochemical destruction of blended feedstocks – oil shale + peat and oil shale + pine bark biomass – show
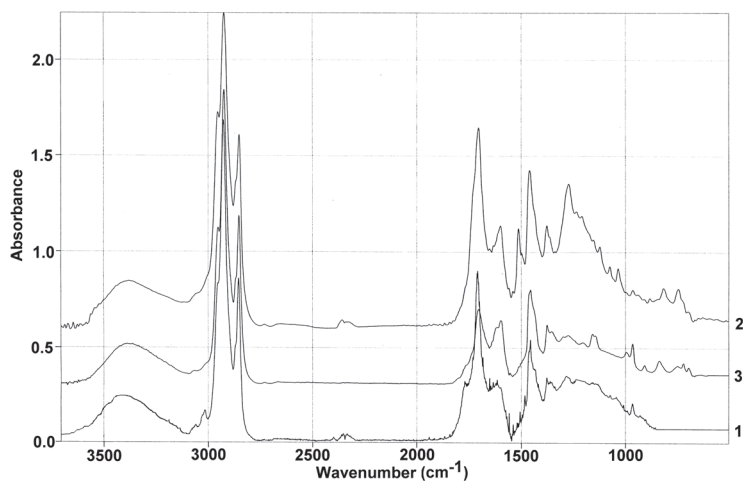

Fig. 7. FTIR-spectra of the benzene soluble oils formed at liquefaction of kukersite oil shale (1), kukersite oil shale + peat (2), and kukersite oil shale + pine bark (3) in an autoclave.

quantitative rather than qualitative differencies in the functional groups' composition compared with shale oil.

The group composition of oils determined by using thin-layer chromatography is presented in Table 5. One can see that neutral and high-polar oxygen compounds prevail, making up 75% of oils investigated. The oil obtained from kukersite differs from other two oils by lower content of monoaromatic hydrocarbons and higher share of polyaromatic hydrocarbons. To elevate hydrocarbon content of oils so as to approximate their chemical composition to that of natural petroleum, additional hydrogenation should be applied.

Table 5. Group composition of oils, %

Compounds	Kukersite	Kukersite + peat	Kukersite + pine bark
Aliphatic hydrocarbons	6.1	5.1	6.4
Monoaromatic hydrocarbons	1.2	3.4	4.1
Polyaromatic hydrocarbons	19.4	14.8	14.2
Neutral oxygen compounds	20.4	13.8	12.8
High-polar oxygen compounds	52.9	62.9	62.5

4. Conclusions

Liquefaction of both peat and pine bark biomass in the mixture with the kukersite oil shale at certain feedstock ratios leads to higher yields of liquid and gaseous products compared with liquefaction of peat and pine bark individually in the same conditions in an autoclave. Liquefaction of the individual and mixed feedstocks can be significantly accelerated in the presence of solvents. Besides, it is obvious that solvent addition decreases the temperature of the maximum oil yield from every kind of feedstock.

It was found that both solvents used increase the yield of oil from individual feedstocks as well as from their mixture in the 1 : 1 ratio studied in this work. The strongest synergistic effect was achieved by co-pyrolysis at 360 °C with water, in which case the liquid product yield from the kukersite-peat mixture is 70% of OM, which is 24.8% more than the corresponding additive yield.

It was found also that it is not rational to use mixture in which bark share is higher than 50%, because in this case oil and gas yields decrease, while coke quantity increases.

The liquid products obtained (including benzene-soluble oil) urgently need upgrading in order to be used as petroleum substitutes because of elevated oxygen content.

Compared with liquefaction of oil shale, that of oil shale mixture with peat or bark biomass generates less harmful gaseous emissions and considerably reduces the amount of solid waste used as landfill.

Acknowledgements

REFERENCES

1. Kumabe, K., Hanaoka, T., Fujimoto, S., Minowa, T., Sakanishi, K. Co-gasification of woody biomass and coal with air and steam. *Fuel*, 2007, **86**(5-6), 684–689.

2. Jones, J. M., Kubacki, M., Kubica, K., Ross, A. B., Williams, A. Devolatilisation characteristics of coal and biomass blends. *J. Anal. Appl. Pyrol.*, 2005, **74**(1), 502–511.

3. Moghtaderi, B., Meesri, C., Wall, T. F. Co-pyrolysis of coal and woody biomass. *Prepr. Symp. Am. Chem. Soc., Div. Fuel Chem.*, 2003, **48**(1), 363–364.

4. Meesri, C., Moghtaderi, B. Lack of synergetic effects in the pyrolytic characteristics of woody biomass/coal blends under low and high heating rate regimes. *Biomass Bioenerg.*, 2002, **23**(1), 55–66.

5. Collot, A.-G., Zhuo, Y., Dugwell, D. R., Kandiyoti, R. Co-pyrolysis and co-gasification of coal and biomass in bench-scale fixed-bed and fluidised bed reactors. *Fuel*, 1999, **78**(6), 667–679.

6. Vuthaluru, H. B. Investigations into the pyrolytic behaviour of coal/biomass blends using thermogravimetric analysis. *Bioresource Technol.*, 2004, **92**(2), 187–195.

7. Vuthaluru, H. B. Thermal behaviour of coal/biomass blends during co-pyrolysis. *Fuel Process. Technol.*, 2004, **85**(2–3), 141–155.

8. Moghtaderi, B., Meesri, C., Wall, T. F. Pyrolytic characteristics of blended coal and woody biomass. *Fuel*, 2004, **83**(6), 745–750.

9. Matsumura, Y., Nonaka, H., Yokura, H., Tsutsumi, A., Yoshida, K. Co-liquefaction of coal and cellulose in supercritical water. *Fuel*, 1999, **78**(9), 1049–1056.

10. Cordero, T., Rodríguez-Mirasol, J., Pastrana, J., Rodríguez, J. J. Improved solid fuels from co-pyrolysis of a high-sulphur content coal and different lignocellulosic wastes. *Fuel*, 2004, **83**(11–12), 1585–1590.

11. Ahmaruzzaman, M., Sharma, D. K. Characterization of liquid products obtained from co-cracking of petroleum vacuum residue with coal and biomass. *J. Anal. Appl. Pyrol.*, 2008, **81**(1), 37–44.

12. Sonobe, T., Worasuwannarak, N., Pipatmanomai, S. Synergies in co-pyrolysis of Thai lignite and corncob. *Fuel Process. Technol.*, 2008, **89**(12), 1371–1378.

13. Zhang, L., Xu, S., Zhao, W., Liu, S. Co-pyrolysis of biomass and coal in a free fall reactor. *Fuel*, 2007, **86**(3), 353–359.

14. Haykiri-Acma, H., Yaman, S. Synergy in devolatilization characteristics of lignite and hazelnut shell during co-pyrolysis. *Fuel*, 2007, **86**(3), 373–380.

15. Rafiqul, I., Lugang, B., Yan, Y., Li, T. Study on co-liquefaction of coal and bagasse by factorial experiment design method. *Fuel Process. Technol.*, 2000, **68**(1), 3–12.

16. Storm, C., Rüdiger, H., Spliethoff, H., Hein, K. R. G. Co-pyrolysis of coal/bio-mass and coal/sewage sludge mixtures. *J. Eng. Gas Turb. Power*, 1999, **121**(1), 55–63.

17. Oriňák, A., Halás, L., Amar, I., Andersson, J. T., Ádámová, M. Co-pyrolysis of polymethyl methacrylate with brown coal and effect on monomer production. *Fuel*, 2006, **85**(1), 12–18.

18. Sakurovs, R. Interactions between coking coals and plastics during co-pyrolysis. *Fuel*, 2003, **82**(15–17), 1911–1916.

19. Ballice, L., Reimert, R. Temperature-programmed co-pyrolysis of Turkish lignite with polypropylene. *J. Anal. Appl. Pyrol.*, 2002, **65**(2), 207–219.

20. Comolli, A. G., Ganguli, P., Stalzer, R. H., Lee, T. L. K., Zhou, P. The direct liquefaction co-processing of coal, oil, plastics, MSW, and biomass. *Prepr. Symp. Am. Chem. Soc., Div. Fuel Chem.*, 1999, **44**(2), 300–305.

21. Dadyburjor, D. B., Shaikh, H. Z., Zondlo, J. W. Co-liquefaction of coal and high-density polyethylene. *Prepr. Symp. Am. Chem. Soc., Div. Fuel Chem.*, 1999, **44**(2), 311–314.

22. Wang, L., Chen, P. Development of first-stage co-liquefaction of Chinese coal with waste plastics. *Chem. Eng. Process.*, 2004, **43**(2), 145–148.

23. Wang, L., Chen, P. Mechanism study of iron-based catalysts in co-liquefaction of coal with waste plastics. *Fuel*, 2000, **81**(6), 811–815.

24. Gimouhopoulos, K., Doulia, D., Vlyssides, A., Georgiou, D. Waste plastics–lignite co-liquefaction innovations. *Resour. Conserv. Recy.*, 1999, **26**(1), 43–52.

25. Ahmaruzzaman, M., Sharma, D. K. Non-isothermal kinetic studies on co-processing of vacuum residue, plastics, coal and petrocrop. *J. Anal. Appl. Pyrol.*, 2005, **73**(2), 263–275.

26. Luik, H. Chemicals and other products from shale oil. In: *UNESCO Encyclopedia of Life Support Systems*. Oxford UK, Publishers Co. Ltd, 2000.

27. Trikkel, A., Kuusik, R., Martins, A., Pihu, T., Stencel, J. M. Utilization of Estonian oil shale semicoke. *Fuel Process. Technol.*, 2008, **89**(8), 756–763.

28. *Ministry of the Environment Obtained Study Results on Semicoke Composition.* 11.04.2003. http://www.envir.ee/66671.

29. Alpern, B., Lemos de Sousa, M. J. Documented international enquiry on solid sedimentary fossil fuels; coal: definitions, classifications, reserves-resources, and energy potential. *Int. J. Coal Geol.*, 2002, **50**(1–4), 3–41.

30. Orru, M. (Ed.). *Estonian Peat Resources.* Tallinn, Geological Survey of Estonia, 1992, P. 146 (in Estonian).

31. Yao, S., Xue, C., Hu, W., Cao, J., Zhang, C. A comparative study of experimental maturation of peat, brown coal and subbituminous coal: Implications for coalification. *Int. J. Coal Geol.*, 2006, **66**(1–2), 108–118.

32. Lishtvan, I. Problems of peat production to be met with in Byelorussia. *Estonian Peat*, 1994, 3, 3–5 (in Estonian).

33. Orru, M. Production cost of surface peat. *Estonian Peat*, 1994, 1, 2–3 (in Estonian).

34. Björnbom, E., Björnbom, P. Some criteria for the selection of peat as a raw material for liquefaction. *Fuel*, 1988, **67**(11), 1589–1591.

35. Björnbom, P., Granath, L., Kannel, A., Karlsson, G., Lindström, L., Björnbom, E. Liquefaction of Swedish peats. *Fuel*, 1981, **60**(1), 7–13.

36. Orru, M. Basic properties of fuel peat. *Estonian Peat*, 1994, 1, 8–10 (in Estonian).

37. Sutcu, H. Pyrolysis of peat: Product yield and characterization. *Korean J. Chem. Eng.*, 2007, **24**(5), 736–741.
38. Fuchsman, C. H. *Peat: Industrial Chemistry and Technology*. New York, Academic Press, 1980.
39. McKendry, P. Energy production from biomass (part 1): overview of biomass. *Bioresource Technol.*, 2002, **83**(1), 37–46.
40. Mohan, D., Pittman, Jr., C. U., Steele, P. H. Pyrolysis of wood/biomass for bio-oil: A critical review. *Energ. Fuel*, 2006, **20**(3), 848–889.
41. Yaman, S. Pyrolysis of biomass to produce fuels and chemical feedstocks. *Energ. Convers. Manage.*, 2004, **45**(5), 651–671.
42. Tiikma, L., Johannes, I., Luik, H. Fixation of chlorine evolved in pyrolysis of PVC waste by Estonian oil shales. *J. Anal. Appl. Pyrol.*, 2006, **75**(2), 205–210.
43. Luik, H., Luik, L., Tiikma, L., Vink, N., Kozyreva, J. Upgrading shale oil heavy fractions with biomass via catalytical hydroprocessing. In: *Success & Visions for Bioenergy. Thermal processing of biomass for bioenergy, biofuels and bio-products* (Bridgewater, A. V., ed). (CD-ROM). CPL Scientific Publishing Services Ltd., 2007. 7 pp.
44. Luik, L., Luik, H., Bityukov, M., Kruusement, K., Sokolova, J., Tamvelius, H. Thermochemical co-liquefaction of biomass wastes and Estonian oil shale. In: *Success & Visions for Bioenergy. Thermal processing of biomass for bioenergy, biofuels and bioproducts* (Bridgewater, A. V., ed). (CD-ROM). CPL Scientific Publishing Services Ltd., 2007. 8 pp.
45. Luik, L., Luik, H., Vink, L., Kruusement, K., Veski, R. Thermochemical co-liquefaction of woody biomass and fossil fuel in supercritical water. In: *15th European Biomass Conference & Exhibition: From Research to Market Deployment*. Florence, Italy, 2007. ETA – Renewable Energies, WIP-Renewable Energies, 1955–1959.
46. Veski, R., Palu, V., Kruusement, K. Co-liquefaction of kukersite oil shale and pine wood in supercritical water. *Oil Shale*, 2006, **23**(3), 236–248.
47. Tiikma, L., Tamvelius, H., Luik, L. Coprocessing of heavy shale oil with polyethylene waste. *J. Anal. Appl. Pyrol.*, 2007, **79**(1–2), 191–195.
48. Luik, H., Palu, V., Tamvelius, H., Luik, L., Sokolova, J. Co-conversion of salix biomass and oil shale in the medium of supercritical water. In: *16th European Biomass Conference & Exhibition: From Research to Industry and Markets*. Proceedings of the International Conference, Valencia, Spain, 2–6 June 2008. Florence, Italy: ETA – Florence Renewable Energies; WIP – Renewable Energies. P. 2007–2009.

Article II

Sokolova, J. (Krasulina, J), Tiikma, L., Bityukov, M., Johannes, I. Ageing of kukersite thermobitumen. – *Oil Shale*, 2011, vol. 28, no. 1, pp. 4-18.

AGEING OF KUKERSITE THERMOBITUMEN

J. SOKOLOVA, L. TIIKMA, M. BITYUKOV, I. JOHANNES[*]

Tallinn University of Technology
Department of polymer materials
Laboratory of oil shale and renewables research
5 Ehitajate Rd., 19086 Tallinn, Estonia

Ageing of the mix of thermobitumen and oil (TBO) formed at low-temperature pyrolysis of kukersite in autoclaves was studied, and the effect of pyrolysis conditions on the share of fractions soluble in hexane, benzene and tetrahydrofurane was described. The results reveal a decrease in the total weight of TBO and solid residue at storage. During a month of ageing in open air the additional weight loss of the initial organic matter reaches 10-15%. At that, the yield of TBO decreases and that of the solid residue increases. The fractions of TBO soluble in hexane (maltenes + oil) and in benzene (asphaltenes) decrease, and the fraction soluble in tetrahydrofurane (pre-asphaltenes) increases.

The initial yields of hexane and benzene solubles depend on the degree of TBO secondary cracking determined by the pyrolysis conditions. The share of the fraction soluble in hexane increases with pyrolysis temperature and duration and attains 40–50% from the initial organic matter on account of decomposition of asphaltenes concurred with decrease in the total yield of TBO to 60–70% because of gas and coke formation.

Introduction

The continually increasing demand for liquid fuels and steadily decreasing petroleum reserves have intrigued investigations aimed at more complete transformation of oil shale organic matter into liquid fuels.

The previous works have shown that the recovery of kukersite organic matter (OM) can be enhanced by its extraction with superheated solvents [1, 2] or by low-temperature pyrolysis of the shale at 340–380 °C [3–6] and subsequent dissolution of the high-molecular (650-1300 u) semi product, thermobitumen (TB), remained in the cubic residue in open retorts or of the mix of thermobitumen and oil (TBO) formed in autoclaves. Under the optimum conditions where the initial kerogen has decomposed almost entirely into TBO but its secondary cracking into coke has scarcely started,

---

[*] Corresponding author: e-mail *ille.johannes@ttu.ee*

the high (up to 90%) extraction yield of TBO from the initial organic matter can be obtained in both devices.

A theoretical basis for the new technology describing the co-effects of pyrolysis duration, nominal temperature and non-linear heating rate on the kinetics of phase transformations in the both laboratory devices by a unified mathematical model was proposed [7–9]. The rate factors and apparent kinetic constants for the parallel decomposition patterns of kerogen into extract (TBO in an autoclave and TB in a retort) and volatiles (gas in auto-claves, and oil and gas in retorts), and for the secondary parallel decomposition of TBO in autoclaves or TB in retorts into gas and coke were estimated.

The next challenge would be the further upgrading of the TBO obtained into liquid fuels by hydrogenation. At that, the first problem revealed in the works mentioned above is instability of the extracts evident from formation of a solid phase in the solutions of TBO during storage.

Ageing of oil shale TBO has not been studied earlier. The structure of TBO that is far being fully understood is quite complex. At that, the free radicals evoking during thermal decomposition may take part in irreversible ageing reactions as polymerization, polycondensation and oxidation, and evaporation of lighter components.

The widely used analytical method chromatography, coupled with mass-spectrometry (GC-MS or LC-MS) is limited by volatility or solubility and cannot readily be adapted to examine high-molecular-mass materials. Currently, above the 450–500 u range, no single method is unambiguously capable of indicating molecular mass distribution or chemical structural features in complex fuel-derived mixtures, and advances in this field require a comparison of several independent analytical methods [10].

At the present time, 95% of the almost 100 Mt of natural and artificial bitumen obtained as the vacuum residue of petroleum distillation, are applied as asphalt mixes in the paving industry. Mainly rheological methods have been proposed to replicate the effect of ageing aimed to foresee bitumen behaviour during application and service life. In this field the first concern has been the effect of time on the viscosity at blending of hot mixes to be pumpable and to allow homogeneous coatings. Second, the coating has to become stiff enough to resist rutting at high pavement temperatures and, oppositely, soft enough to resist cracking at the lowest temperatures. Viscosity, penetration, softening point, and weight loss tests were applied to investigate the rheological properties of fresh and aged Arabian asphalts [11]. It has been shown [12, 13] that ageing produces fundamental modifica-tions in the colloidal structure of both vacuum residues and their maltenes fractions shifting all the solubility classes (asphaltenes, resins and saturates plus aromatics) towards the preceding, adjacent less soluble class. However, in contrast to the previous findings, the macrostructure of asphaltenes both in solutions and in a vacuum residue was found not being representative of the age hardening process, in spite of the fact that the content of asphaltenes increased and the ratio of resins, aromatics and saturates against asphaltenes

decreased being strongly dependent on temperature ranges [14]. The chemical changes during ageing of several bitumens have been found to include the formation of carbonyl compounds and sulfoxides, and to increase in amount of large molecular associations and polydispersity [15].

Lamontagne [16] has shown, basing on the indexes of aromaticy ($A_{1600}/\Sigma A$), aliphatic [$(A_{1460} + A_{1376})/\Sigma A$], carbonyl ($A_{1700}/\Sigma A$) and sulphoxide ($A_{1030}/\Sigma A$) where $\Sigma A = A_{1700} + A_{1600} + A_{1460} + A_{1376} + A_{1030} + A_{864} + A_{814} + A_{743} + A_{724} + A_{2953,2923,2862}$, that an hour of oxidation of road bitumens by the air inside a FTIR heated (163 °C) cell is equivalent to two years of ageing on site. This work demonstrated that during the first two years, an increase in aromatisation was observed.

Masmoudi [17] measured by FTIR a decrease in instauration index and an increase in carbonyl index during stability studies of cosmetic "oil in water" emulsions taking as instauration index $A_{3006}/(A_{3006} + A_{2921} + A_{2851})$ and as carbonyl index $A_{1746}/\Sigma A$ (the sum of the area between 1800 and 650 cm^{-1}).

The over-year ageing of an hydrocracked extract of coal was examined using size exclusion chromatography assessed in terms of shorter elution times and parallel changes in UV-fluorescence spectra [18]. The extent of the changes in the first week of the study was significant. No further changes were detected after the first month. At that, the ageing phenomenon was more marked for the product kept at room temperature in the air than in a freezer in a non-oxidising atmosphere. It was supposed that the changes observed involve the formed less reactive free radicals that have not reacted during the hydrocracking reaction itself.

The most part of thermobitumen consists of difficult to process asphaltenes, the high-molecular very complex compounds insoluble in *n*-hexane (*n*-pentane) but soluble in benzene (toluene). Asphaltenes are made up from units of condensed aromatic nuclei carrying alkyl groups and hetero elements. The difference in the size of units and chemical structure of asphaltenes depend on their source. The tendency of asphaltenes to aggregate distinguishes them from other oil constituents. According to Evdokimov [19], asphaltenes form aggregate-free solutions only at concentrations below 1–5 mg/l, between 10–20 mg/l dimers become the predominant species, while at concentrations 90–100 mg/l quasispherical dimer pairs are formed, whereas Beer's law is fulfilled only at concentrations exceeding 700 mg/l. In more diluted solutions a non-monotonic multi-peak relationship exists in the plot of absorbencies versus concentrations at any wave-length. On the contrary, a linearity of that plot was demonstrated in the range 0–400 mg/l of asphaltenes at 532 nm in [20]. Later, kinetics of asphaltenes aggregation was studied by conifocal microscopy [21]. The authors concluded that the aggregation process depended on the nature of the crude oil studied, and it was affected by the asphaltenes concentration.

Thermo-optical studies of solutions of asphaltenes in toluene and tetra-hydrofurane [22] have shown that the solvent molecules can be trapped

during aggregation of asphaltenes resulting in minimum diffusivities (D) before 50 mg/l and an increase in D at higher concentrations until a constant value is reached near 2000 mg/l.

Basing on the Hansen solubility parameter for bitumen determing solubility data of bitumen in a set of 48 solvents with known solubility parameters, Masmoudi [23] found that the asphaltenes may be dissolved in the maltenes rather than dispersed, indicating that no asphaltene micelles can exist. It was shown that the small difference between solubility parameters of asphaltenes and maltenes of the paving asphalt contributes to its good aging resistance [24].

Ageing of bio-oils, in some ways, analogous to the behaviour of asphaltenes found in petroleum, was observed as a viscosity increase and some phase separations. This instability is believed to result from a breakdown in the stabilized micro emulsion and to chemical reactions, which continue to proceed in the oil [25].

The artificial maturation of asphaltenes has been studied by hydrous and confined pyrolysis. The results support the idea that a competition between water and hydro-aromatics as hydrogen sources exists in hydrogen transfer reactions [26]. It was suggested that hydrogen transfer reactions between water and the newly formed hydrocarbons are catalyzed by the asphaltenes.

Besides, alteration of the share of the maltenes and asphaltenes with pyrolysis conditions should affect the hydrogenation results. For example, the formation of two structurally different cokes during thermal hydro-cracking of Tabasco bitumen is attributed to differences in coking properties of the asphaltenes and the deasphalted heavy oils [27].

In this work, the ageing of TBO obtained at low-temperature pyrolysis of kukersite in autoclaves is studied for the first time, and the effect of pyrolysis conditions on the yield of hexane and benzene soluble fractions is described.

Experimental

In all the experiments 4.0 g of finely powdered (0.04-0.1 mm) kukersite, containing 0.9% moisture and 40.15% organic matter (OM) were poured into a glass tube with inner diameter 8 mm, weighed and put into a 20-cm^3 micro-autoclave. The autoclaves were placed in a muffle oven at room temperature. The desired nominal temperature (360–410 °C) was reached during 100 min. After two hours residence time the autoclaves were cooled to room temperature and opened. The mass of gas formed was determined by the weight loss after discharging. The solid residue was not removed from TBO to avoid any loss of the lighter fractions during evaporation of the organic solvents applied. So, it was possible to find out that the mass of the pyrolyzed products decreased with time. The samples were weight in open and closed tubes kept at room temperature and in a refrigerator during

3 months. After different durations of the storage, the solid pyrolyzed product was extracted exhaustively in Soxhlet extractor successively with hexane, benzene and tetrahydrofurane. The mass of the corresponding extracts – so-called maltenes, asphaltenes and pre-asphaltenes, was found from the decrease in the sample mass at the extraction after drying of the corresponding residue. The extracts obtained were dissolved in 100-ml measuring flasks. The absorbance of the solutions was recorded on the spectrophotometer SPECOL 10 at wave lengths 420–450 nm. At that, the too dark solutions of asphaltenes and pre-asphaltenes were diluted in the ratio 1:10 with tetrahydrofurane.

Iodine value for hexane and benzene extracts was determined according to ASTM D-1959.

Results and discussion

Ageing

Changes in the yield of the phases

Several series of pyrolysis experiments in the six on hand micro autoclaves were conducted in this study. The heating time (100 min.) up to the nominal temperature (380 °C) was chosen, like it was made in the major autoclaves (500 cm^3) used, and followed by two hours isothermal retention. Distribution of the pyrolysis products between the three phases: gas, hexane + benzene extract (TBO) and organic solid residue is depicted in Fig. 1.

One can see from Fig. 1 that the experimental results obtained in different series fluctuate. Nevertheless, a continuous increase in the yields of volatiles and solid residue on account of the target product, TBO, is evident at ageing.
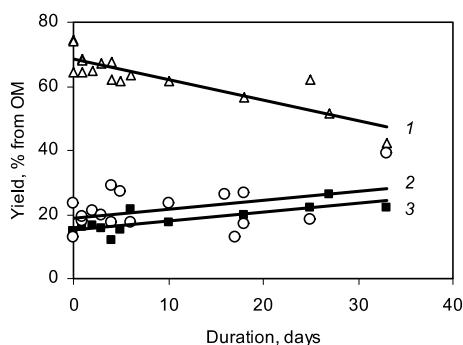

Fig. 1. Effect of ageing on the yield of different phases, % from initial OM: Total hexane and benzene extract, TBO (curve *1*), gas (curve *2*), and solid residue, coke and THF extract (curve *3*).

These changes in time (t) can be approximated to the following linear relationships:

$$Y(\text{Gas}) = 18.6(\pm1.6) + 0.39(\pm0.11)t \tag{1}$$

$$Y(\text{Extract}) = 68.5(\pm1.4) - 0.58(\pm0.10)t \tag{2}$$

$$Y(\text{Solid residue}) = 15.2(\pm1.0) + 0.222(\pm0.073)t \tag{3}$$

The experiments above revealed an unexpected result – the mass of pyrolysates consisting of TBO and solid residue decreased at ageing. This phenomenon was studied in more details monitoring in time the weight of the glass tubes containing pyrolysates obtained at different nominal temperatures in several parallel experiments from different series. The results presented in Fig. 2 prove that, independently of the initial gas yield depending on the pyrolysis conditions, a sharp increase in the yield of volatiles occurs during the first week of ageing followed by a trivial monotonous increase even after three month.

Noteworthy is that when the initial gas yield is subtracted from the current yield (curve 4), the loss of volatiles stored under the same conditions practically coincides independently from the pyrolysis temperature. It suggests that evolution of the light components dissolved and saturating TBO can take place. The opinion is supported by the fact that storage of the glass tubes with pyrolysate under different conditions (Fig. 3) affects the weight loss.

So, the rate of weight loss at room temperature (curve *1*) overcomes that in the refrigerator (curve *2*), both approaching the same constant value. Probably, in open air the content of volatiles at equilibrium conditions between TBO and gas phase approaches the total exhaustion of the light
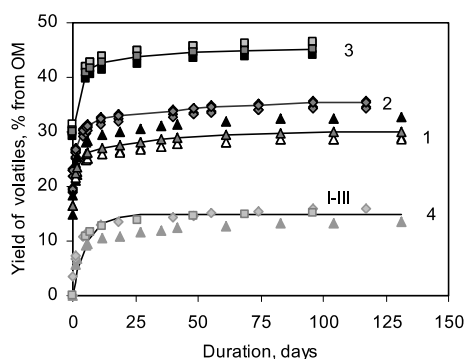

Fig. 2. Effect of ageing on the total yield of volatiles from the pyrolysate obtained at nominal temperatures, °C: 360 (curve *1*), 380 (curve *2*), 410 (curve *3*), and on the corresponding weight losses at room temperature storage (points *I-III*, curve *4*). Points experimental, curves calculated means.
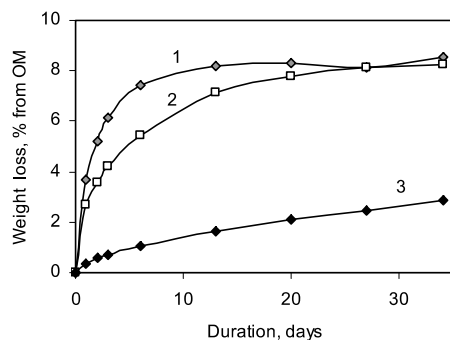
Fig. 3. Effect of ageing conditions on the weight loss of pyrolysate at storage in open tubes at room temperature (curve *1*), in open tubes in a refrigerator (curve *2*) and in closed tubes at room temperature (curve *3*).

fractions in TBO. Somewhat surprising weight loss of the closed tube (curve 3) can be explained by the volatiles leaving through the cork under the gas pressure increasing with time.

Extracts
The results obtained extracting the pyrolysates after different storage duration in Soxhlet apparatus subsequently with hexane (here and after maltenes), benzene (asphaltenes) and tetrahydrofurane (pre-asphaltenes) are presented in Fig. 4.

The experimental points in the figure show again pretty diffusive clouds of the extract yields, probably because the pyrolysates from different series
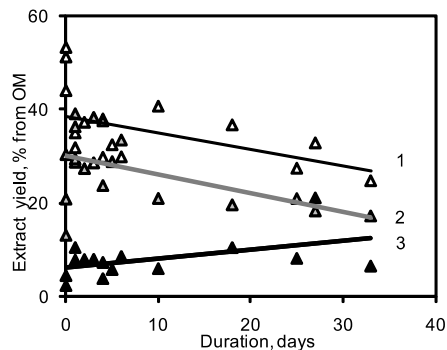

Fig. *4.* Effect of ageing on the yield of the fractions soluble in hexane (curve *1*), benzene (curve *2*) and tetrahydrofurane (curve *3*).

were applied for extraction. Yet, the results prove that the decrease in TBO yield described above by curve 1 in Fig. 1 is compiled from decreases in the yield of both maltenes and asphaltenes, and the yield of solid residue increases due to the increase in the yield of preasphaltenes. The changes can be approximated to linear relationships as follows:

$$Y(\text{Maltenes}) = 38.4(\pm2.3) - 0.31(\pm0.17)t \qquad (4)$$

$$Y(\text{Asphaltenes}) = 29.8(\pm2.2) - 0.42(\pm0.16)t \qquad (5)$$

$$Y(\text{Pre-asphaltenes}) = 5.8(\pm1.4) + 0.14(\pm0.10)t \qquad (6)$$

It can be concluded that a condensation of the both TBO fragments takes place at ageing. The noteworthy changes in the group composition of the extracts are evident in the results of thin layer chromatography presented in Fig. 5.

A decrease in the share of aliphatic compounds in the hexane fraction could be explained by their volatilization from the pyrolysate. Appearance of Nhet, PCHC and MCHC in benzene fraction, and the decrease in the share of HPhet compounds in benzene and tetrahydrofurane can be explained by their aggregation. As far the yields of the extracts are different, it is more informative to compare the changes of the compounds by yields of the chemical groups from the initial kerogen (Table 1). The results in Table 1 explain that depicted in Fig. 1 decrease in the total yield of the extract at ageing takes place mainly in the fraction of hexane soluble, especially aliphatic hydrocarbons, and in the fraction of high-polar heterocompounds precipitating due to stabilization of the unsaturated intermediate products by aggregation.

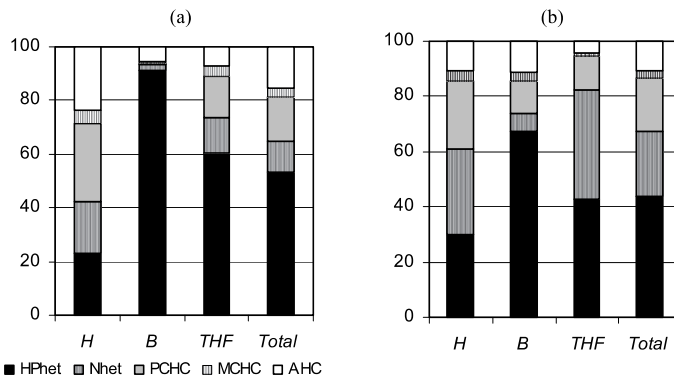

Fig. 5. Chemical group composition of the fractions soluble in hexane (column *H*), benzene (column *B*), tetrahydrofurane (column *THF*) and total extract (*Total*) separated from the fresh pyrolysate (*a*) and after its 34 days ageing (*b*).

Table 1. **Effect of ageing on the yield of chemical groups at subsequent extraction of the pyrolysate into hexane (H), benzene (B) and tetrahydrofurane (THF), % from OM**

Compound	After 0 day				After 34 days			
	H	*B*	*THF*	*Total*	*H*	*B*	*THF*	*Total*

Hydrocarbons:
    aliphatic (AHC)
    aromatics:
	9.02	1.70	0.17	10.89	3.15	2.01	0.22	5.38

monocyclic (MCHC)	1.96	0.06	0.08	2.10	1.01	0.53	0.05	1.59
polycyclic (PCHC)	11.17	0.24	0.35	11.76	7.10	2.05	0.60	9.75
Neutral hetero compounds (Nhet)	7.30	0.57	0.30	8.17	9.04	1.21	1.97	12.22
High polar hetero-compounds (HPhet)	8.95	27.24	1.37	37.56	8.57	11.86	2.11	22.54
Total yield of the extract	38.40	29.81	2.27	70.48	28.87	17.66	4.95	51.48

Iodine value

Estimation of an unsaturation characteristic, iodine value, depicted in Fig. 6, reveals that there is no practical change in the iodine values of remaining soluble malthenes and asphaltenes (clouds of experimental points *1* and *2*) at ageing.

The mean iodine value for maltenes is 15.6 g/100 g and for asphaltenes 26 g/100 g. But iodine value of the total pyrolysate including solid residue (experimental points *3*) shows a tendency to decrease a little according to the trendline

$$Y \text{ (Iodine value of total pyrolysate)} = 39.1 - 0.42t \qquad (7)$$

According to Fig. 1 the yield of solid residue increases with time. Obviously, such a precipitation of maltenes and asphaltenes by condensation
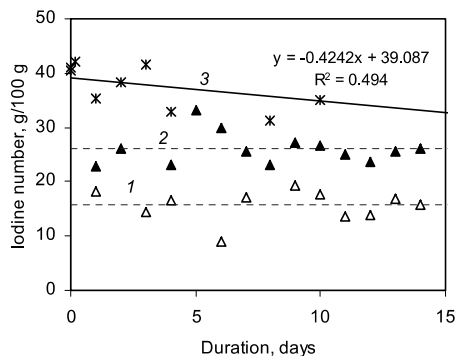

Fig. 6. Effect of ageing on the iodine number of the fractions soluble in hexane (curve *1*), benzene (curve *2*) and total OM in the pyrolysate (curve *3*).

on account of their double bonds and unsaturated radicals decreases the total iodine value of the pyrolysate. The remaining dissoluted maltenes and asphaltenes do not change their unsaturation degree per mass unit.

Discussion

Independently on the mine and content of mineral matter, the kerogen of kukersite is unique in composition, and products of its thermal decomposition contain large quantities of acid and neutral oxygen compounds as well as unsaturated, saturated, and aromatic hydrocarbons. According to Lille [28] the macromolecules of kerogen are highly aliphatic, with the ratio of aliphatic to aromatic carbons *ca* 4–5. The model of the kerogen empirical formula is $C_{421}H_{638}O_{44}S_4NCl$ which corresponds to the elemental composition, %: C − 76.9; H − 9.7; O − 10.7; S − 1.9; N − 0.2; Cl − 0.5, and the atomic ratio of H/C 1.515. The composition and physical characteristics of polycomponental TB reflect the structural groups of kerogen and depend on pyrolysis conditions. There were found various polycyclic compounds of different molecular masses in the composition of TB. For example after pyrolysis of the kerogen concentrate during 132 hours at 330 °C and 4 hours at 360 °C, Kask [29] estimated the elemental composition of thermobitumen as follows, %: C − 86.9 and 83.6; H − 8.43 and 9.56; O+N − 4.4 and 6.3; S − 0.40 and 0.50, and the corresponding atomic ratio of H/C 1.16 and 1.37. The decrease in the H/C ratio in TB and the high content of oxygen can be the main causes of TB ageing.

The experimental results above have revealed that at ageing of the pyrolysate obtained at low-temperature pyrolysis of kukersite in an autoclave an aggregation of the compounds takes place that shifts maltenes and asphaltenes to the preceding adjacent class − pre-asphaltenes and solid residue, and the content of aliphatic, monocyclic and polycyclic hydrocarbons soluble in hexane decreases and those soluble in benzene increases. The aggregation might be resulted by chemical condensation reactions between phenolic and neutral oxygen groups or by formation of hydrogen bonded complexes between oxygen-containing molecules. At the same time an opposite process takes place − the yield of the volatile phase increases. It might be supposed that the weight decrease would be brought about volatile side-products of condensation or just by evolution of trapped in TBO light fractions. A decrease in the yield of aliphatic hydrocarbons supports rather the latter idea. The chemical changes in the products will be a challenge of the future works.

Effect of pyrolysis conditions on the share of maltenes and asphaltenes in TBO

The experimental results above have revealed that asphaltenes overcome malthenes in their ageing rate and iodine number. Besides, production of liquid fuels by hydrogenation from asphaltenes is more complicated than from maltenes. So, conditions where maltenes prevail would be of interest. It

is known that the share of maltenes and asphaltenes in TBO depends on the pyrolysis conditions [4], but the effect is not quantitatively clear.

In this part of work, the effects of pyrolysis temperature and duration on the yield of maltenes and asphaltenes from oil shale were elaborated.

Basing on the photometric measurements described in [19–21] an attempt was done to evaluate the effect of main factors of the low-temperature pyrolysis on changes in the optical densities (E) of the solutions (Fig. 7).
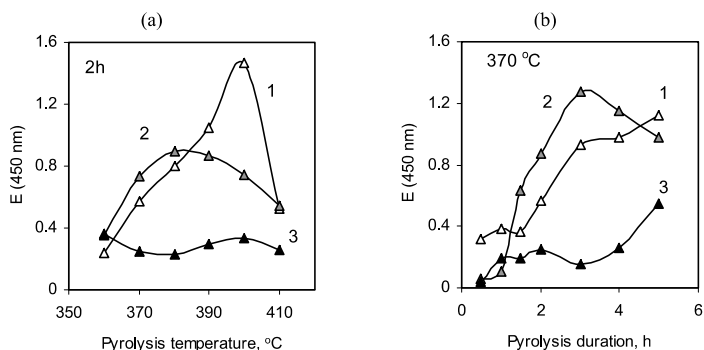

Fig. 7. Effect of pyrolysis nominal temperature (*a*) and pyrolysis duration (*b*) on the optical density of the solutions of the fractions soluble in hexane (curve *1*), benzene (curve *2*) and tetrahydrofurane (curve *3*).

The results obtained prove that at 2-h duration the maximum in optical density of the hexane solutions occurs at 400 °C, and of the benzene solutions at 380 °C, whereas the temperature effect is insignificant for the tetrahydrofurane solutions. The increasing duration increases optical density of the hexane and tetrahydrofurane solutions on account of the benzene solution at 370 °C.

Building of calibration curves evidences that the special absorbance per gram of the extracts having pale yellow to dark brown colour increased in the row: maltenes<asphaltenes<<pre-asphaltenes. The graphs obtained by dilution of any definite sample followed good linearity. But the graphs built using diluted extracts from different pyrolysis series resulted in a cloud of discursive experimental points with quite unsatisfactory linear regression. Besides, the solutions became darker and turbid in time. Therefore, the optical density measurements were excluded in the further study.

The analogous but much more informative and authentic is depiction of the effect of pyrolysis conditions on the yield of the main products. The effect of pyrolysis nominal temperature on the yield of products extracted on the next day after 2-h pyrolysis duration is given in Fig. 8a. One can see that an increase in the temperature increases the yield of gas, and decreases the

yield of asphaltenes and pre-asphaltenes, whereas the yield of maltenes has its maximum at 400 and the yield of solid residue its minimum at 370 °C. The effect of pyrolysis duration on the yield of products at the temperature found as the maximum for separation of OM from mineral matter, 370 °C, is presented in Fig. 8b. The results show that the changes in the yields with increase in duration are analogous to the increase in temperature – the decomposition degree of the products increases, whereas preasphaltenes and organic solid residue have a minimum before the secondary cracking of asphaltenes starts. At 410 °C and after two hours also decomposition of the benzene solubles starts. The behaviour of the curves explains that the secondary cracking of asphaltenes increases mainly the yield of benzene solubles but unwontedly also the coke and gas yields.

Fig. 8. Effect of pyrolysis nominal temperature (*a*) and duration (*b*) on the yield of the fractions soluble in hexane (curve *1*), benzene (curve *2*), and of the total TBO (curve *1+2*), gas (curve *3*) and solid organic residue (curve *4*). Heating-up time 100 min.

In all the experiments above the heating-up time was 100 minutes. The data in Table 2 explain that when the heating-up time is shorter the yields of gas, TBO and pre-asphaltenes decrease, the yield of solid residue increases, whereas the yield of asphaltenes has a maximum and that of maltenes a minimum. The results prove that under the pyrolysis duration 2 hours and nominal temperature 370 °C formation of TBO and its secondary cracking start before the nominal temperature is attained.

The experimental results in Figures 8*a* and 8*b* and Table 2 agree with the maximum in the yield of total TBO and minimum of the organic solid residue under an appropriate combination of pyrolysis temperature and duration described earlier mathematically in [7, 8].

Table 2. **Effect of heating up time to 370 °C on the yield of kerogen decomposition products, % from OM**

Product	Heating-up time, min, and (rate, °/min)		
	6 (58)	60 (5.8)	100 (3.5)
Gas	8.38	9.73	10.18
Maltenes + oil	12.3	10.45	28.24
Asphaltenes	65.67	69.66	52.43
TBO	77.97	80.11	80.67
Pre-asphaltenes	1.15	4.15	4.8
Organic solid residue	14.73	7.26	5.7

Conclusions

The target product, a mix of thermobitumen and oil (TBO), forming at low-temperature (360-410 °C) pyrolysis of oil shale in autoclaves, is not stable. The following phenomena have been revealed at storage of the product:

- An additional volatilization of the light fractions captured in the sticky TBO leads to the continuous decrease in the weight of the total product. Independently of the pyrolysis temperature, the weight loss reaches in open air 10–15% from the initial organic matter during a month of ageing.
- The yield of extractable with organic solvents products decreases on account of the increasing yields of solid residue and gas.
- The yields of hexane solubles (maltenes + oil) and benzene solubles (asphaltenes) decrease and of tetrahydrofurane solubles (pre-asphaltenes) increases.
- The main decrease in the hexane solubles takes place in the most preferable fraction – aliphatic hydrocarbons – and also in the fraction of aggregating high polar heterocompounds.
- The initial yield of maltenes and asphaltenes at pyrolysis depends on the degree of secondary cracking of TBO. The share of the hexane-soluble fraction increases with pyrolysis temperature and duration and attains 40-50% from the initial organic matter on account of the decrease in the total yield of TBO to 60-70%.
- The process of upgrading of TBO to liquid fuels by hydrogenation should follow the pyrolysis process as soon as possible to avoid any loss at ageing.

Acknowledgements

REFERENCES

1. *Luik, H., Palu, V., Bitjukov, M., Luik, L., Kruusement, K., Tamvelius, H., Pryadka, N.* Liquefaction of Estonian kukersite oil shale kerogen with selected superheated solvents in static conditions // Oil Shale. 2005. Vol. 22, No. 1. P. 25–36.
2. *Luik, H., Luik, L.* Extraction of fossil fuels with sub- and supercritical water // Energ. Source. 2002. Vol. 23, No. 5. P. 449–459.
3. *Zaidentsal, A. L., Soone, J. H., Muoni, R. T.* Yields and properties of thermal bitumen obtained from combustible shale // Solid Fuel Chem. 2008. Vol. 42, No. 2. P. 74–79.
4. *Tiikma, L., Zaidentsal, A., Tensorer, M.* Formation of thermobitumen from oil shale by low-temperature pyrolysis in an autoclave // Oil Shale. 2007. Vol. 24, No. 4. P. 535–546.
5. *Tiikma, L., Johannes, I., Luik, H., Zaidentsal, A., Vink, N.* Thermal dissolution of Estonian oil shale // J. Anal. Appl. Pyrol. 2009. Vol. 85, No. 1–2. P. 502–507.
6. *Tiikma, L., Sokolova, Yu., Vink, N.* Effect of the concentration of organic matter on the yield of thermal bitumen from Baltic oil shale Kukersite // Solid Fuel Chem. 2010. Vol. 44, No. 2. P. 89–93.
7. *Johannes, I., Zaidentsal, A.* Kinetics of low-temperature retorting of kukersite // Oil Shale. 2008. Vol. 25, No. 4. P. 412–425.
8. *Johannes, I., Tiikma, L., Zaidentsal, A., Luik, L.* Kinetics of kukersite low-temperature pyrolysis in autoclaves // J. Anal. Appl. Pyrol. 2009. Vol. 85, No. 1–2. P. 508–513.
9. *Johannes, I., Tiikma, L., Zaidentsal, A.* Comparison of the thermobituminization kinetics of Baltic oil shale in open retorts and autoclaves // Oil Shale. 2010. Vol. 26, No. 1. P. 17–25.
10. *Herod, A. A., Bartle, K. D., Kandiyoti, R.* Characterization of heavy hydrocarbons by chromatographic and mass spectrometric methods: An overview // Energ. Fuel. 2007. Vol. 21, No. 4. P. 2176–2203.
11. *Siddiqui, M. N., Ali, M. F.* Studies on the ageing behaviour of the Arabian asphalts // Fuel. 1999. Vol. 78, No. 9. P. 1005–1015.
12. *Leseur, D.* The colloidal structure of bitumen: consequences on the rheology and on the mechanisms of bitumen modification // Adv. Colloid Interface Sci. 2009. Vol. 145, No. 1–2. P. 42–82.
13. *Mastrofini, D., Scarsella, M.* The application of rheology to the evaluation of bitumen ageing // Fuel. 2000. Vol. 79, No. 9. P. 1005–1015.
14. *Scarsella, M., Mastrofini, D., Barré, L., Espinat, D., Fenistein, D.* Petroleum heavy ends stability: Evolution of residues macrostructure by ageing // Energ. Fuel. 1999. Vol. 13, No. 3. P. 739–747.
15. *Lu, X., Isacsson, U.* Effect of ageing on bitumen chemistry and rheology // Constr. Build. Mater. 2002. Vol. 16, No. 1. P. 15–22.
16. *Lamontagne, L., Dumas, P., Mouillet, V., Kister, J.* Comparison by Fourier transform infrared (FTIR) spectroscopy of different ageing techniques: application to road bitumens // Fuel. 2001. Vol. 80, No. 4. P. 483–488.
17. *Masmoudi, H., Dréau, Y. L., Piccerelle, P., Kister, J.* The evaluation of cosmetic and pharmaceutical emulsions aging process using classical techniques and a new method: FTIR // Int. J. Pharm. 2005. Vol. 289, No. 1–2. P. 117–131.

18. *Begon, V., Suelves, I., Herod, A. A., Dugwell, D. R., Kandiyoti, R.* Structural effects of sample ageing in hydrocracked coal liquefaction extracts // Fuel. 2000. Vol. 79, No. 12. P. 1423–1429.

19. *Evdokimov, I. N., Eliseev, Y. N., Akhmetov, B. R.* Assembly of asphaltenes molecular aggregates as studied by near-UV/visible spectroscopy: II. Concentration dependencies of absorptivities // J. Petrol. Science. Eng. 2003. Vol. 37, No. 3–4. P. 145–152.

20. *Castillo, J., Hung, J., Fernández, A., Mujica, V.* Nonlinear optical evidences of aggregation in asphaltene-toluene solutions // Fuel. 2001. Vol. 80, No. 9. P. 1239–1243.

21. *Hung, J., Castillo, J., Reyes, A.* Kinetics of asphaltenes aggregation in toluene-heptane mixtures studied by confocal microscopy // Energ. Fuel. 2005. Vol. 19, No. 3. P. 898–904.

22. *Acevedo, S., Ranaudo, M. A., Pereira, J. C., Castillo, J., Fernández, A., Pérez, P., Caetano, M.* Thermo-optical studies of asphaltene solutions: evidence for solvent-solute aggregate formation // Fuel. 1999. Vol. 78, No. 9. P. 997–1003.

23. *Redelius, P.* Bitumen solubility model using Hansen solubility parameter // Fuel. 2004. Vol. 18, No. 4. P. 1087–1092.

24. *Yang, P., Cong, Q., Liao, K. J.* Application of solubility parameter theory in evaluating the aging resistance of paving asphalts // Petrol. Sci. Technol. 2003. Vol. 21, No. 11–12. P. 1843–1850.

25. *Mohan, D., Pittman, Jr., C. U., Steele, P. H.* Pyrolysis of wood/biomass for bio-oil: A critical review // Energ. Fuel. 2006. Vol. 20, No. 3. P. 848–889.

26. *Michels, R., Langlois, E., Ruau, O., Mansuy, L., Elie, M., Landais, P.* Evolution of asphaltenes during artificial maturation: a record of the chemical process // Energ. Fuel. 1996. Vol. 10. P. 39–48.

27. *Nandi, B. N., Belinko, K., Ciavaglia, L. A., Pruden, B. B.* Formation of coke during thermal hydrocracking of Athabasca bitumen // Fuel. 1978. Vol. 57, No. 5. P. 265–268.

28. *Lille, Ü., Heinmaa, I., Pehk, T.* Molecular model of Estonian kukersite kerogen as evaluated by ^{13}C MAS NMR spectra // Fuel. 2003. Vol. 82, No. 7. P. 799–804.

29. *Kask, K. A.* About bituminizing of kerogen of oil shale-kukersite. Report I // Transactions of Tallinn Polytechnic Institute. Series A. 1955. No. 63. P. 51–64 [in Russian].

Article III

Tiikma, L., **Sokolova, J. (Krasulina, J.)**, Vink, N. Effect of the concentration of organic matter on the yield of thermal bitumen from the Baltic oil shale kukersite. – *Solid Fuel Chemistry*, 2010, vol. 44, no. 2, pp. 89-93.

Effect of the Concentration of Organic Matter on the Yield of Thermal Bitumen from the Baltic Oil Shale Kukersite

L. Tiikma, Yu. Sokolova, and N. Vink

Tallinn University of Technology, Ehitajate tee 5, Tallinn, 19086 Estonia
e-mail: laine.tiikmaa@ttu.ee

Received May 25, 2009

Abstract—The low-temperature (360°C) autoclave pyrolysis of the oil shale kukersite, which has carbonate-type mineral matter, with various organic matter (OM) concentrations of 31.8–90.1% and the separation of the pyrolyzate from the mineral matter at the stage of thermal bitumen formation by extraction with various solvents such as benzene, ethanol, and their mixtures were considered. The OM distribution between a gas, an extract, and a residue insoluble in a given solvent was characterized. It was found that, in the pyrolysis of oil shale in an autoclave, the extract yield on an OM basis somewhat increased as the OM content of oil shale increased because the concentration of OM adsorbed on the mineral matter of oil shale remained constant.

DOI: 10.3103/S0361521910020035

In the pyrolysis of Baltic oil shale, kerogen sequentially transformed to a plastic state at the first step of decomposition; that is, thermal bitumen soluble in organic solvents was formed. This intermediate step was characterized by the lowest release of gaseous substances and minimum OM losses as coke in a solid residue. As compared with kerogen, thermal bitumen contained smaller amounts of both oxygen and hydrogen. Hydrogen losses occurred through water and hydrogen sulfide, whereas the main amount of oxygen was eliminated as carbon dioxide. In the subsequent pyrolysis, thermal bitumen was converted into oil, gas, and coke. Minimal losses of kerogen occurred in the separation of the pyrolyzate from the mineral matter at the step of thermal bitumen formation.

The formation of thermal bitumen from kukersite has been described in a number of publications [1–8], where the conditions and kinetics of formation of thermal bitumen and its mixture with oil (TBO) in a retort and an autoclave have been reported. In these studies, standard oil shale was used as a test material. The process of TBO formation from shale with various kerogen contents and the effect of mineral matter on thermal degradation were not considered.

Undoubtedly, the mineral matter of fossil fuels affects the thermal degradation of solid fuels; however, the degree and character of this effect depend on not only the amount and composition of mineral components but also the type of fuel and the behavior of the process. This can explain contradictory conclusions on the effect of the mineral matter of shale on the yield of tar in the semicoking of shale.

According to reference data [9], a linear relationship between the yield of tar and the concentration of

OM was observed. However, Urov and Klesment [10], who studied the composition and properties of oil shale, concluded that the yield and composition of tar depend on the chemical structure of kerogen, the adsorption properties of mineral matter, and the conditions of pyrolysis.

Luts [11] and Efimov et al. [12] stated that the yield of semicoking tar on a kerogen basis increased with the OM content of the kukersite shale and this tar mainly contained primary decomposition products. Burnham et al. [13] studied the effect of minerals on the pyrolysis of Green River oil shale and concluded that they exerted a noticeable effect on the yield and composition of pyrolysis products.

The effect of the mineral matter of oil shale on the processes of pyrolysis was mainly studied using model mixtures in a Fischer retort. The pyrolysis of standard and enriched shale, as well as kerogen mixtures with various mineral substances (aluminum oxide, bentonite, kaolinite, and calcium carbonate), demonstrated that the yield of pyrolizates increased upon the pyrolysis of artificial mixtures [14].

Vysotskaya [15] studied the effect of carbonate–clay mineral matter on the yield and composition of the pyrolysis products of oil shale from Yakutsk, Belorussian, and Kashpirskoe deposit and Estonian Dictyonema oil shale. A negative effect of mineral matter on the yield of semicoking tar in a Fischer retort in the presence of both carbonate and clay mineral substances regardless of the type of kerogen was mainly noted. However, the effects of carbonate and clay rocks were noticeably different in this case. Clay rocks exhibit both adsorption (retention of a tar portion by the solid residue and the subsequent additional

Table 1. Characteristics of kukersite samples used in the experiments

Shale	OM content*
Concentrate 90	90.1
Concentrate 76	76.0
K-59	59.3
K-51	51.0
K-40	40.5
K-32	31.8

* With no pyrite correction.

Table 2. Composition of the mineral matter of kukersite, % [23]

Clay minerals	5.0
Quartz	8.5
Orthoclase	8.5
Gypsum	0.8
Pyrite	3.1
Calcium carbonate	64.0
Magnesium carbonate	1.9
The rest	8.2

decomposition of tar as a result of secondary reactions) and catalytic properties (favorable for tar formation because of a more complete redistribution of hydrogen between tar and nonvolatile residue). The adsorption effect is mainly characteristic of carbonates; this shifts the process of tar formation to the higher temperature region and preserves the primary products of degradation to prevent the formation of volatile substances. An increase in the concentration clay mineral substances having a developed surface in oil shale results in a dramatic decrease in the yield of tar on a kerogen basis.

Khisin [16] believed that calcium carbonate, silica, and semicoke did not exert a noticeable effect on the yield of tar. This was supported in experiments on the pyrolysis of Colorado and Thailand oil shale in a flow system [17]. However, a decrease in the yield of tar on an OM basis was observed in the industrial processing of kukersite in a plant with a solid heat carrier using a mixture with ash from the same plant [18]. The same occurred in the semicoking of oil shale in a retort, where the concentration of high-boiling and unsaturated hydrocarbons in tar increased in a mixture with free calcium oxide [19].

Pan et al. [20] studied the effect of the acidity of the mineral matter of Estonian oil shale on tar formation by adding various mineral matter components to the OM of kukersite in a ratio of 1 : 16 (in this case, the

OM concentration was about 6%). They found an increase in tar formation as the acidity of the mineral matter was increased, whereas calcites and dolomites, which are alkaline components of kukersite, did not facilitate the formation of thermal bitumen even in the presence of a large amount of water.

The OM of kukersite before pyrolysis was almost insoluble in organic solvents. For example, less than 1% OM passed into solution upon dissolving with benzene or ethanol–benzene. Thermal bitumen was defined as a high-molecular-weight product of kukersite pyrolysis at the primary stage of decomposition; this product is nonvolatile but soluble in organic solvents. As a rule, benzene or, in some cases, a mixture of benzene with ethanol was used for separating thermal bitumen in research works [2, 4, 6]. Pentane was used for the fraction separation of hydrocarbons [20], and a dichloromethane–methanol mixture or tetrahydrofuran was used for exhaustive extraction. It was found that the pyrolysis of kukersite in solvents (so-called thermal dissolution) can accelerate the process of kukersite liquefaction. Ethanol, shale gasoline, and supercritical water belong to these solvents [21]. According to Luik et al. [22], the dissolving power of the test solvents toward the OM of kukersite changed in the following order: dimethyl ketone > ethanol > benzene > hexane > diethyl ether > water.

In this paper, we consider the low-temperature pyrolysis of the oil shale kukersite, which has a carbonate type of mineral matter. We studied the yield and composition of TBO obtained by the low-temperature pyrolysis of the kukersite with various OM contents in an autoclave and the efficiency of TBO separation from the mineral matter with various solvents (benzene, ethanol, and their mixture). We also determined kerogen losses with the residue insoluble in these solvents.

EXPERIMENTAL

The pyrolysis of shale samples (1–4 g) with various OM contents was performed in 20-ml autoclaves, which were placed in a preheated muffle furnace. The pyrolysis temperature was 360°C, and the pyrolysis time was 3.5 or 4 h, which is close to that required for obtaining a maximum yield of thermal bitumen under these conditions [3]. The separation of TBO from the mineral matter was performed using various solvents: benzene, ethanol, and a mixture of benzene with ethanol in a ratio of 1 : 1. Dissolution was performed using two procedures: (a) with stirring a sample with 100 ml of a solvent for 30 min in a heated flask at 60°C and (b) with boiling solvents in a Soxhlet apparatus.

The amount of gases formed upon pyrolysis was determined by difference between sample weights in closed and open autoclaves, and the OM in the dry residue was determined using the following two proce-
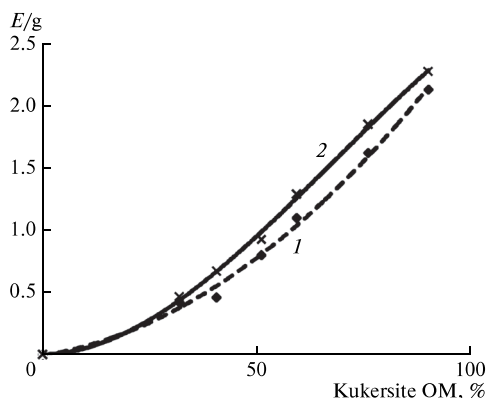
Fig. 1. Dependence of the absorbance of a benzene extract on the OM content of kukersite at pyrolysis times of (*1*) 3.5 and (*2*) 4 h.
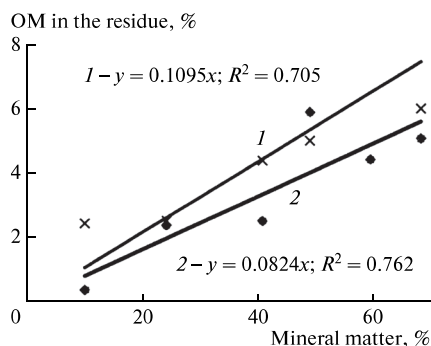

Fig. 2. Dependence of the total amount of OM_{diff} in the insoluble residue (% on a kukersite basis) on the mineral matter of kukersite at pyrolysis times of (*1*) 3.5 and (*2*) 4 h.

dures: (a) OM_{diff}, by difference between the weights of the dry residue and the mineral matter and (b) OM_{HCl}, by difference between the residue after separating carbonates with 10% hydrochloric acid and calcination losses (825°C). The amount of TBO formed was determined after dissolving a sample in a Soxhlet apparatus: (a) TBO_{HCl}, by difference between the initial OM, gas (on an OM basis), and OM in the residue (OM_{HCl}), (b) TBO_{diff}, by the weight difference of dry shale, gas, and residue dried at 105°C on an OM basis, (c) TBO_{dist}, by the weight of dissolved tar after distilling a solvent in a rotary evaporator and drying the residue in a flask at 75°C for 1 h, and (d) TBO_{color}, by the absorbance of a dilute extract. The absorbance was determined on a colorimeter at a wavelength of 420 nm, and the results were converted to 1 g of kukersite at a sample dilution to 1 l.

The composition of TBO was determined by thin-layer chromatography according to Luik et al. [22].

The experiments were performed with six samples of kukersite shale (Table 1); Table 2 summarizes the composition of the mineral matter of this shale.

RESULTS AND DISCUSSION

Effect of the OM content of oil shale on its distribution. The pyrolysis of oil shale with OM contents from 31.8 to 90.1% was performed at 360°C for 3.5 and 4 h. For comparison, we demonstrated the distribution of OM between gas, TBO, and benzene-insoluble residue for pyrolysis times of 3.5 (Table 3) and 4 h (Table 4). The losses of OM with the residue were determined according to Stadnikov (OM_{HCl}) or by difference (OM_{diff}). Figures 1 and 2 show the graphical dependences.

The yields of gas and TBO upon pyrolysis for 4 h were somewhat higher than those upon pyrolysis for 3.5 h, and their weights increased with the OM content of kukersite. The amount of insoluble organic residue

Table 3. Distribution of OM between the pyrolysis products (%) of shale (360°C; 3.5 h)

OM of kuker-site, %	Gas	Amount of TBO			OM content of the dry residue	
		OB_{HCl}	OB_{diff}	OB_{dist}	OB_{HCl}	OB_{diff}
90.1	13.6	84.1	83.4	89.4	2.3	3.0
76.0	10.7	85.8	84.5	97.3	3.5	4.8
59.3	7.9	86.1	84.0	98.6	6.0	8.1
51.0	11.1	80.7	76.7	77.7	8.2	12.2
40.5	7.9	78.6	70.1	78.0	13.5	22.0
31.8	6.4	69.8	54.6	70.8	23.8	39.0

Table 4. Distribution of OM between the pyrolysis products (%) of shale (360°C; 4 h)

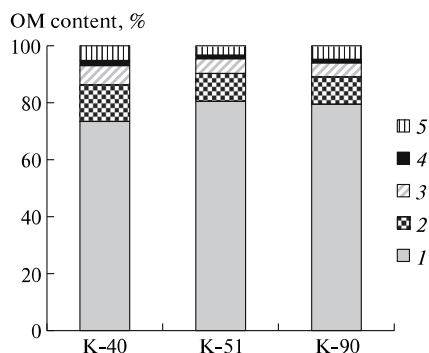| OM of kuker-site, %	Gas	Amount of TBO			OM content of the dry residue	
		OB_{HCl}	OB_{diff}	OB_{dist}	OB_{HCl}	OB_{diff}
90.1	15.6	82.7	82.3	87.9	1.7	2.1
76.0	11.5	86.0	85.4	95.5	2.5	3.1
59.3	9.5	86.4	85.3	96.2	4.1	5.2
51.0	9.5	84.5	85.0	75.0	6.0	5.5
40.5	9.4	79.9	78.6	80.1	10.7	12.0
31.8	7.3	75.2	73.0	72.7	17.5	19.7

TIIKMA et al.

Fig. 3. Group composition of TBO at various OM contents of oil shale: (*1*) high-polarity, (*2*) oxygen-containing, (*3*) polyaromatic, (*4*) monoaromatic, and (*5*) paraffin–naphthene compounds.

depended on pyrolysis time and increased with increasing mineral matter of kukersite.

The dependence of the amount of coke on mineral matter was described by an equation of a straight line that passes through the origin regardless of determination methods. The slope of a straight line (*m*) in Fig. 2 expresses the amount of OM bound to mineral matter under the specified conditions. The constancy of this value (*m* was 0.08% on a mineral matter (MM) basis for a pyrolysis time of 4 h) suggests that a saturated monomolecular Langmuir adsorption layer was reached in the autoclave. Of course, this saturation occurred when the amount of OM was sufficient for saturation, that is, $OM > m_{MM}$ or $100/MM > m + 1$.

Group composition of TBO and its solubility in various solvents. Upon the semicoking of kukersite in a

retort, tar is separated from the mineral matter by distillation; however, the extraction of TBO is required upon pyrolysis in an autoclave. We performed experiments on the extraction of TBO with various solvents in order to determine the best suited solvent in terms of the completeness of TBO separation and a decrease in nonextracted OM in the residue. Because the yields of gas and TBO in previous experiments after pyrolysis for 4 h were higher than those after 3.5 h, we performed pyrolysis for 4 and 6 h in this series.

To determine the composition of TBO at different reaction times, we extracted the pyrolyzed samples at 60°C with stirring for 30 min using 100 ml of a solvent (benzene, ethanol, or their mixture in a volume ratio of 1 : 1). After removing the solvent, the samples were analyzed by TLC. Table 5 summarizes the results of the analysis of TBO and the distribution of the OM of kukersite between pyrolysis products.

High-polarity compounds were the main components of thermal bitumen regardless of the extracting agent, the time of pyrolysis, and the OM content of shale. The total concentration of paraffin–naphthene and monoaromatic compounds, which are most appropriate for liquid fuels, was lower than 7%. At a reaction time of 6 h, the yield of target products somewhat decreased (as compared with 4-h exposure) because of the secondary decomposition of TBO into gas and coke.

Figure 3 shows the composition of TBO obtained upon the pyrolysis of shale with various OM contents (40, 51, and 90%). As expected, the previously found constant composition of kerogen in various kukersite samples leads to the same group composition of TBO obtained under the same conditions of pyrolysis.

Table 5. Distribution of the OM of kukersite (%) between the pyrolysis products

Compounds	Pyrolysis time of 4 h			Pyrolysis time of 6 h		
	benzene	benzene + ethanol mixture	ethanol	benzene	benzene + ethanol mixture	ethanol
Gas	9.4	9.4	9.4	12.5	12.5	12.5
OM_{HCl}	10.7	15.0	39.9	11.2	20.6	43.7
Yield of TBO_{diff}	79.9	75.6	50.7	76.3	66.9	43.8
including the following compounds:						
high-polarity	58.7	62.6	34.2	53.3	39.8	27.6
oxygen-containing	10.2	7.0	9.0	9.6	15.5	9.1
polyaromatic	5.4	3.5	4.3	8.1	8.3	4.7
monoaromatic	1.3	0.5	0.8	1.4	1.2	0.4
paraffin–naphthene	4.2	2.0	2.4	3.9	2.1	2.1

CONCLUSIONS

We found that 80–85% of the OM of kukersite can be extracted from its mineral matter at the stage of the formation of a TBO mixture. The yield of pyrolysis products from the kukersite shale depends on the concentration of OM in it. The formation of gas and TBO from OM somewhat increased as the OM content of oil shale increased, whereas the formation of a benzene-insoluble residue decreased. We determined that this behavior was due to a constant adsorption capacity of the mineral matter of kukersite under the given conditions of pyrolysis (temperature, grain size, and the degree of decomposition of kerogen and TBO).

Benzene is an efficient solvent for the separation of TBO. A mixture of benzene + ethanol, which has been preferred previously, is inferior to the above because solvent regeneration is unsuccessful. Ethanol is a poor solvent for TBO, with the use of which the greatest OM losses with the residue were observed. The dissolution of shale pyrolysis product with stirring allows us to separate TBO from mineral matter.

The main components of TBO mixtures obtained from oil shale with various OM contents are high-polarity compounds regardless of extracting agent and pyrolysis time, and the total concentration of paraffin–naphthene and monoaromatic compounds is lower than 10%.

ACKNOWLEDGMENTS

REFERENCES

1. Aarna, A.Ya., *Tr. TPI, Ser. A.*, 1954, no. 57, p. 32.
2. Kask, K.A., *Tr. TPI, Ser. A.*, 1955, no. 63, p. 51.
3. Tiikma, L., Zaidentsal, A., and Tensorer, M., *Oil Shale*, 2007, vol. 24, no. 4, p. 535.
4. Zaidentsal', A.L., Soone, Yu.Kh., and Muoni, R.T., *Khim. Tverd. Topl.* (Moscow), 2008, no. 2, p. 14.
5. Johannes, I. and Zaidentsal, A., *Oil Shale*, 2008, vol. 25, no. 4, p. 412.
6. Aarna, A.Ya. and Lippmaa, E.T., *Tr. TPI, Ser. A.*, 1958, no. 97, p. 3.
7. Fomina, A.S., Pobul', L.Ya., and Degtereva, Z.A., *Priroda kerogena Pribaltiiskogo goryuchego slantsa-kukersita i ego khimicheskie syr'evye kachestva* (Nature of Kerogen in the Baltic Oil Shale Kukersite and Its Chemical Properties), Tallinn: Izd. Akad. Nauk ESSR, 1965.
8. Shul'man, A.I. and Proskuryakov, V.A., *Khimiya i tekhnologiya goryuchikh slantsev i produktov ikh pererabotki* (Chemistry and Technology of Oil Shales and Products of Their Conversion), Myasnikova, L.B., Ed., Leningrad: Khimiya, 1968.
9. *Spravochnik slantsepererabotchika* (Shale Processor's Handbook) Rudin, M.G. and Serebryannikov, N.D., Eds., Leningrad: Khimiya, 1988.
10. Urov, K.E. and Klesment, I.R., *Khim. Tverd. Topl.* (Moscow), 1981, no. 3, p. 16.
11. Luts, K., *Der Estländische Brennschiefer—Kukersit, Seine Chemie, Technologie und Analyse,* Reval: Revalen Buchverlag, 1944.
12. Efimov, V.M., Petukhov, E.F., Doilov, S.K., and Kundel', Kh.A., *Khim. Tverd. Topl.* (Moscow), 1981, no. 1, p. 56.
13. Burnham, A.K., Huss, E.B., and Singleton, M.F., *Fuel*, 1983, vol. 62, no. 10, p. 1199.
14. Horsfild, B. and Douglas, A., *Geochim. Cosmochim. Acta*, 1980, vol. 44, no. 8, p. 1119.
15. Vysotskaya, V.V., *Cand. Sci. (Chem.) Dissertation*, Tallinn: Tallinn Polytech. Inst., 1987.
16. Khisin, Ya.I., *Termicheskoe razlozhenie goryuchikh slantsev* (Thermal Decomposition of Oil Shale), Leningrad: Gostoptekhizdat, 1948.
17. Enomoto Minoru, Sate Shinya, Takahashi Shiro, and Matsuzawa Sadao, *J. Jap. Petrol. Inst.,* 1985, vol. 28, no. 2, p. 126.
18. Kyll', A.T., *Goryuchie slantsy. Khimiya i tekhnologiya* (Oil Shale: Chemistry and Technology), Moscow: Gostoptekhizdat, 1954, issue 1, p. 246.
19. Efimov, V.M., Doilov, S.K., Lille, Yu.E., et al., *Khim. Tverd. Topl.* (Moscow), 1975, no. 2, p. 72.
20. Pan, C., Geng, A., Zhong, N., et al., *Fuel,* 2008, vol. 88, p. 909.
21. Tiikma, L., Johannes, I., Luik, H., et al., *JAAP,* 2009, vol. 85, p. 502.
22. Luik, H., Palu, V., Bityukov, M., et al., *Oil Shale*, 2005, vol. 22, no. 1, p. 25.
23. Pokonova, Yu.V. and Fainberg, V.S., *Itogi Nauki Tekh., Ser.: Tekhnol. Org. Veshchestv*, 1985, vol. 10.

Article IV

Luik, H., Luik, L., Johannes, I., Tiikma, L., Vink, N., Palu, V., Bitjukov, M., Tamvelius, H., **Krasulina, J.**, Kruusement, K., Nechaev, I. Upgrading of Estonian shale oil heavy residuum bituminous fraction by catalytic hydroconversion. – *Fuel Processing Technology*, 2014, vol. 124, pp. 115-122.

Upgrading of Estonian shale oil heavy residuum bituminous fraction by catalytic hydroconversion

CrossMark

Hans Luik *, Lea Luik, Ille Johannes, Laine Tiikma, Natalia Vink, Vilja Palu, Mihhail Bitjukov, Hindrek Tamvelius, Julia Krasulina, Kristjan Kruusement, Igor Nechaev

Tallinn University of Technology, Faculty of Chemical and Materials Technology, Department of Polymeric Materials, Laboratory of Oil Shale and Renewables Research, 5 Ehitajate Rd., 19086 Tallinn, Estonia

ARTICLE INFO

ABSTRACT

Possibilities for upgrading of the Estonian shale oil rectification residuum boiling above 360 °C by hydroconversion were studied for the first time with the aim to maximize the fractions boiling below 360 °C and between 275–360 °C.

The single- and two-step hydroprocessing were performed in a 500 cm^3 periodic autoclave under the range of temperatures 340–420 °C, duration 40–240 min, and the hydrogen initial pressure 6.4-7.5 MPa. Three types of catalysts foreseen for hydropurification (KGU-950, KF-848), for hydrocracking (GO-30-7, KF-1015, KC-3210) and for universal purpose (DN-3100 Th) were added in the quantity of 10% per the residuum. The effectiveness of the treatment was evaluated by yields of oil, gas, coke and water, by boiling curves, elemental composition, and group composition (hydrocarbons, aromatics, polyaromatics, low-polar heterocompounds and high-polar heterocompounds) of the hydrogenated oil, by FTIR spectra and GC/MS analysis, and by composition of the gases formed.

Any characteristic of the hydrogenated products depended on the complicated co-effects of the pyrolysis conditions, temperature, time and catalysts. So, there was no unique solution for the best conditions and catalysts for the best total result. The highest yield of the fraction boiling below 360 °C obtained was 82.7%.

1. Introduction

The increasing demand for liquid fuels and their rising prices have revived interest in shale oil. The world oil shale reserves are estimated to exceed 4.8 trillion barrels of recoverable oil [1].

The oil obtained by semicoking of Estonian Kukersite oil shale, is known as an unstable, extremely complex mixture of compounds and is specific one by its high content of oxygen. Therefore, the oil and even its distillation fractions are unsuitable for exploitation as a feed-stock for motor fuels without visbreaking, stabilization and removing of the heteroatoms.

Recent advances in the production of high quality transportation fuels have been focused on the upgrading technologies of high boiling fractions of crude oils and residua by hydroprocessing. Unfortunately, a general upgrading scheme suitable for all heavy oil refineries is absent because there are many factors to take into consideration like: chemical and physical properties of the heavy oil and residua, available catalysts, local needs, as well as refinery configuration and prices of products [2]. Laboratory-scale research of shale oil upgrading has been studied intensively in the US, Estonia, Russia, Israel, Australia, Brazil, China, Near East countries and elsewhere [3–9].

In spite of the opening of the first industrial oil shale liquefaction factory in Estonia as early as 1924 [10], and advancing the oil distillation technology temporally by several modifications of the retorting units (tunnel ovens, shaft retorts, solid heat carrier varieties up to efforts to use for heating of fluidized bed oil retorts the circulating hot ash from the fluidized bed incineration of the semicoke and shale oil), neither the oil nor its distillation fractions have been hydroprocessed industrially. Extensive analysis and pilot plant testing of the Estonian shale oil obtained in Enefit Oil and Gas to upgrade the oil to Euro V diesel were conducted in Haldor Topsoe A/s in Denmark [11].

A comprehensive review of the previous investigations on the theory and practice of Estonian shale oil formation and its laboratory upgrading was given by Luik in [12]. The lion's share of oil shale was used for the production of electricity, the minor part for production of

* Corresponding author.
  E-mail address: hans.luik@ttu.ee (H. Luik).

heating oil. Now, considering the large reserves of oil shale as high syncrude potential in Estonia, the elaboration of the possibilities and perspectives of employing the shale oil as synoil has again become relevant.

Catalytic hydrotreatment of different distillation fractions of Kukersite oil was studied by Luik [13–18] in a laboratory batch autoclave using Co–Mo and Ni catalysts. The fraction "heavy mazute" (heavy gas oil) boiling over 320 °C gave 90–91% of refined oil whereas the content of hetero-compounds decreased from 66.1 to 24.9%, and iodine number from 84 to 43.

Hydrotreating of the oil shale thermobitumen [19] under conditions 400 °C, 5 MP, 60 min. resulted 19.8% of gas and water and 76.9% of benzene soluble oil from the totally soluble in benzene initial matter whereas the content of hetero-compounds decreased from 90 to 66.7% and content of liquid hydrocarbons increased from 10 to 34%.

Noteworthy longer durations, 8 to 56 h, and higher hydrogen pressure, 15.0 MPa, were applied by Chishti and Williams [20] for hydroprocessing at 400 °C of the Kimmeridge Clay shale oil. With increasing duration the content of three and four ring polyaromatic hydrocarbons decreased; and the content of single ring and two ring ones increased. Concentration of nitrogen and sulfur containing three and four ring aromatic hydrocarbons in the oils was reduced with increasing hydrotreatment time to reach negligible concentrations after 56 h.

The heavy residuum bituminous shale oil fraction boiling above 360 °C obtained as a result of industrial semicoking of Kukersite makes up roughly 50% of the total oil and its further utilization is limited to coke production only [21]. The data concerning upgrading of the heavy residuum into liquid fuels are absent.

The goal of this work was the upgrading by catalytic hydroconversion of the heavy bitumenous oil boiling above 360 °C to the liquid fuel boiling below 360 °C. For this purpose, the effect of hydroprocessing conditions on the yield and characteristics of the upgraded liquid products was studied in a laboratory batch autoclave.

2. Experimental

2.1. Materials and reagents

The shale oil heavy residuum bituminous fraction boiling above 360 °C (called later as "initial oil") was an industrial fraction produced by VKG, the biggest oil shale processor in Europe [22].

The six Mo–Co- and/or –Ni catalysts on the alumina support with three purposes tested in this work are given in Table 1.

All the Akzo Nobel catalysts were activated by presulfiding of the oxides before use by feeding sulfur containing light gas oil and hydrogen.

2.2. Hydroprocessing procedure

The single- or two-step hydroprocessing of the initial oil and of the dephenolated residuum was conducted in a rocking 500 cm³ batch autoclave with varying hydrogenation conditions. The products obtained

Table 1
Applied catalysts.

Type	Producer	Purpose
KGU-950	OAO AZKiOS, Irkutsk, Russia	Hydropurification
GO-30-7	OAO AZKiOS, Irkutsk, Russia	Hydrocracking
DN-3100 Th	Shell Chemicals LP, US	Universal
KF-848	Akzo Nobel, Netherlands	Hydropurification
KF-1015	Akzo Nobel, Netherlands	Hydrocracking
KC-3210	Akzo Nobel, Netherlands	Hydrocracking

Here and in succeeding Tables the hydrocracking catalysts are highlighted with 50% gray color, the hydropurification catalysts are not highlighted, and the universal catalyst or the mixes of the hydropurification and -cracking ones are highlighted with 25% gray color.

in the first stage of hydropurification and in the second stage of hydrocracking at an elevated temperature after addition of a cracking catalyst were separated by filtration, extraction, distillation, and drying. The liquid products were characterized by their yield, phenol content, fractional composition, and elemental and group composition.

The reactor was provided with controlled heating system connected with an inside thermocouple, a manometer, and inlet and outlet valves. About 50 g of the initial oil or the dephenolated residuum, 10% of catalyst per the residuum, and hydrogen up to the pressure 6.4–7.5 MPa (at ambient temperature) were charged. The initial reaction time was taken when the nominal temperature (340–420 °C) was attained. The current temperatures and pressures were recorded. After the duration prescribed (40–240 min) the autoclave was cooled down to room temperature, the residual pressure was registered, and the samples for gas analysis were taken. After that, the autoclave was opened, and the solid phase (catalyst applied and coke formed) was separated from the hydrogenated oil by filtration through a filter paper. The filtrate was analyzed. The solid residuum in the filter cake was washed with benzene, dried and weighed. Benzene was evaporated from the washing filtrate in a vacuum rotator and the residuum obtained was considered in calculation of the total yield of liquid products.

2.3. Methods of analysis

Phenols were determined by their weight after separation by alkali dephenolation of the initial oil according to the five different extraction procedures described below in Section 3.1.

The alkali-extracted phenols were re-extracted after acidification of the phenolate solutions with diethyl ether. The total phenols were weighed after diethyl ether evaporation.

Water-soluble phenols were determined analogously, by water extraction of the initial oil diluted with benzene.

Asphaltenes were estimated by weight after dissolution of the samples in benzene (1:10), precipitation of asphaltenes by addition of n-hexane (1:50), and their filtration on the next day.

Boiling range of the oils recovered was estimated by Engler distillation.

Chemical group composition of the liquid products was estimated by adsorption thin-layer chromatography. For this aim, 300–500 mg of the oil was fractionated on the 2 mm high silica gel (Fluka 60 μm) spread on a plate 24 × 24 cm, and eluted with n-hexane: The following fractions of hydrocarbons (HC) and hetero-compounds (Het) were separated: aliphatic hydrocarbons (AlHC), monoaromatic hydrocarbons (MAHC), polyaromatic hydrocarbons (PAHC), low-polar hetero-compounds (LPHet) and high-polar hetero-compounds (HPHet), and weighed after their desorption with diethyl ether and desiccation.

Functional group composition was characterized by a Fourier transform infrared (FTIR) spectrometer "Interspect 2020 FT-IR".

The GC/MS analysis was conducted on a Shimadzu QP 2010 Plus using 30 m capillary columns ZB-5 and HP-5MS.

Gas composition was analyzed by gas chromatography (Chrom 5).

Content of H_2S and NH_3 in the gases diluted with an excess of hydrogen were below sensitivity of the chromatographic methods. Therefore their yield was estimated by bubbling of the gas formed through alkali and acidic solutions followed by iodometric titration of sulfide ions and photometric measurement of ammonia content with Nessler reagent.

Ultimate analysis of C, H, S, N and O in oil was conducted on "Elementar Vario EL" analyzer.

3. Results and discussion

3.1. Phenolic compounds

In the previous works concerning hydrotreatment of Kukersite oil fractions [13–18], as a rule, the first stage has been separation of

phenolic compounds that would reduce the quality of liquid fuels, waste hydrogen at hydrogenation, and could be used for synthesis of resins, adhesives, antioxidants, plastificators, etc.

The direct dephenolation of the sticky heavy residuum by extraction with an alkali water solution failed because the organic and water phase did not give different layers.

The results concerning dephenolation of the diluted oil are presented in Tables 2 and 3.

The data obtained evidence that the yield of total phenols extracted depends on the solvent applied for dilution. The two phases do not separate when diethyl ether is added. The yield of phenols reaches 17% at higher ratios of the alkali solution using ethyl ether or the light fraction of shale oil, called naphtha. When benzene or toluene is used the yield reaches 26.9%. Probably, hydrogen bonding arises between the molecules of oxygen containing solvents and the heavy residuum. So, distribution of the phenols is reduced to the organic solutions, and only the anionic phenolates with shorter alkyl radicals can be extracted into the alkali water solution. In aromatic solvents the bonding is weaker, and the so-called neutral phenols (where the hydrophilic anionic site of phenolates is balanced with hydrophobic polyaromatic nuclea and longer side-chain hydrocarbons) can be extracted into the alkali solution also.

The results of dephenolation prove the extremely complicated nature of the heavy residuum. As can be expected, the share of water soluble phenols in the heavy residuum is trivial.

3.2. Hydroprocessing of the initial and dephenolated oil

The hydroprocessing conditions tested and the yields of the products are given in Table 4.

The results in Table 4 reveal that the mean need for hydrogen is 0.227 dm^3/g oil at normal conditions.

Noteworthy is that the dephenolation of the heavy residuum does not promote efficiency of the hydroprocessing for several reasons:

• the recovery of the secondary oil from the initial oil surpasses that from the dephenolated one at hydroprocessing,
• a part of the target hydrocarbons in long side chains of the phenols would be wasted at dephenolation,
• the complicated "heavy" phenols separated are unique but have not found sufficient market value so far,
• the polyfunctionality of the "heavy" phenols makes their distribution between water and organic phases very sensible for the solvent type and extraction method.

So, the major experiments were conducted with the initial oil without prior dephenolation.

According to Table 4, the highest total yield of liquid product soluble in benzene (95.7%) was obtained in the two stage experiment 11-I-II where the mix of universal catalysts DN-3100 Th and the hydrocracking catalyst GO-30-7 was used in the first stage at 340 °C, and in the second

Table 2
Extraction of total phenols from initial oil.

Oil dilution		Extraction with NaOH aqueous solution		
Solvent	Oil:solvent (g/g)	NaOH solution:oil (g/g)	NaOH (%)	Yield of phenols (% from oil)
Diethyl ether	1:1	2:1	10	0[a]
Ethyl ether	1:1	4:1; 4:1; 4:1	2.5; 5; 10	17.0[b]
Gasoline	1:2	2:1; 1:1; 1:1	2.5; 5; 10	16.4[b]
Toluene	1:4	4:1; 4:1; 4:1	2.5; 5; 10	26.8[b] (25.98, 0.739 and 0.113)[c]
Benzene	1:4	5:1; 5:1; 5:1	2.5; 5; 10	26.9[b]

[a] Phases did not separate.
[b] Total yield.
[c] Yield in the subsequent steps.

Table 3
Extraction of the water soluble phenols.

Oil dilution		Extraction with water	
Solvent	Oil:solvent (g/g)	Water:oil (g/g)	Yield of phenols (% from oil)
None	–	3:1, three times	0.18
None	–	10:1, once	0.196
Benzene	1:4	10:1, once	0.11

stage the temperature was increased to 380 °C. In both stages the duration was 40 min and the initial hydrogen pressure 7.1 MPa. The total oil yield was high also in the second stage of the experiments 6-II, 15-II, and 7-II (93.8, 92.8 and 91.6% from the first stage oil) loosing 3.5–8.4% as gas, coke and water. It is understandable that the oil yield 100% at hydroprocessing can evidence that there has been no transformation of the initial oil.

3.3. Fractional composition of the hydrogenated oils

Fractional composition of the secondary oils obtained under various conditions of the hydroprocessing is depicted in Fig. 1.

The distillation curves show principal similarity when the dephenolated (Fig. 1a) and initial heavy residuum (Fig. 1b) were used as feedstocks. As can be expected, the cracking catalysts GO-30-7 (experiments 4, 6-II, 7-II, and 11-II) and KF-1015 (experiment 14-II) obviously enhance formation of the lower boiling fractions in comparison with the hydropurification catalysts applied in the first stage (I). The results obtained revealed that in the distillation most of the hydrogenated shale oil samples decline to secondary thermal decomposition, especially in the cases without dephenolation (Fig. 1b). As a specific feature, a sharp increase in the fraction share takes place at a constant temperature above 250 °C. The phenomenon can be explained by thermal disassociation of the hydrogen-bonded associates characteristic of the shale oil polar molecules. Decomposition of the associates results in an increase in the quantity of lighter fractions concurrently with a decrease in temperature.

The fact that a part of Kukersite retort oil decomposes during its repeated distillation resulting incongruity of the fractions with the initial oil has been known earlier [23]. The analogous behavior of the hydrogenated oils proves that their stabilization under hydroprocessing conditions tested has been insufficient.

Distribution of the hydrogenated oils between the fractions of gasoline (200 °C–), kerosene (200–275 °C) and gas oil (275–360 °C) is depicted in Fig. 2.

Yields of the main fractions of the hydrogenated oils and the iodine numbers are presented in Table 5.

According to Figs. 1, 2, and Table 5, kerosene, the most desired fraction, prevails (53%) in the hydrocracked oils 6-II and 7-II where the secondary decomposition of the oils at fractional distillation has begun near 250 °C already. The highest share of the gas oil (275–360 °C), was obtained in the tests 14-I and 11-II where the secondary cracking was delayed close to 360 °C.

The data obtained suggest that at fractional distillation the gaseous products dissolved in the hydrogenated oils or quit at decomposition of the unstable associates formed volatilize as an additional gas phase. Dilution of the viscous initial oil with the gasoline fraction (1:1) in test 10 does not benefit the hydroprocessing but only increases adequately the light fraction. According to Table 5, the highest share of the fraction 200–360 °C was formed in experiments 14-I and 14-II, 11-II and 6-II (72.7 and 64.6, 59.7 and 62.6 g/100 g) where the hydropurification catalyst KF-848 and the mix of catalysts consisting of the universal catalyst DN-3100 Th and the hydrocracking catalyst GO-30-7 were applied. So, for further analysis the following hydrogenated oils were chosen: 14-I, 14-II, 11-II and 6-II, and for comparison, oil 9-III where the yield of the fraction boiling above 360 °C remained was one of the highest (48.4%).

Table 4
Hydroprocessing conditions and yields of the products.

Test number	Object	Catalyst	Temperature (°C)	Duration (min)	H₂ pressure (MPa)			Yields (% from the object)				Hydrogen consumption (dm³, n. c.)
					Initial	Working	Residual	Hydrogenated oil	Gas	Coke	Water	
1	Dephenolated	GO-30-7	400	60	7.7	17.3	5.0	75.8	17.4	3.2	3.6	15.7
2	Dephenolated	GO-30-7	430	60	8.8	22.5	6.2	46.4	36.6	15.1	1.9	16.3
3	Dephenolated	GO-30-7	380	60	7.0	16.0	5.5	75.0	19.8	5.2	below sensitivity	9.1
4	Dephenolated	GO-30-7	400	240	6.4	16.0	4.5	58.9	29.8	10.0	1.3	11.4
5	Dephenolated	DN-3100 Th	400	60	6.5	16.5	5.4	60.2	25.7	12.8	1.3	7.9
6-I	Initial	DN-3100 Th	380	120	6.3	13.2	3.5	90.5	6.1	1.2	2.2	18.3
6-II	Liquid and solid products from 6-I	DN-3100 Th + GO-30-7	400	60	7.5	17.0	4.8	93.8	3.5	0.9	1.8	15.7
6-I+II								84.9[a]	9.3[a]	2.0[a]	3.8[a]	34.0
7-I	Dephenolated	KGU-950	360	60	6.2	13.3		89.5	7.6	1.5	1.4	9.7
7-II	Liquid product from 7-I	GO-30-7	420	60	6.4	14.6	4.6	91.6	4.8	1.4	2.2	11.0
7-I+II								82.0[a]	11.9[a]	2.7[a]	3.4[a]	20.7
8-I	Initial	DN-3100 Th	360	60	6.4	13.3	4.6	n. d.	n. d.	n. d.	n. d.	n. d.
8-I+II	Liquid and solid products from 8-I	DN-3100 Th GO-30-7	400	40	6.5	15.0	4.7	83.9[a]	10.4[a]	1.6[a]	4.1[a]	22.4[a]
9-I	Initial	KGU-950 GO-30-7	360	60	6.4	13.3	4.6	n.d.	n.d.	n.d.	n.d.	n.d.
9-I+II	Liquid and solid products from 9-I	KGU-950 GO-30-7	400	40	6.5	15.4	4.6	n.d.	n.d.	n.d.	n.d.	n.d.
9-I+II+III	Liquid and solid products from 9-II	KGU-950 GO-30-7	340	60	6.5	15.6	6.0	86.5[a]	9.8[a]	1.3[a]	2.4[a]	36.5[a]
10	Initial + gasoline fraction (1:1)	DN-3100 Th	380	120	6.3	13.5	3.1	90.6	6.8	0.9	1.7	18.7
11-I	Initial	DN-3100 Th+GO-30-7	340	40	7.1	15.5	–	n.d.	n.d.	n.d.	n.d.	n.d.
11-I+II	Liquid and solid from 11-I	DN-3100 Th GO-30-7	380	40	7.1	14.9	5.4	95.7[a]	2.6[a]	0.9[a]	0.8[a]	11.8[a]
12	Hydrogen	No	400	60	6.7	15.3	6.7	0	0	0	0	0
13	Initial	No	400	120	0	5.5	0.9	34.5	25.0	39.3	1.2	0
14-I	Initial	KF-848	380	60	7.0	14.8	4.5	90.0	7.9	0.7	1.4	17.2
14-II	Oil from 14-I	KF-1015	400	60	6.5	13.9	4.8	83.6	12.9	1.9	1.6	11.0
14-I+II								75.2[a]	19.6[a]	2.4[a]	2.8[a]	28.2
15-I	Initial	KF-848	380	60	7.3	15.0	4.8	90.8	7.3	0.5	1.4	17.6
15-II	Oil from 15-I	KC 3210	380	40	6.3	13.3	5.6	92.8	5.3	1.9	traces	6.1
15-I+II								84.3[a]	12.1[a]	2.2[a]	1.4[a]	23.7
16	Initial	No	420	90	7.5	20.6	6.8	54.0	28.9	16.5	0.6	9.0

[a]Total yield of the product from the initial object in step I; n. d. — not determined because the temperature was regulated without opening of the autoclave.

3.4. Group composition of the hydrogenated oils

The results of the thin layer adsorption chromatography of the representative oil samples are presented in Table 6.

The data explain that under the selected conditions (6-II) hydroprocessing can increase the content nonaromatic hydrocarbons from 1.8 to 16.1% whereas the total content of hydrocarbons is increased from 19.2 to 62.9%, and the content of undesirable low- and high-polar
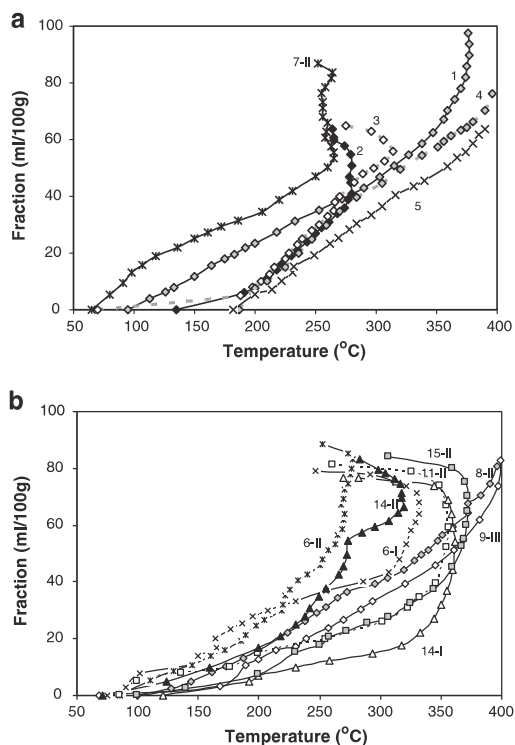
Fig. 1. Fractional composition of the hydrogenated oils obtained by hydroprocessing of the dephenolated (a) and initial (b) heavy residuum under conditions given in Table 4.

Table 5
Yield of distillation fractions and iodine number of the hydrogenated oils (g/100 g initial oil).

Test No	Yield					Iodine number
	200 °C−	200–360 °C	360 °C−	360 °C+	Gas	
1	21.2	49.7	70.9	25.0	4.1	9.7
2	7.0	59.3	66.3	30.7	3.0	n. d.
3	10.3	55.0	65.3	29.6	5.1	n. d.
4	6.1	49.4	55.5	41.5	3.0	n. d.
5	4.4	46.3	50.7	46.8	2.5	n. d.
6-I	22.8	49.4	72.2	25.4	2.4	21.6
6-II	20.1	62.6	82.7	16.0	1.3	5.6
7-II	27.9	54.5	82.4	15.0	2.6	18.7
8-II	13.2	41.8	55.0	42.8	2.2	18.3
9-III	10.3	37.2	47.5	48.4	4.1	21.5
10	37.2	46.9	84.1	9.9	6.0	23.3
11-II	20.5	59.7	80.2	15.3	4.5	35.4
14-I	5.7	72.7	78.4	16.1	5.5	34.3
14-II	13.8	64.6	78.4	18.3	3.3	14.3
15-II	5.3	33.5	38.8	56.5	4.7	23.4

It becomes evident from Table 7 that hydroprocessing can increase the amount of phenols, as what occurred in test 1 with the dephenolated initial oil and in the first stages of tests 14 and 15 where the hydropurification catalyst KF-848 was applied at 380 °C. Contrariwise, the content of phenols is significantly decreased during the next stage of experiments 6, 7, and 8 where the universal catalyst DN-3100 Th (8-I) or the hydrocracking catalyst GO-30-7 (7-II) were used at temperatures 400–420 °C. Noteworthy is that more than 90% of the initial phenols were not decomposed at hydrogenation in the presence of the mix of the latter catalysts at 380 °C (11-II). The results obtained suggest an essential role of temperature in the decomposition of phenols.

According to Table 3, the content of water soluble phenols in the initial oil was between 0.11 and 0.20% depending on their isolation conditions. As shown in Table 8, the content of water soluble phenols extracted three times with water in ratio 1:10 is increased for some scores of times in the stage of hydropurification (14-I and 15-I) whereas in the cracking stage (7-II, 8-II, 11-II) decomposition of the newly formed phenols takes place.

3.6. Ultimate analysis

The results of the ultimate analysis of the more interesting hydrogenated oils are presented in Table 9.

The data in Table 9 demonstrate that dephenolation of the heavy residuum according to Table 3 increases a little the mole ratio of H/C (from 1.16 to 1.21 or 1.18) but somewhat unexpectedly, the contents of both oxygen and nitrogen increase, and the sulfur content decreases from 0.73 to 0.64 and 0.60%. The elemental composition of the dephenolated oils suggests that the phenols in the heavy residuum are very complicated polyfunctional compounds, and the hydrocarbon part extracted

hetero-compounds being 46.8 and 34.0% in the initial oil decrease to 24.3 and 12.8%.

3.5. Secondary phenols and asphaltenes in hydrogenated oils

The total phenols after hydroprocessing of the dephenolated and initial oils were extracted with 5% NaOH (1:5) from the oils diluted with benzene (1:1), and thereafter re-extracted from the acidified water phase with diethyl ether. The results are presented in Table 7.
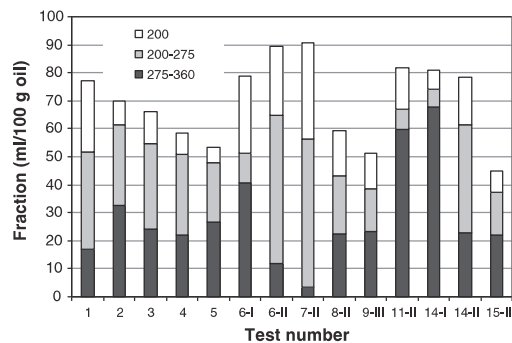

Fig. 2. Distribution of the hydroprocessed oils between naphtha, kerosene and gas oil fractions.

Table 6
Group composition of oils (%).

Compound group	Initial oil	6-II	9-III	11-II	14-I	14-II
Aliphatic hydrocarbons (AlHC)	1.8	16.1	13.2	7.4	3.9	12.7
Monoaromatic hydrocarbons (MAHC)	2.9	11.2	10.4	4.5	5.2	7.0
Polyaromatic hydrocarbons (PAHC)	14.5	35.6	35.9	21.0	21.8	33.1
Low-polar hetero-compounds (LPHet)	46.8	24.3	22.8	35.8	37.5	25.3
High-polar hetero-compounds (HPHet)	34.0	12.8	17.7	31.3	31.6	21.9

Table 7
Total phenols in hydrogenated oils (%).

Test number	1	6-II	7-II	8-II	8-II(360+)[a]	11-II	14-I	14-II	15-I
Phenols in the initial oil (%)	0	26.8							
Phenols in the hydrogenated oil (%)	6.73	3.88	3.57	3.23	9.06	24.8	29.6	7.61	31.7
Hydrogenation temperature (°C)	400	400	420	400	360	380	380	400	380

[a] Engler distillate fraction boiling above 360 °C+ of oil 8-II.

in dephenolation overcomes the phenolic oxygen removed. The elemental composition supports the conclusion drawn in Section 3.3 that pre-dephenolation applied for lighter fractions of shale oil [13–16] is inadvisable for the heavy residuum.

The effect of hydrogenation on the H/C ratio for the initial heavy residuum has less effect than expected. So, mono- and polyaromatic rings have been stable under the conditions tested. But an obvious hydropurification of the oil from heteroatoms has taken place under most conditions tested. For example, in experiment 8-II (where the mix of universal catalyst DN-3100 Th and the hydrocracking catalyst GO-30-7 were applied at 400 °C) the content of sulfur has decreased by 82%, the content of oxygen by 76%, but the content of nitrogen only by 5%. The highest removal of sulfur, by 89%, was obtained in experiment 9-III using the mix of KGU-950 and GO-30-7. In spite of nitrogen having been easily removed from the derivatives of pyridine and pyrrole common in raw oils [24], the removable 5% in this work suggest that nitrogen might exist in an unusual form in the residuum. But more likely, the ammonia and carbon dioxide formed could react and be trapped in the batch autoclave as ammonium carbonate.

Coincidence of the best stability (see Fig. 1) and the lowest content of heteroatoms in the oils from experiments 8-II and 9-III supports the idea that the instability expressed by the peculiar back turning shape of the most distillation curves in Fig. 1 might have resulted from the decomposition of hydrogen bonded labile hetero-associates.

3.7. FTIR analysis

The FTIR spectrum of the initial heavy oil and, as an example, the spectrum of hydrogenated oil 14-II are presented in Fig. 3.

Everyone of the spectra obtained contains absorptions at 748, 1376, 1455, 2853, and 2924 cm^{-1} caused by methyl and methylene groups in aliphatic chains, and complex absorptions at 838, 1150, and 1600 cm^{-1} characteristic for aromatic compounds. The spectrum of the initial

Table 8
Water soluble phenols in hydrogenated oils (%).

Test number	7-II	8-II	11-II	14-I	15-I
Water soluble phenols	0.26	0.16	0.57	4.90	4.17

Table 9
Elemental composition of oils (wt.%, and atomic ratios).

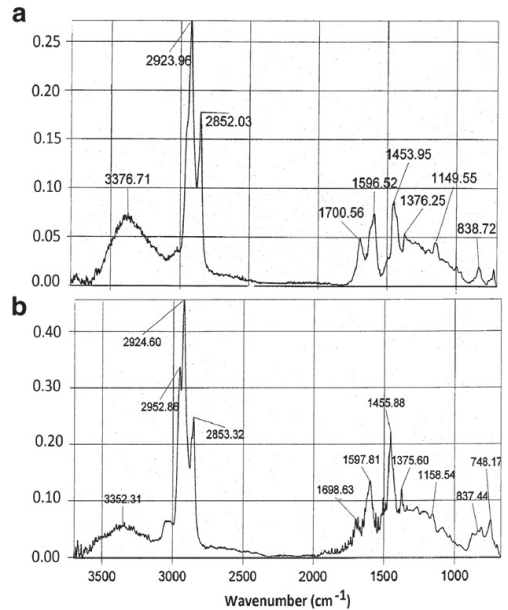| Oil sample	C	H	N	O	S
Initial oil	84.11	8.16	0.20	6.80	0.73
Dephenolated oil (after separation of 27% as phenols)	83.66	8.42	0.21	7.07	0.64
Dephenolated oil (after separation of 17% as phenols)	82.74	8.14	0.21	8.31	0.60
8-I	86.02	8.70	0.18	4.85	0.25
8-II	89.28	8.74	0.19	1.66	0.13
9-III	86.68	9.07	0.21	3.96	0.08
14-I	86.36	8.84	0.14	4.33	0.33
14-II	88.35	8.78	0.11	2.57	0.19

Fig. 3. FTIR spectra of the initial heavy residuum (*a*) and the hydrogenated oil 14-II (*b*).

sample differs from others by an intense absorption at 3377 characteristic for hydroxyl groups. Together with an absorption at 1600 cm^{-1} referring to benzene derivatives a significant concentration of phenolic
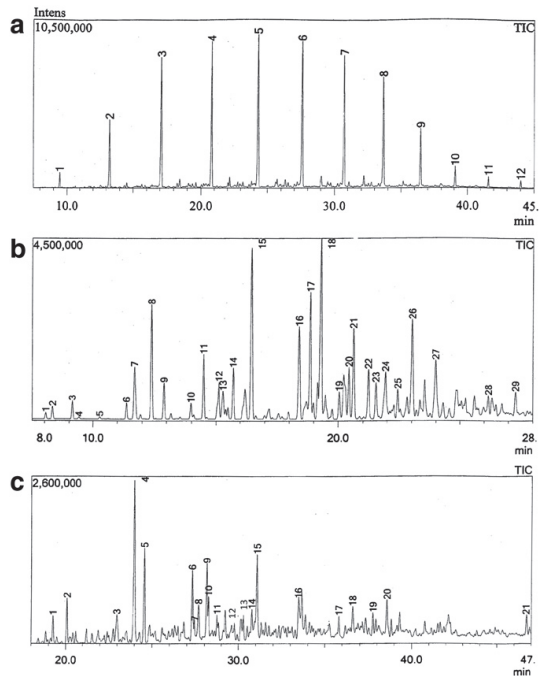

Fig. 4. Total ion chromatograms (TICs) of the hydrogenated oil 14-II compound groups: aliphatic hydrocarbons (*a*), monoaromatic hydrocarbons (*b*), and polyaromatic hydrocarbons (*c*).

compounds in the heavy bituminous oil is evident. Besides, an intense absorption at 1700 cm^{-1} belonging to carbonyl groups is present. As a result of hydrogenation most of the hydroxyl and carbonyl groups

Table 10
Distribution of compounds in the compound groups by GC/MS analysis of hydrogenated oil 14-II.

Peak number	Compound	Base m/z	Retention time (min)	Peak area (%)
Aliphatic hydrocarbons (AlHC)				
1	*n*-Nonane	43	9.5	1.1
2	*n*-Decane	57	13.3	6.1
3	*n*-Undecane	57	17.1	13.3
4	*n*-Dodecane	57	20.8	15.5
5	*n*-Tridecane	57	24.3	16.8
6	*n*-Tetradecane	57	27.6	14.3
7	*n*-Pentadecane	57	30.7	13.6
8	*n*-Hexadecane	57	33.7	10.4
9	*n*-Heptadecane	57	36.5	5.4
10	*n*-Octadecane	57	39.1	1.7
11	*n*-Nonadecane	57	41.6	0.8
12	*n*-Eicosane	57	44.0	0.5
Sum:				100
Monoaromatic hydrocarbons (MAHC)				
1	Ethylbenzene	91	8.0	0.3
2	o-; m-, p-Xylene	91	8.3	0.7
3	o-; m-, p-Xylene	91	9.1	0.9
4	*n*-Nonane	57	9.4	0.1
5	1,2,3-Trimethylbenzene	105	10.3	0.1
6	*n*-Propylbenzene	91	11.4	0.9
7	o-; m-, p-Ethyltoluene; Isopropylbenzene	105	11.7	3.9
8	o-; m-, p-Ethyltoluene; Isopropylbenzene	105	12.4	6.6
9	o-; m-, p-Ethyltoluene; isopropylbenzene	105	12.9	2.0
10	1,3-Diethylbenzene	105	14.0	0.7
11	Indane	117	14.5	3.7
12	o-; m-, p-Propyltoluene	105	15.1	1.4
13	*n*-Butylbenzene	91	15.3	1.5
14	*sec*-Butylbenzene	105	15.7	2.9
15	1-; 4-; 5-Methylindane	100	16.5	11.3
16	1-; 4-; 5-Methylindane	100	18.4	6.4
17	1-; 4-; 5-Methylindane	100	18.9	7.1
18	Tetralin	100	19.3	13.5
19	Naphtalene	100	20.0	1.6
20	2-Ethylindane	117	20.4	3.3
21	1,3-Dimethylindane	100	20.6	5.6
22	2-Methyltetralin	100	21.2	3.0
23	6-Methyltetralin	100	21.5	2.3
24	1-Ethylindane	117	21.9	3.6
25	1,6-; 4,7-Dimethylindane	131	22.4	1.4
26	5-; 6-Methyltetralin	100	23.0	7.0
27	2,7-Dimethyltetralin	100	24.0	5.6
28	6-Ethyltetralin	131	26.2	0.9
29	5,7-Dimethyltetralin	100	27.3	1.5
Sum:				100
Polyaromatic hydrocarbons (PAHC)				
1	Tetralin	104	19.3	2.5
2	Naphtalene	128	20.1	4.5
3	5-Methyl-tetralin	105	23.0	2.8
4	2-Methyl-naphtalene	142	24.0	19.4
5	1-Methyl-naphtalene	142	24.6	9.8
6	1-Ethyl-naphtalene	141	27.3	7.5
7	2-Ethyl-naphtalene	141	27.4	1.7
8	2,7-Dimethyl-naphtalene	156	27.6	3.5
9	2,6-Dimethyl-naphtalene	156	28.1	8.0
10	1,5-Dimethyl-naphtalene	156	28.2	3.8
11	2,3-Dimethyl-naphtalene	156	28.7	1.4
12	1-Propyl-Naphtalene + Ace-Naphtalene	141	30.1	2.7
13	1-Propyl-naphtalene + ace-naphtalene	141	30.3	2.5
14	2-Isopropyl-naphtalene	155	30.8	2.0
15	Butylated hydroxytoluene??	205	31.1	7.9
16	Allyl-naphtalene??	168	33.5	6.5
17	Diphenylmethylcarcinol??	105	35.8	1.9
18	2,2′-Dimethylbiphenol	165	36.6	3.0
19	1,2,3,4-Tetrahydrophenanthrene	182	37.8	2.2
20	Anthracene/phenanthrene	178	38.6	4.6
21	Pyrene	202	46.7	1.9
Sum:				100

have been eliminated, and content of methyl and methylene groups in aliphatic changes has increased. The ratios of absorption intensities in the initial oil for the hydroxyl groups (3377–3352 cm^{-1})/aromatic compounds (1597–1598 cm^{-1}) and carbonyl groups (1700–1699 cm^{-1})/aromatic compounds (1597–1598 cm^{-1}) have decreased accordingly 4.3 and 1.7 times, and those for the methyl- and methylene groups in aliphatic chains (1376 cm^{-1})/aromatic compounds (1597–1598 cm^{-1}) have increased 1.5 times in comparison with the ratios in hydrogenated oil 14-II. The results agree with changes in the compound groups described in Section 3.6.

3.8. GC-MS

The initial bituminous heavy oil and the fractions of high-molecular heterocompounds were too heavy for the GC separation whereas the main components in the compound groups of aliphatic, aromatic and polyaromatic hydrocarbons were clearly identified. As a typical example, the results obtained for hydrogenated oil 14-II are presented in Fig. 4 and Table 10.

The results show practically neither unsaturated nor iso-alkanes among the 12 aliphatic hydrocarbons (C$_9$–C$_{20}$) recognized. At that, the share of C$_{11}$–C$_{16}$ each peak area exceeds 10% and their sum in the group attains 84.25%. The main representatives of monoaromatic hydrocarbons are more varied. Among the 29 compounds identified only two, methyl-indanes and tetralin exceed 10% whereas the group of (di)methyl- and ethylindanes reaches 37.3%, that of tetralin 33.8% and alkyderivatives of benzene 13.9%. 2-Methylnaphtalene is the main component comprising 19.4% among the 21 polyaromatic hydrocarbons found. The share of the other representatives of PAHC, mainly naphtalene (di)methyl- and ethyl derivatives remains below 8%.

3.9. Yield and composition of gases

Variations in the total gas yield under the hydroprocessing conditions tested are given in Table 5. The results of GC gas analysis presented in Table 11 confirm that composition of the gases evolved is affected by the conditions as follows.

The share of hydrogen charged to the autoclave decreases due to exhaustion and dilution with the gases produced under the conditions studied at least to 66.5 (11-II), and maximal to 22.9 vol.% (6-I). According to Table 10, the main gas components by vol.% are hydrocarbons C$_1$–C$_3$ whereas the shares of carbon oxide and dioxide depend on the conditions and catalyst applied. As a rule, the catalysts increase substantially the departure of carbon atoms in the form of hydrocarbons and decrease that of carbon oxides in the hydroprocessing procedures.

Table 11
Composition of the gases evolved at hydroprocessing of the initial oil (vol.%).

Test number	H$_2$	CO	CO$_2$	CH$_4$	C$_2$H$_6$	C$_3$H$_6$	C$_3$H$_8$
6-I	22.9	6.8	17.5	26.1	11.2	3.1	11.8
6-II	37.6	7.2	7.8	27.4	11.5	3.8	3.9
7-II	45.3	29.4	0.9	13.3	5.3	1.4	3.8
8-I	34.9	4.3	8.2	20.1	11.0	5.7	15.8
8-II	57.9	10.0	2.5	18.0	4.7	1.6	5.3
9-I	47.9	3.7	7.4	13.8	8.0	4.6	14.6
9-II	60.3	11.6	2.8	13.4	5.8	1.2	4.9
9-III	52.4	0.8	7.9	8.6	5.0	4.3	21.0
10	39.3	12.3	5.4	19.6	7.4	3.0	13.0
11-II	66.5	5.5	3.8	10.6	4.6	3.4	5.6
14-I	24.8	5.1	11.3	17.8	11.0	5.8	23.4
14-II	30.2	29.5	3.5	17.7	6.9	2.2	10.0
15-I	46.4	7.0	8.8	15.0	9.2	2.8	10.8
15-II	26.3	6.0	10.7	20.9	11.4	6.1	18.6
16	33.1	48.9	0.5	13.7	2.5	0.0	1.3

Table 12
Yields of H_2S and NH_3 evolved in hydroprocessing of the initial oil (wt.% of the heavy residuum).

Component	9			10	11	13	14		15		16
	I	II	III		II		I	II	I	II	
H_2S	0.056	0.048	0.016	0.501	0.301	0.118	0.09	0.058	0.15	0.031	0.326
$S_{gas}/S_{residuum\,I}$	7.22	6.19	2.06	64.59	38.81	15.21	11.60	7.48	19.34	4.00	42.03
$NH_3 \times 10^4$	2.70	0.11	0.075	0.22	n.d.	n.d.	n.d.[a].	n.d.	n.d.	n.d.	n.d.
$N_{gas}/N_{residuum}$	0.111	0.005	0.003	0.009	n.d.	n.d.	n.d.	n.d.	n.d.	n.d.	n.d.

[a] n.d. – not determined.

The data in Table 12 characterize the yield of gaseous H_2S and NH_3 in hydroprocessing.

Heteroatoms such as sulfur and nitrogen are known to leave the reactor as gaseous products at hydroprocessing of heavy crude oils in a fixed-bed reactor system [25]. In this work, only a minor part of the initial sulfur (0.73%) was transformed into toxic H_2S (except in test 16 without any catalyst at 420 °C, test 10 where the initial oil was diluted with gasoline before hydroprocessing, and 11-II using the catalyst DN-3100 Th at 380 °C). It can be concluded, that most of sulfur is transformed into the coke formed. Gasification of the initial oil nitrogen (0.20%) was extremely low, but unlike sulfur, most of the nitrogen remained in the hydroprocessed oil (Table 9).

4. Conclusions

Upgrading of the Estonian shale oil heavy bituminous residuum has been studied for the first time. It has been found that more than 70% of the residuum boiling above 360 °C can be transformed into liquid fuels boiling below 360 °C by two-step (360 and 400–420 °C) hydroprocessing (H_2 6.4–7.5 KPa) in the presence of 10% of various Mo–Co and/or –Ni catalysts: KGU-950, GO-30-7, DN-3100 Th, KF-848, KF-1015 and KC-3210.

Dephenolation before hydroprocessing, known as a common practice for the Estonian shale oil lower fractions, cannot be suggested for the complicated heavy residuum because a lot of hydrocarbons would be wasted as side chains of the high molecular alkylphenols not having yet any marketable value.

Characteristics of the hydrogenated products depend on the co-effects of the pyrolysis conditions, temperature, time and catalysts. So, there cannot be any unique solution for the best conditions and catalysts.

The general regularities of the upgrading are as follows:

- according to FTIR spectra, hydrogenation eliminates most of the hydroxyl and carbonyl groups, and increases the content of methyl and methylene groups in aliphatic chains;
- the H/C ratio increases insignificantly, 1.04–1.06 times in the first stage and 1.01–1.02 times in the second stage, whereas the ratios of O/C decreases accordingly 1.4–1.6 and 2.8–4.4 times and S/C 4.0–6.0 times;
- according to GC/MS, there are only n-alkanes (C_9–C_{20}) in the group of aliphatic hydrocarbons in the hydrogenated oils. The main representatives of monoaromatic hydrocarbons are methylindanes and tetralin, and of polyaromatic hydrocarbons – 2-methylnaphtalene.

The highest yield, 82.7 wt.%, of the fraction boiling below 360 °C was obtained using in the two-stage process the mix of the universal catalyst DN-3100 Th and GO-30-7 (test 6-II). The highest yield, 72.7 wt.%, of the fraction 200–360 °C, concurring with 78.4 wt.% of the total fraction boiling below 360 °C, was obtained using the catalyst KF-848 (test 14-I).

References

[1] 2010 Survey of Energy Resources, World Energy Council, http://www.worldenergy.org/documents/ser_2010_report.pdf (ISBN 978-0-946121-02-1, 98).
[2] M.S. Rana, V. Sámano, J. Ancheyta, J.A.I. Diaz, A review of recent advances on process technologies for upgrading of heavy oils and residua, Fuel 86 (2007) 1216–1231.
[3] R.S. Goodrich, A synfuels era for the United States? Energy Conversion and Management 23 (1983) 1–9.
[4] V. Oja, A brief overview of motor fuels from shale oil of kukersite, Oil Shale 23 (2006) 160–163.
[5] A. Krichko, Hydrogenation of oil shale and polymers, Oil Shale 17 (2000) 271–285.
[6] M.V. Landau, M. Herskowitz, D. Givoni, S. Laichter, D. Yitzhaki, Medium-severity hydrotreating and hydrocracking of Israeli shale oil. II. Testing of novel catalyst systems in a trickle bed reactor, Fuel 77 (1998) 3–13.
[7] M.V. Landau, M. Herskowitz, D. Givoni, S. Laichter, D. Yitzhaki, Medium severity hydrotreating and hydrocracking of Israeli shale oil. III. Hydrocracking of hydrotreated shale oil and its atmospheric residue for full conversion to motor fuels, Fuel 77 (1998) 1589–1597.
[8] A. Muradian, L. Stephenson, Jet and diesel fuels derived from Julia Creek shale oil, Proceedings of the Second Australian Workshop on Oil Shale, Brisbane, 6–7 December, 1984, 1984, pp. 239–244.
[9] S.J. Smidth, New directions for shale oil: path to a secure new oil supply well into this century, Oil Shale 20 (2003) 333–346.
[10] I. Rooks, A historical review of RAS "Kiviter", Oil Shale 11 (1994) 283–285.
[11] G. Low, R. Egelberg, O. Alkilde, Upgrading of Estonian shale oil to high quality Euro V diesel, Oil Shale Symposium, International Oil Shale Symposium, Tallinn, Estonia, June 10–13, 2013, 2013, p. 28, (http://www.oilshalesymposium.eu).
[12] H. Luik, Hydrogenation of Estonian oil shale and shale oil, Oil Shale 11 (1994) 151–160.
[13] H. Luik, E. Lindaru, N. Vink, L. Maripuu, Upgrading of Estonian shale oil distillation fractions. 1. Hydrogenation of the "diesel fraction", Oil Shale 16 (1999) 141–148.
[14] H. Luik, N. Vink, E. Lindaru, L. Maripuu, Upgrading of Estonian shale oil distillation fractions. 2. The effect of time and hydrogen pressure on the yield and composition of "diesel fraction" hydrogenation products, Oil Shale 16 (1999) 249–256.
[15] H. Luik, L. Maripuu, N. Vink, E. Lindaru, Upgrading of Estonian shale oil distillation fractions. 3. Hydrogenation of light mazute, Oil Shale 16 (1999) 331–336.
[16] H. Luik, N. Vink, E. Lindaru, L. Maripuu, Upgrading of Estonian shale oil distillation fractions. 4. The effect of time and hydrogenation pressure on the yield and composition of light mazute hydrogenation products, Oil Shale 16 (1999) 337–342.
[17] H. Luik, N. Vink, E. Lindaru, L. Maripuu, Upgrading of Estonian shale oil distillation fractions. 5. Hydrogenation of heavy mazute, Oil Shale 17 (2000) 25–30.
[18] H. Luik, N. Vink, L. Maripuu, E. Lindaru, Upgrading of Estonian shale oil distillation fractions. 6. The effect of time and temperature on the yield and composition of heavy mazute hydrogenation products, Oil Shale 17 (2000) 31–36.
[19] H. Luik, L. Luik, I. Johannes, L. Tiikma, J. Sokolova, Co-processing of biomass and heavy shale oil using catalytical hydrocracking method, 17th European Biomass Conference & Exhibition, Proceedings of the International Conference, Hamburg, Germany, 29 June–3 July, 2009, Florence, Italy, ETA-Florence Renewable Energies; WIP-Renewable Energies, 2009, pp. 1082–1084.
[20] H.M. Chishti, P.T. Williams, Aromatic and hetero-aromatic compositional changes during catalytic hydrotreatment of shale oil, Fuel 78 (1999) 1805–1815.
[21] H. Luik, Alternative technologies for oil shale liquefaction and upgrading, International Oil Shale Symposium, Tallinn, Estonia, June 8–11, 2009, 2009, p. 44, (http://www.oilshalesymposium.com).
[22] VKG - Viru Keemia Grupp AS (http://www.vkg.ee).
[23] L. Tiikma, L. Mölder, H. Tamvelius, Resources of water-soluble alkylresorcinols in distillates of the shale oil from generators of high unit capacity, Oil Shale 9 (1992) 330–335.
[24] M.R. Gray, Upgrading Petroleum Residuums and Heavy Oils, Marcel Dekker, New York, 1994.
[25] A. Alvarez, J. Ancheyta, Effect of liquid quenching on hydroprocessing of heavy crude oils in a fixed-bed reactor system, Industrial and Engineering Chemistry Research 48 (2009) 1228–1236.

Article V

Johannes, I., Tiikma, L., **Sokolova, J. (Krasulina, J.**). Dissolution rate of oil shale thermobitumen in different solvents. – *Oil Shale*, 2009, vol. 26, no. 3, pp. 399-414.

DISSOLUTION RATE OF OIL SHALE THERMOBITUMEN IN DIFFERENT SOLVENTS

I. JOHANNES[*], L. TIIKMA, J. SOKOLOVA

Laboratory of Oil Shale and Renewables Research
Tallinn University of Technology
5 Ehitajate Rd., Tallinn 19086, Estonia

Dissolution kinetics of the mix of thermobitumen and oil (TBO) formed at low-temperature pyrolysis of oil shale in autoclaves was studied for the first time. The pyrolysis temperature was varied in the range of 350–370 °C and duration between 3 and 9 hours. The dissolution of TBO obtained was conducted in a thermostated stirred class reactor and evaluated by the increase in optical density of the solutions with time varying temperature (25–60 °C) and solvent type (benzene, toluene, oil shale petrol and ethanol). A mathematical model was deduced for quantitative description of dissolution kinetics by approximation of the process to the first-order parallel dissolution of two fractions. The dissolution rate coefficients for the fractions were estimated, and contribution of their partial optical densities on the current optical density was described under the conditions studied.

Introduction

It is known that at pyrolysis of Estonian oil shale (kukersite) between temperatures 250–350 °C the unwanted plasticization takes place resulting in formation of sticky thermobitumen (TB) and some light fractions. The TB formed is a mix of soluble in organic solvents high-molecular non-volatile intermediate products of kerogen thermal decomposition. At 325–350 °C begins the secondary pyrolysis of TB into oil fractions, gas and semicoke. The physical characteristics and molecular weight of TB depend on its formation conditions [1].

At the present time, formation of TB from oil shale studied intensively in the middle of the last century is of interest again [2–6] in order to perform the isolation of a maximum amount of organic substances from kukersite. Reviews about previous works and the recent experimental results concerning formation of TB from oil shale in Fischer retort and of the mix of TB and oil (TBO) in autoclaves were published in [2] and [3]. The results proved the

---

[*] Corresponding author: e-mail *ille.johannes@ttu.ee*

possibility for dissolution about 90% of oil shale organic matter as TBO when the thermal treatment is conducted below the temperature range for coke formation. The yield of the decomposition products in the form of TBO overcomes 1.5 times the oil yield at retorting of kukersite in a laboratory Fischer assay. Besides, the content of hazardous organic matter in semicoke is decreased drastically. The main disadvantage of the thermobituminization process is the comparatively slow formation of TBO (3-5 h) at the low-temperature region required. Kinetics of parallel formation of TB, oil and gas from kukersite, and consecutive formation of gas and coke from TBO or TB was modeled in [4] and [5] for the temperatures range 350–410 °C. It was found [6] that when thermal decomposition of kukersite was conducted in the environment of supercritical water, ethanol or oil shale petrol, the formation of TBO was accelerated whereas the solvents benzene, toluene and sub-critical water had no effect on the decomposition rate in comparison with the process without any solvent. The papers [7] and [8] showed that at liquefaction of the enriched kukersite, kerogen-70, during 4 hours at 360 °C in an autoclave the solvents applied arranged by the yield of liquid products from organic matter as follows, %: water (69.6), *n*-hexane (72.2), benzene (81.5), ethanol (99.0!), diethyl ether (106.3!) and dimethyl ketone (145.7!). At that, the surprisingly high liquid yields obtained with the last three solvents were explained by incorporation of the solvents into TBO.

The liquid and solid products formed at thermal decomposition of oil shale, independently of the solvents applied, were diluted in benzene [3–8] or in the mix of benzene and ethanol [1, 2]. In the next step, the phases were separated by time-consuming Soxhlet extraction with boiling benzene [1–6] or by filtration and washing with benzene at room temperature [7, 8]. Filtration of some gel-like products was travail.

The goal of this work, dissolution rate of TBO formed, has not been studied earlier.

Survey of dissolution models

In [9] an overview about history of dissolution research during the last century was published. According to this report, already in 1897 Noyes and Witny [10] in Massachusetts Institute of Technology proposed the following expression for dissolution rate of solid substances

$$\frac{dC}{dt} = k(S - C), \tag{1}$$

where C was the current concentration at time t, S represented the solubility of the substance, and k was a constant.

Already in the beginning of the 20th century it was shown [1] that the dissolution rate coefficient depended on the stirring rate, temperature, and surface and on the arrangement of the dissolution device. According to

Nernst-Brunner equation [11] dissolution rate expression was advanced basing on the diffusion layer concept as follows:

$$\frac{dC}{dt} = \frac{DA}{Vh}(C_S - C), \tag{2}$$

where D was the diffusion coefficient, A the exposed surface area of the solid, h the thickness of the diffusion layer, and V the volume of the diffusion medium (which was stirred rapidly to insure homogeneity), C_S was the concentration of the dissolved solid in the diffusion layer surrounding the solid.

When a solvent reacts throughout the particle at all times, and the amount of the particles is exhaustible, the dissolution rate can be given in the same form as for a homogeneous reaction where instead of C_S the maximum concentration being attained (the steady state) under the dissolution conditions, C_{max}, is applied.

Up to now, the first order kinetic equation (2) and its integrated form

$$\ln(1 - x) = \frac{DA}{Vh}t, \tag{3}$$

where x is C/C_S or C/C_{max} have been widely applied in dissolution kinetics [12].

When the plot of C/C_{max} versus t has an asymmetric sigmoidal shape, the semi-empirical "Power Law" model

$$\frac{C}{C_{max}} = kt^n \tag{4}$$

has been proposed by Peppas [13] where n is a non-physical fit parameter that does not satisfy any physico-chemical model being mathematically derived to-date for phase transformation kinetics.

The generalized integral rate equation of the physico-chemical models is as follows:

$$g(x) = kt, \tag{5}$$

where conversion function $g(x)$ is determined by the process mechanism and should be proportional with time.

A selection from the set of formulas for calculation of $g(x)$ in the most frequently used models for solid-state reactions published in [14] and later applied by several researchers [16–22] are given in Table 1.

The aim of this work was quantitative description of the effect of solvent type on the dissolution rate of TBO. For this aim, the suitable kinetic model was obtained, and the effects of solvent volume and temperature, and of pyrolysis temperature and duration on the total dissolution rate coefficients, k, were elucidated. The individual contribution of the factors of k (D, A, V and h) depending mainly on the substance being dissolved was not discussed in this work handling only TBO.

Table 1. **Integral forms of the conversion function, *g*(*x*) [14-22]**

Model type	$g(x)$	Formula No
First-order, Eq. (3)	$-\ln(1-x)$	*I*
n–order	$[1-(1-x)^{1-n}]/(1-n)$	*II*
1D diffusion	x^2	*III*
2D-diffusion	$x+(1-x)\ln(1-x)$	*IV*
3D-diffusion	$[1-(1-x)^{1/3}]^2$	*V*
4D-diffusion	$1-2x/3\text{-}(1-x)^{2/3}$	*VI*
Zero-order	x	*VII*
Contracting area	$[1-(1-x)]^{1/2}$	*VIII*
Contracting volume	$[1-(1-x)]^{1/3}$	*IX*
Power law, Eq. (4), *n* = 2	$x^{1/2}$	*X*

Experimental

Materials

The initial air-dry oil shale contained 40% organic matter (kerogen) and 0.57% hygroscopic water. The purity of the solvents applied was of analytical grade, except oil shale petrol. The latter was obtained from the industrial Galoter process [23]. Its density at 20 °C was 0.780 kg/dm^3.

Pyrolysis

The samples of TBO for dissolution tests were prepared by pyrolysis of 1 gram of the initial kukersite in a glass test-tube with inner diameter 10 cm inserted into a 20 cm^3 autoclave. The autoclaves were placed into a muffle oven heated up to various nominal temperatures between 350–370 °C. Pyrolysis duration was varied in the range of 3–9 hours. The gas yield was estimated by the weight loss of the cooled to room temperature and opened autoclaves. The yield of TBO per organic matter was found by subtraction of the yields of gas and solid residue from 100%. The yield of organic solid residue remaining after dissolution was estimated by weight loss at incineration of the acid treated residue. In this way the artifacts concerning over-estimated yields of TBO due to incorporation of solvents discussed in [6, 8] were avoided.

   The yields of TBO obtained under various conditions are presented in the second column of Tables 2 and 3, and in Fig. 1. The results prove the essential effect of the pyrolysis temperature and duration on the yield of TBO from kukersite known earlier [2–8]. At that, about 30-minute prolongation of the time to reach the maximum yield in comparison with that given earlier [3 and 4] can be explained by an increase of the heating-up time due to additional glass tubes applied for the samples in autoclaves in this work. Noteworthy is the negligible effect of dissolution temperature on the total yield of TBO. The vital effect of the dissolution conditions on the dissolution kinetics will be discussed later below.

Table. 2. **Characteristic constants for TBO dissolution in benzene**

The default conditions: benzene volume per kukersite 100 cm^3/g; dissolution temperature − 60 °C; dilution factor of the solutions before estimation of their optical density − 10; wave length − 420 nm, l = 1 cm.

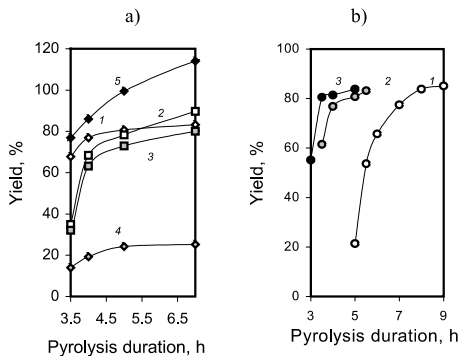| Variable	Yield of TBO, % from kerogen	Maximum optical density		Rate coefficient, min^{-1}	
		E_{1max} Eq. (23)	E_{2max} Eq. (23)	k_1 Eq. (24)	k_2, Eq. (21)
Pyrolysis nominal temperature 350 °C					
Pyrolysis duration, h					
5	21.4	0.271	−	10.25	−
5.5	53.6	0.652	0.021	0.591	0.021
6	65.7	0.765	0.074	0.625	0.022
7	69.7	0.796	0.059	0.705	0.036
8	83.8	1.049	−	1.109	−
Pyrolysis nominal temperature 360 °C					
Pyrolysis duration, h					
3.5	67.8	0.803	0.053	0.539	0.0517
4	76.8	0.917	0.095	0.686	0.0306
5	80.7	1.023	−	1.208	−
7	83.2	1.038	−	1.164	−
Dissolution temperature, °C					
25	67.4	0.640	0.216	0.133	0.0060
40	67.4	0.743	0.112	0.205	0.0292
60	67.8	0.803	0.053	0.539	0.0517
Pyrolysis nominal temperature 370 °C					
Pyrolysis duration, h					
3	55.1	0.652	0.0506	0.395	0.0481
3.5	80.54	1.021	−	2.257	−
4	81.4	1.032	−	3.175	−
5	83.8	1.062	−	4.096	−

Fig. 1. Effect of pyrolysis duration on the total yield of TBO from kerogen, %, (*a*) solvent type: 1 − benzene, 2 −toluene, 3 − oil shale petrol, 4 − ethanol, 5 − benzene + ethanol; (*b*) pyrolysis nominal temperature: 1 − 350, 2 − 360, 3 − 370 °C.

The default conditions: pyrolysis nominal temperature 360 °C; pyrolysis duration 3.5 h; solvent volume 100 cm^3/g; dissolution temperature 60 °C, solvent − benzene.

Table. 3. **Characteristic constants for TBO dissolution in different solvents**

The default conditions: pyrolysis nominal temperature 360 °C; pyrolysis duration 3.5 h; solvent volume per kukersite 100 cm^3/g; dissolution temperature – 60 °C; dilution factor of the solutions before estimation of their optical density – 10; wave length – 420 nm, l = 1 cm.

Variable	Yield of TBO, % from kerogen	Maximum optical density		Rate coefficient, min^{-1}	
		E_{1max} Eq. (23)	E_{2max} Eq. (23)	k_1 Eq. (24)	k_2 Eq. (21)
Toluene					
Pyrolysis duration, h					
3.5	34.9	0.353	0.054	0.486	0.058
4	68.4	0.822	0.050	0.892	0.035
5	78.3	0.838	0.153	0.960	0.400
7	89.7	1.137	–	2.460	–
Ethanol					
Pyrolysis duration, h					
3.5	13.9	0.086	0.091	0.0632	0.0025
5	24.3	0.202	0.106	0.157	0.0189
7	25.2	0.249	0.070	0.597	0.0402
Solvent volume, cm3/g					
75	15.8	0.057	0.118	0.171	0.0161
100	13.9	0.086	0.091	0.0632	0.0025
150	13.9	0.055	0.101	0.065	0.0016
Oil shale petrol, $d = 0.780$ g^3/cm^3					
Pyrolysis duration, h					
3	30.8	0.391	–	0.246	–
3.5	32.1	0.407	–	0.322	–
4	63.3	0.802	–	0.983	–
8	83.0	1.052	–	1.998	–
Ethanol + benzene, (1:1)$_V$					
Pyrolysis duration, h					
3	69.5	0.801	0.078	0.763	0.159
3.5	76.9	0.915	0.078	0.544	0.047
5	91.6	1.261	–	0.983	–
8	116.0	1.471	–	1.261	–

Dissolution

The pyrolyzed sample stuck, as a rule, in the form of the stick-like inner volume of the glass test-tube. Dissolution of the product with any solvent in a flow tube-reactor without stirring failed revealing that an active agitation of the suspension was required. For this aim, in the next experiments the pyrolyzed sample was quantitatively poured into 100 cm^3 thermostated (20-60 °C) dissolution solvent in a refluxed flask stirred with an anchor mixer with constant rotation rate, 3000 turns/min. After certain intervals a volume V_{an} was taken from the solution for photometric determination of optical density (E^*) of the solutions by a spectrophotometer SPEKOL 11. As far the solution volume per mass of the sample decreased with every volume taken

for the analysis, the corrected current optical densities (E_n) were calculated as follows:

$$E_n = \left\{ \sum_{i=1}^{n-1} E^*_i V_{an} + E^*_n \left[V - (n-1) V_{an} \right] \right\} / V. \qquad (6)$$

The plot of optical density at the wave length 420 nm *versus* TBO concentration estimated by weight has given a linear calibration graph with slope 3.21 $dm^3(cm\ g)^{-1}$. So, the current yield of TBO at dissolution from its total soluble quantity in the solvent, C/C_{max}, should be equal with the ratio of the corresponding optical densities, E/E_{max}.

The experimental results prove the modeled earlier regularities [4] – the yield of TBO increases with pyrolysis time and temperature (Fig. 2a). Besides, as it can be expected, the rate increases with dissolution temperature (Fig. 2b). But the effects of the solvent volume (Fig. 2c) and type (Fig. 2d) are insignificant, except ethanol whose dissolution possibility is remarkably lower.

Fig. 2. Effect of dissolution time on the dissolution degree of TBO formed at different variables: (*a*) pyrolysis duration, h; (*b*) dissolution temperature, °C; (*c*) solvent type (see the symbols in Fig. 1a).
    The default conditions see in Fig. 1.

TBO dissolution kinetics

Suitability of the known dissolution models

For quantitative comparison of the effect of various solvents on the TBO dissolution kinetics, the rate coefficient k was estimated by different kinetic models. Fitness of the models was evaluated by invariability of their k during dissolution. For this aim, linearity between $g(x)$ and t according to Eq. (5) was tested using the models given in Table 1 for calculation of $g(x)$.

At first, the typical dissolution model described by Eq. (3) was tested. For estimation of the two unknown constants, E_S and k, the equation was written as

$$k = \frac{\ln\left(1 - \dfrac{E}{E_S}\right)}{t},\tag{7}$$

and the least squares method was applied introducing the series of experimentally found E and t values. At that, for the most of the dissolution conditions studied the best fit of k was obtained at a value of E_S proposed that provided unacceptable systematically decreasing in time values of k with a high (10–30%) mean dispersion. So, the model with diffusion layer concentration does not agree with experimental results.

In the following calculations, considering the exhaustible amount of TBO, the dissolution degree, $x = E/E_{max}$ was used where the maximum value of optical density was found experimentally as the mean during 2–3 hours dissolution.

Unsuitability of the "Power law" model, Eq. (4), was proved by curvilinear shape of the logarithmic relationship between x and t.

The plots of $g(x)$ calculated according to the formulas given in Table 1 *versus* dissolution time for the default conditions given in Tables 2 and 3 are presented in Fig. 3a. At that, the values of $g(x)$ in Fig. 3a are normalized by dividing with their values at 30 min., and in 3b with those at 10 min. The curves obtained evidence that Models *I* and *III–X* give quite similar convex-type curves suggesting decreasing in time rate coefficients, and Model II ($n = 2$, 3, and 4) oppositely, concave-type ones. But there are some experi-
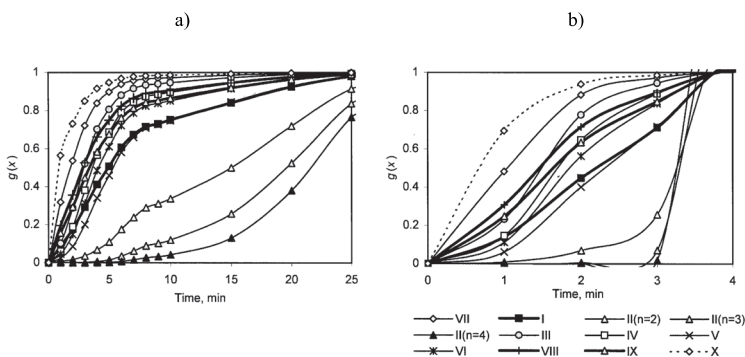
a)   b)

Fig. 3. Effect of dissolution time on the current values of $g(x)$ calculated by different models: (*a*) for the default conditions, (*b*) for pyrolysis temperature 370 °C and time 3.5 h. The numbers of curves are equivalent with their formula numbers in Table 1.
   The default conditions see in Fig. 1.

mental conditions whose results can be approximated to a linear relationship, particularly following the first order kinetic model I, (Fig. 3b, curve *I*). These phenomena will be discussed later below.

Model for the two-stage parallel dissolution

For more adequate modeling of TBO dissolution kinetics, all the curves in Fig. 3a can be more or less satisfactorily approximated to two intersecting straight lines belonging to two stages. The first stage is compiled from parallel dissolution of two fractions with different dissolution rate coefficients. As soon as dissolution of the first component has reached its steady state, the next stage begins where dissolution of the single second component takes place. Basing on Fig. 3b, the first order Model *I* has been chosen from the bulk of formulas *I–X*.

The two straight lines are expressed by the following formulas:

$$Y_1 = b_1 t \qquad (8)$$

and

$$Y_2 = a_2 + b_2 t \qquad (9)$$

having their intersection point at time

$$t' = a_2/(b_1 - b_2). \qquad (10)$$

Admitting that in the first stage the parallel dissolution of the lower-molecular weight fraction (1) and higher-molecular weight fraction (2) takes place, an increase in the total optical density of the solution should follow the relationship

$$dE/dt = k_1(E_{1max} - E_1) + k_2(E_{2max} - E_2), \qquad (11)$$

where the rate coefficients k_1 and k_2, and the maximum optical densities E_{1max} and E_{2max} are four unknown constants to be estimated. Besides, the current optical densities of the two components (E_1 and E_2) having coinciding spectra cannot be measured separately either. The experimentally recorded values are their sums

$$E_{max} = E_{1max} + E_{2max} \qquad (12)$$

and

$$E = E_1 + E_2. \qquad (13)$$

Algorithm for estimation of k_2

For estimation of the unknown constants, the second stage beginning from t' determined by Eq. (10) is handled at first. As far during this stage the current and maximum total optical densities differ from those of the second component by E_{1max}, the following equalities are valid:

$$\mathrm{d}E/\mathrm{d}t = k_2(E_{\max} - E),\tag{14}$$

$$\mathrm{d}E_2/\mathrm{d}t = k_2(E_{2\max} - E_2).\tag{15}$$

Integration of Eq. (14) in the boundaries from E' to E and t' to t gives

$$\ln\frac{1-\dfrac{E'}{E_{\max}}}{1-\dfrac{E}{E_{\max}}} = k_2(t-t').\tag{16}$$

Eq. (16) can be presented in the form of a linear regression

$$y = A_2 + B_2 x,\tag{17}$$

where

$$y = \ln\left(1-\frac{E}{E_{\max}}\right),\tag{18}$$

$$x = (t - t'),\tag{19}$$

and the regression coefficients

$$A_2 = \ln\left(1-\frac{E'}{E_{\max}}\right),\tag{20}$$

$$B_2 = -k_2.\tag{21}$$

Algorithm for estimation of $E_{1\max}$ and $E_{2\max}$

The integrated form of Eq (11) describes the time-dependence of the total optical density

$$E = E_{1\max}[1 - \exp(-k_1 t)] + E_{2\max}[1 - \exp(-k_2 t)].\tag{22}$$

In the second stage where dissolution of the first component is completed

$$E = E_{1\max} + E_{2\max}[1 - \exp(-k_2 t)].\tag{23}$$

Eq. (23) should express a straight line of the current optical densities versus the current shares of not dissolved second component expressed as $[1 - \exp(-k_2 t)]$. So, the regression constants in Eq. (23) correspond directly to the maximum optical densities of the components.

Algorithm for estimation of k_1

The value of k_1 can be found as a slope of the linear regression obtained after replacements in Eq. (22) as follows:

$$Y = -\ln\{1 - [E - E_{2\max}(1 - \exp(-k_2 t)]/E_{1\max}\} = k_1 t\tag{24}$$

introducing the constants k_2, $E_{1\max}$ and $E_{2\max}$ found as described above and the current optical densities in the first stage where $t < t'$.

The values of k_2, $E_{1\max}$, $E_{2\max}$ and k_1 and found by Eqs. (16), (21), (23) and (24) are gathered in Tables 2 and 3.

Algorithm for estimation of current dissolution yields

The current concentration of TBO in the dissolution solutions is calculated as

$$C = \frac{EV}{BV_{an}l},\tag{25}$$

where V/V_{an} is the dilution degree of the solution for analysis, B is the special absorptivity of TBO equal to the slope of the calibration curve at the wavelength applied, and l is the length of the optical path.

The current yield of TBO from the sample being dissolved, in grams per 100 gram of the initial organic matter (kerogen)

$$\alpha_{OM} = 100CV/G,\tag{26}$$

where V is volume of the dissolution solution (dm^3), and G is mass of the initial sample or its kerogen at the low-temperature pyrolysis.

Results and discussion

Estimation of the dissolution rate coefficients and maximum optical densities

The values of E estimated in every series were introduced into the first order kinetic formula *I* given in Table 1 and plotted against the corresponding dissolution time. As examples, the curves for dissolution of TBO in benzene at 360 and 370 °C are presented in Fig. 4a. The distinct difference between the two stages evident for 360 °C (curves 1–3) allows estimation of the regression coefficients b_1, a_2 and b_2 according to Eqs. (8) and (9). For 370 °C (curve 4) a linear relationship is kept up to the function value –4.3 corresponding to the dissolution degree 0.986 from the total soluble TBO. So, the single stage model can be applied for description of the dissolution process under the last conditions, and similar ones. In such cases the slope is equivalent to the single dissolution rate coefficient $-k$.

According to Eq. (21), the value of $-B_2$ for the second stage is equal to k_2. All the second stage rate coefficients for the two-stage processes revealed under the conditions studied are given in the last columns of Tables 2 and 3. In conditions where the one-stage mechanism describes the kinetics satisfactorily, the values of k_2 are absent in the columns.

For estimation of $E_{1\max}$ and $E_{2\max}$, the current optical densities estimated in the second stage were plotted against the function $1 - \exp(-k_2 t)$ according

to Eq. (23). Some examples are given in Fig. 4b. The values of the maximum optical densities found from the slope and intercept are presented in the third and fourth columns of Tables 2 and 3.
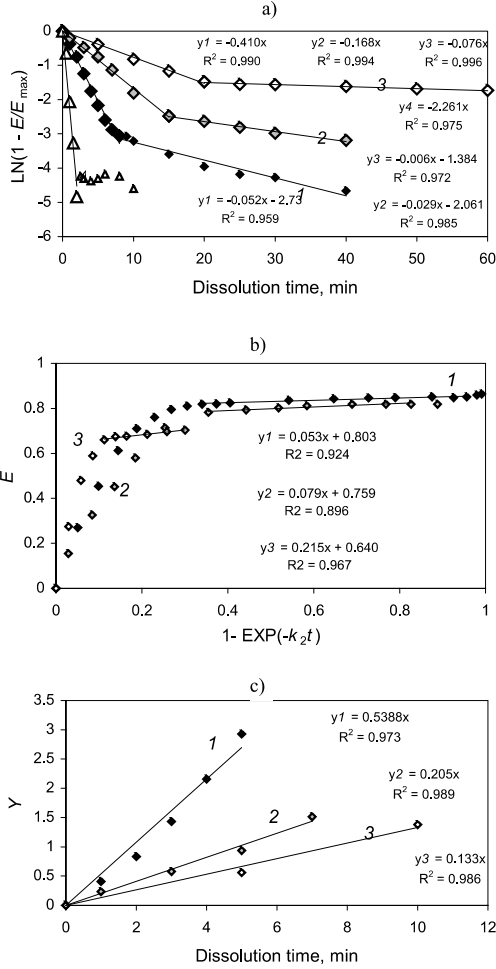

Fig. 4. Plot of the assisting functions for calculation of the constants: (*a*) k_2 by Eq. (14, 19); (*b*) E_{1max} and E_{2max} by Eq. (21); (*c*) k_1 by Eq. (22) for dissolution temperatures: 1 – 60; 2 – 40 and 3 – 25 °C, and 4 in Fig. (*a*) – for pyrolysis temperature 370 °C.

The default conditions see in Fig. 1.

At last, the values of k_1 were estimated as the slope introducing the values of t and E of the first stage into Eq. (24). Some examples are depicted in Fig. 4c. The values found are given in the fifth column of Tables 2 and 3.

The data obtained (Tables 2 and 3) evidence that, as a rule, the dissolution kinetics characterized by a single stage and rate coefficient is appropriate in conditions resulting in higher (over 80%) decomposition degree of oil shale organic matter, for example at prolonged pyrolysis durations or at higher pyrolysis temperatures. On the contrary, the one-stage dissolution scheme can be applied also at the beginning of thermal decomposition (below 25%) at 350 °C. Noteworthy is that, despite the low yield, the dissolution process of TBO in ethanol consists of two stages, and the dissolution in oil shale petrol is an one-stage process at any pyrolysis duration and corresponding yield of TBO obtained.

Prediction of the current optical densities of the dissolution solutions

When the values of k_1, k_2, E_{1max} and E_{2max} have been estimated, the current values of optical density over the both stage can be predicted by Eq. (22). As examples, the plots of E versus t are depicted in Fig. 5 for the two-stage dissolution scheme of TBO obtained by pyrolysis at 360 °C under the three dissolution temperatures 25, 40 and 60 °C (curves 1–3), and an one-stage process under temperature 60 °C of TBO obtained at 370 °C (curve 4).

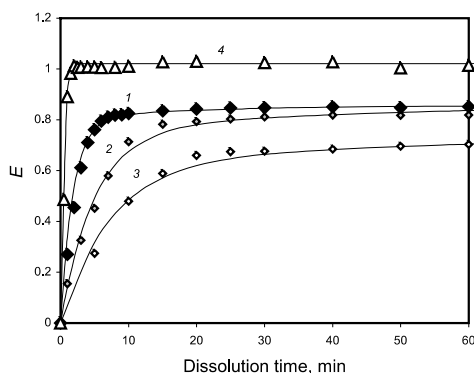The current concentration and yield of TBO can be calculated according to Eqs. (25) and (26).

Fig. 5. Plot of optical density versus dissolution time for dissolution temperatures, °C: 1 − 60, 2 − 40, 3 − 25, and 4 − for pyrolysis temperature 370 °C.
  Points experimental, curves − calculated.
  Dilution factor of the solutions before estimation of their optical density − 10; wave length − 420 nm, l = 1 cm. The default conditions see in Fig. 1.

Conclusions

Dissolution kinetics of the mix of thermobitumen and oil (TBO) obtained at low-temperature pyrolysis of kukersite in various solvents was studied for the first time. The main results of the study were as follows:

- Dissolution of the sticky TBO needs an active stirring and allows under optimal conditions separation of 80–90% from the kukersite organic matter as a liquid product.
- The yield of TBO into the solvents applied increases in the row: ethanol $\ll$ oil shale petrol $\approx$ benzene < toluene < benzene + ethanol whereas part of ethanol incorporates into TBO.
- The dissolution of TBO at an active stirring is faster (less than 30 min) than formation of TBO (3.5–5 hours) and depends mainly on the decomposition degree of the initial kerogen determined by the pyrolysis temperature and duration, and on the dissolution temperature. The effect of solvent type on the dissolution rate is negligble, except in ethanol.
- The dissolution kinetics under the conditions enabling low (below 25%) and high (over 80%) total yield of TBO can be described by the first-order kinetic model, except in ethanol. Under conditions enabling the total yield of TBO in the range of 25–80%, and in ethanol at any yield, the fourteen known kinetic models tested were unsuitable for description of the process.
- A mathematical model basing on the scheme of parallel first-order dissolution of two fractions has been deduced for satisfactory description of the dissolution kinetics of TBO not fitting under the models known earlier.
- The rate coefficients for dissolution of the fractions, and the maximum optical densities of their solutions were estimated for the conditions studied.

Acknowledgements

REFERENCES

1. *Aarna, A. Y., Lippmaa, E. T.* Thermal destruction of oil shale-kukersite // Trans. Tallinn Polytechnic Institute. Series A. 1958. No. 97. P. 3–27 [in Russian].

2. *Zaidentsal', A. L., Soone, J. H., Muoni, R. T.* Yields and properties of thermal bitumen obtained from combustible shale // Solid Fuel Chemistry. 2008. Vol. 42, No. 2. P. 74–79.

3. *Tiikma, L., Zaidentsal, A., Tensorer, M.* Formation of thermobitumen from oil shale by low temperature pyrolysis in an autoclave // Oil Shale. 2007. Vol. 24, No 4. P. 535–546.

4. *Johannes, I., Tiikma, L., Zaidentsal, A., Luik, L.* Kinetics of kukersite low-temperature pyrolysis in autoclaves // J. Anal. Appl. Pyrolysis. 2009. Vol. 85, No. 1–2. P. 508–513.

5. *Johannes, I., Zaidentsal, A.* Kinetics of low-temperature retorting of kukersite oil shale // Oil Shale. 2008. Vol. 25, No 4. P. 412–425.

6. *Tiikma, L., Johannes, I., Luik, H., Zaidentsal, A., Vink, N.* Thermal dissolution of Estonian oil shale // J. Anal. Appl. Pyrolys. 2009. Vol. 85, No. 1–2. P. 502–507.

7. *Luik, H., Klesment, I.* Liquefaction of kukersite concentrate at 330-370 °C in supercritical solvents // Oil Shale. 1997. Vol. 14, No. 4. P. 419–432.

8. *Luik, H., Palu, V., Bityukov, M., Luik, L., Kruusement, K., Tamvelius, H., Pryadka, N.* Liquefaction of Estonian kukersite oil shale kerogen with selected superheated solvents in static conditions // Oil Shale. 2005. Vol. 22, No. 1 P. 25–36.

9. *Dokoumetzidis, A., Macheras, P.* A century of dissolution research: From Noyes and Whitney to the biopharmaceutics classification system // Int. J. Pharm. 2006. Vol. 321, No. 1–2. P. 1–11.

10. *Noyes, A., Whitney, W. R.* The rate of solution of solid substances in their own solutions // J. Am. Chem. Soc. 1897. Vol. 19, No. 12. P. 930–934.

11. *Nernst, W.* Theorie der Reaktionsgeschwindigkeit in heterogenen Systemen // Z. Phys. Chem. 1904. Vol. 47. P. 52–55.

12. *Skrdla, P. J.* A simple model for complex dissolution kinetics: A case study of norfloxacin // J. Pharm. Biomed. Anal. 2007. Vol. 45, No. 2. P. 251–256.

13. *Peppas, N. A.* Analysis of Fickian and non-Fickian drugrelease from polymers // Pharm. Acta Helv. 1985. Vol. 60, No. 4. P. 110–111.

14. *Galwey, A. K., Brown, M. E.* Thermal Decomposition of Ionic Solids: Chemical Properties and Reactivities of Ionic Crystalline Phases, 1st ed. – Elsevier, Amsterdam, 1999. P. 75.

15. *Khawam, A., Flanagan, D. R.* Role of isoconversional methods in varying activation energies of solid-state kinetics. I. Isothermal kinetic studies // Thermochim. Acta. 2005. Vol. 429, No. 1. P. 93–102.

16. *Khawam, A., Flanagan, D. R.* Role of isoconversional methods in varying activation energies of solid-state kinetics. II. Nonisothermal kinetic studies // Thermochim. Acta. 2005. Vol. 436, No. 1–2. P. 101–112.

17. *Skrdla, P. J., Robertson, R. T.* Dispersive kinetic model for isothermal solid state conversions and their application to the thermal decomposition of oxacillin // Thermochim. Acta. 2007. Vol. 453, No. 1. P. 15–20.

18. *Aboulkas, A., El Harfi, K., El Bouadili, A., Benchanaa, M., Mokhlisse, A., Outzourit, A.* Kinetics of co-pyrolysis of Tarfaya (Morocco) oil shale with high-density polyethylene // Oil Shale. 2007. Vol. 24, No. 1. P. 14–33.

19. *Aboulkas, A., El harfi, K., El bouadili, A.* Kinetics and mechanism of Tarfaya (Morocco) and LDPE mixture pyrolysis // J. Mat. Proc. Technol. 2008. Vol. 206, No. 1–3. P. 16–24.

20. *Yang Xulai, Zhang Jian, Zhu Xifeng*. Thermal degradation kinetics of calcium-enriched bio-oil // AIChE J. 2008. Vol. 54, No. 7. P. 1945–1950.
21. *Farjas, J., Roura, P.* Simple approximate analytical solution for nonisothermal single-step transformations: kinetic analysis // AIChE J. 2008. Vol. 54, No. 8. P. 2145–2154.
22. *Ortega, A.* A simple and precise linear method for isoconversional data // Thermochim. Acta. 2008. Vol. 474, No. 1–2. P. 81–86.
23. *Öpik, I., Golubev, N., Kaidalov, A., Kann, J., Elenurm, A.* Current status of oil shale processing in solid heat carrier UTT (Galoter) retorts in Estonia // Oil Shale. 2001. Vol. 18, No. 2. P. 99–108.

Article VI

Johannes, I., Tiikma, L., Luik, H., Tamvelius, H., **Krasulina, J.** Catalytic thermal liquefaction of oil shale in tetralin. – *International Scholary Research Netrwoek (ISRN), Chemical Engineering*, (ID 617363), 2012, pp. 1-11.

Research Article

Catalytic Thermal Liquefaction of Oil Shale in Tetralin

I. Johannes, L. Tiikma, H. Luik, H. Tamvelius, and J. Krasulina

Laboratory of Oil Shale and Renewables Research, Department of Polymeric Materials, Tallinn University of Technology, 5 Ehitajate Road, 19086 Tallinn, Estonia

Correspondence should be addressed to I. Johannes, ille.johannes@ttu.ee

A short review on the publications concerning thermal liquefaction of solid fuels in the environment of hydrogen donor solvents and catalysts is compiled. New experimental results on the catalytic thermal dissolution of oil shale in tetralin as the hydrogen donor solvent in a batch autoclave are presented. The impacts of pyrolysis temperature, duration, and catalyst type on the yields of gas, maltenes, asphaltenes, preasphaltenes, and coke in the presence of tetralin are described.

1. Introduction

Since 1980, discovery of new locations of "conventional" oil sources has fallen below production, and by 2050 discovery of new deposits is supposed to fall to zero [1]. As reserves of conventional crude oil continue to decline, unconventional feedstocks have to be investigated and upgraded to meet the increasing demand for transportation fuels.

In our previous studies [2–5], procedures were developed to increase the extraction yield of liquid products from Estonian oil shale kukersite about 1.5 times. For this aim, the theoretical basis for supercritical dissolution and low-temperature pyrolysis (350–420°C) of the oil shale up to the intermediate product of thermal destruction, thermobitumen (TB), followed by its solvent extraction were worked out. The high molecular and viscous TB obtained needs upgrading to liquid fuels by hydroprocessing. Hydrogenation of the unstable TB [6] has not been systematically studied.

In general, the more asphaltenes present in a fuel, the poorer its burning quality. The ability of hydrogen-donor solvents to depress coke formation releasing hydrogen and thereby converting asphaltenes and heavy hydrocarbons to more valuable lower boiling products has been wellknown. At that, paraffines and single-ring naphthenic compounds are ineffective hydrogen transfer agents, a condensed ring naphthenic compound such as decalin is somewhat more effective, whereas a mixed naphthenic-aromatic condensed ring compound such as 1,2,3,4-tetrahydronaphthalene (tetralin) is much more effective.

In this work, effectiveness of tetralin and several catalysts on the formation of gas, liquid fractions soluble in *n*-hexane, benzene and tetrahydrofurane, and solid residue in thermal decomposition of kukersite, rather on the upgrading of the unstable TB *in statu nascendi*, has been studied.

1.1. Thermal Decomposition of Tetralin Alone.

Hooper et al. [7] have shown that tetralin (T_{bp} = 207.6°C) alone is quite stable. In the range of low-temperatures pyrolysis, 300–450°C, tetralin decomposes only insignificantly into naphthalene by dehydrogenation of the saturated ring, and into 1-methyl-indan by rearrangement of the ring. For example, after two hours reaction at 400 and 450°C, the yield of naphthalene was only 0.5% and 0.8% and that of 1-methyl-indan 0.7 and 5%. In the conversion of tetralin, there was a sharp increase, 10% in hour, after 2 hours duration at 450°C.

Benjamin et al. [8] studied the pyrolysis products of 1-^{13}C-tetralin by [13]C n.m.r. spectroscopy. He found that heating of tetralin during 18 hours at 400°C caused about 1% decomposition. But at 500°C after 1 hour, only about 25% of tetralin remained. Naphthalene was the major product besides small amounts of 1-methyl-indan, ethyl benzene, toluene, and several other minor compounds. Inspite of the fact that hydrogenation-dehydrogenation reactions of hydrocarbons without changes in carbon skeleton can reach state of equilibrium, it was found that no equilibrium between tetralin and naphthalene in an atmosphere of hydrogen (6.20

and 12.75 MPa) was established without catalysts or in the presence of 30% vitrinite. When tetralin was heated under hydrogen pressure, benzene and its alkyl substituents were formed.

1.2. Reaction of Solid Fuels with Tetralin in Inert Atmosphere. Tetralin, being heated in the mix with a solid fuel, mainly with coals, acts as an active hydrogen donor.

Franz [9] found that when $1,1$-d_2-tetralin was added to subbituminous Kaiparowitz coal, the total transformation of the coal into tetrahydrofurane extract and gases from the dry coal reached 80% after heating during 35 min at $427°C$. As indicated by ^2H n.m.r. results, in the first 10 min introduction of deuterium was favored at aliphatic sites, and afterwards in aromatic structures. At that, varieties of solid fuels differed strongly in reactivity with tetralin.

Pajak and Socha [10] showed on the basis of naphthalene formation that the coals with high content of functional groups being readily reduced (quinones, ketones, certain aromatic compounds) were the most reactive with tetralin, and the rate of the reactions was accelerated by pressure of inert gases (5–50 MPa N_2). The bimolecular mechanism of the reaction of hydrogen with coal was suggested for the low-rank coals (content of O_2 about 20%), whereas the high-rank coals (content of O_2 about 5%) were less reactive, and their hydrogenation was rather unimolecular and not affected by pressure.

Robinson and Cummins [11] studied decomposition of 350 g carbonaceous Colorado oil shale containing 35% of OM in 810 mL tetralin in the range of temperatures 25–350°C and durations 24–144 h. The total yield of extract using subsequently tetralin and benzene increased sharply in the range of temperatures 300–350°C reaching 85% after 48 h and 95% from kerogen after 144 h. The gas yield was about 6% consisting mainly of moles of hydrogen, carbon dioxide, and methane. The extract obtained at 350°C was fractionated between 45–50% of pentane insolubles and pentane soluble material. The latter was fractionated in an alumina column with different solvents as follows: 25–30% of oils, 20–25 % of resins, and 5% of wax. The composition of oil (eluted with pentane) and wax (precipitated in 2-butanone at $-5°C$) was nearly the same over the temperature range. But oxygen content of the resins (eluted with mix of benzene, ethanol, and acetone) and pentane insoluble fractions decreased with increase in temperature. The average molecular weights of the oil (350–375), wax (355–480), resin (575–650), and pentane insoluble fractions (1200–1300) did not change appreciably with increase in temperature.

1.3. Influence of Catalysts on the Hydrogenation of Coals in the Environment of Hydrogen Donor Solvents and Gaseous Hydrogen. The impact of various catalysts (iron oxide, metallic tin and lead, tin oxide, and supported nickel-molybdenum as reference) on the transfer of hydrogen from the gaseous phase to coal with and without donor solvent tetralin was investigated by Bacaud [12]. It was found that tetralin donated hydrogen in the absence of catalysts but addition of the catalysts increased the consumption of gaseous hydrogen.

Hirano et al. [13] investigated liquefaction of an Australian subbituminous coal under the pressure of 5–7.5 MPa hydrogen at 420°C in batch autoclaves using as solvents 150% of 1-methyl-naphthalene or the hydrogenated mixture of anthracite oil and creosote oil, and as catalysts inexpensive pyrite and synthesized α-FeOOH in the amount 0.02 mmol/g of Fe. The slurry product was distilled under vacuum (ASTM D1160) into moisture, naphtha fraction (T_{bp} < 220°C), solvent fraction (T_{bp} 220–538°C), and residue. The oil yield was determined as the sum of the yields of naphtha and solvent fractions, subtracting the solvent amount applied supposed to be invariable during the liquefaction. Both pulverized catalysts increased the coal total conversion (%, d.a.f.) from 49.5 to 80–85% and oil yield from 29% to 44–45%.

Kafesjian [14] investigated in his doctoral work the thermal dissolution of oil shale from US Green River formation Hell's Hole Canyon in cyclohexane and tetralin. The experiments were conducted in a 1-litre autoclave reactor during 24 hours in the range of temperature 274–410°C using 70 gram of the shale and 500 mL of the solvents. Cyclohexane, being in the supercritical state under the extraction temperatures (T_c = 280°C, T_{bp} = 84.16°C), resulted in somewhat greater yields than tetralin extraction (T_c = 449°C, T_{bp} = 206–208°C) in runs below 365°C but approximately the same yields as tetralin at higher temperatures. As far the kerogen of Hell's Hole Canyon oil shale was relatively low aromaticy (f_a = 0.19), both solvents were found to be capable of removing over 90% of the original organic material at temperatures between 360–375°C, whereas in extraction of highly aromatic Antrim oil shale (f_a = 0.5) the oil yield was 71.2% in tetraline and 50.5% in cyclohexane at 364°C. The simulated distillation analysis showed that the high boiling fraction, 375–425°C, was about twice larger for tetralin extracts (35–40%) than that for cyclohexane extracts (19–20%). The difference was attributed to the supercritical phase of cyclohexane penetrating the kerogen longer fragments whereas being cooled to liquid-phase tetralin recovered only kerogen, which had undergone sufficient thermolysis to become soluble. Cyclohexane was easily removed from the extract by distillation at 0.7-0.8 whereas complete removal of tetralin failed. So, an approximate value of the weight percent of the remaining solvent was determined by chromatography and its contribution was eliminated from the results of analysis. The mole ratio H/C being 1.56–1.67 in the organics of the initial samples increased in cyclohexane extracts to 1.65–1.71 and decreased in tetralin extracts to 1.46-1.54. The peculiar hydrogen-donor ability of the reagents was not discussed in this work.

In Colorado School of Mines [15] direct hydrogenation of Australian oil shale (77.83% of ash) with gaseous hydrogen was studied in the environment of tetralin, and hydrogen nondonor solvents as light gas oil (LGO) and heavy gas oil (HGO) produced by fractionation of the pyrolysis oil. The solvent-to-shale ratio was 10 : 1 and initial pressure of hydrogen 2.1–5.5 MPa. Liquids were separated by acetone washing of the product slurry, followed by Soxhlet extraction of the residue with a solution of 50% methanol and 50% benzene. The oil yield obtained under the optimum

conditions of the hydroprocessing (425°C, 5.5 MPa H$_2$ pressure, and 60 min residence time) surpass that formed in Fischer assay (92.7 L/t) as much as 1.58 times in tetralin, 1.44 times in LGO, and 1.39 times in HGO. The increase in oil yield was explained by two primarily factors: (i) the lower temperatures employed inhibited secondary condensation/coking reactions and (ii) the presence of donatable hydrogen quenched free radicals. Noteworthy is that organic carbon conversion was found to be unchanged in the run in tetralin when hydrogen was replaced by helium. So, it was concluded that no molecular hydrogen is needed, as long as hydrogen donors were present in the liquid phase. Simulated distillation of the product oil obtained in tetralin showed 62% to boil below 343°C and 44% of the oil to be in the diesel oil range (218–316°C). Regrettably, compositions of the oils obtained in helium and hydrogen were not compared, and the procedure of how the high boiling solvents (tetralin—207, LGO—215–321, and HGO—321–391°C) were separated from the oils was not presented in this paper.

1.4. Hydrogenation of Heavy Residues and Asphaltenes in Hydrogen-Donor Solvents. The most research works in the field of hydro treatment by means of hydrogen donors deal with heavy residues and asphaltenes.

It was found [16] that the ratio 2 : 1 of tetralin to Arabian heavy vacuum residuum provided a sufficient excess of tetralin at noncatalytical hydrocracking at temperatures 400, 420, and 435°C and pressure of nitrogen 0.5 MPa. At that, overmuch tetralin was not decomposed under the conditions studied, whereas the spent donor was dehydrogenated. As results, coke formation was inhibited, 50% of asphaltenes were converted to lighter fractions and degree of desulphurization was increased.

Behar and Pelet [17] studied thermal cracking of asphaltenes precipitated from Boscan crude oil. In this work (0-1): 1 of benzene or tetralin and/or water was added to asphaltenes. The temperature range tested was 350–430°C and heating time 0–9 h. The cracking was conducted in sealed gold tubes under initial pressure of nitrogen 0.5 MPa to keep the solvents in the liquid state. The fractions C$_6$–C$_{13}$ and C$_{14}$+ were extracted subsequently from the cut tube with pentane and chloroform. The maximum conversion degree overcame 90% under the conditions 390°C and 3 h. At that, about 50% from the asphaltenes was transformed into coke without solvents and also in the environment of benzene, water, and their mix. But there was no coke formed in the environment of 10% or more tetralin, whereas the conversion degree of the asphaltenes was only 41–50%. Appearance of naphthalene showed that tetralin had acted as a hydrogen donor. Inhibition of coke formation revealed that hydrogen-transfer reactions were largely dominant over aromatization and condensation reactions. So, when tetralin was present, radicals, once formed, preferentially underwent H-transfer reaction. The resulting hydrocarbons were inactive and had the same carbon number as the initial radicals from primary cracking. In the same way, aromatic moieties did not undergo condensation reactions to form coke but remained small enough to be soluble in chloroform.

The presence of tetralin hindered completely coke formation at 390°C, but at higher temperatures there was a competition between polycondensation and hydrogen-transfer reactions.

The objective of the study of Rahmani et al. [18] was to examine the kinetics of coke formation from Athabasca asphaltenes separated from Athabasca vacuum residue in a closed reactor under a 4 MPa nitrogen atmosphere at 430°C in the environments of 1-methyl naphthalene, maltenes, and tetralin having hydrogen donor abilities 10, 3.44, and 0.12 mg/g of the corresponding solvents. It was shown that the hydrogen donating ability of the solvents and the hydrogen accepting ability of asphaltenes both played an important role in determining the ultimate yield of the target product in the work [18], coke. Tetralin as a donor solvent significantly enhanced conversion of asphaltenes and helped to suppress coke formation. Replacement of one third or more from 1-methyl naphthalene with tetralin decreased the coke formation rate factor from 0.17 to 0.028 min^{-1}.

Upgrading of an extra heavy crude oil (22% asphaltenes, viscosity at 80°C 1810 cP) from Orinoco Belt (Venezuela) was carried out [19] in a 300 mL batch Parr reactor at 315°C during 24 h adding as a radical initiator the mixture of 1 : 1.7 tertamylmethyl ether and methyl-tertbutyl ether, and to the mixture as a hydrogen donor tetralin and water in the ratios 1 : 1 : 10. The presence of the radical initiator had little effect, but the presence of tetralin decreased viscosity at 80°C to 110 cP. After completing the experiment, water and tetralin were separated from the oil and sand by vacuum distillation at 280°C. The remained oil was removed from the sand by solvent extraction with dichloromethane. The content of asphaltenes in the initial extra-heavy crude being 22% decreased up to 18% after upgrading in the environment of tetralin under the low severity conditions tested (315°C, 24 h).

A patent claim was published [20] for pyrolytic upgrading of the Venezuelan extra heavy crude oil (>500°C), to lighter distillates (<500°C) at least at temperature 380°C and pressure 5.5 MPa in the presence of 1–10% (2%) of octyl nitrate, MTBE or TAME as free radical generators having activity towards cracking reactions (resulting both, lighter distillates and coke), and as hydrogen donors 1–35% (33%) of tetralin or other like materials for inhibiting cycling reactions to produce coke.

Already in 1962 Langer et al. [21] have demonstrated that in visbreaking of crude residuum formation of asphaltenes could be decreased from 55% to 12% adding partially hydrogenated (71.2 H$_2$ n.v/v) tar fraction 371–482°C obtained from catalytic cracking of West Texas gas oil. It was shown that balance between the rates of hydrogen transfer and cracking was very dependent upon temperature, as far residuum cracking was initiated at about 371°C, whereas hydrogen transfer did not become appreciable below 427°C. Consequently, in any thermal cracking operation, regardless of hydrogen donor content, the concentration of polymeric products (asphaltenes) underwent an initial increase until the activation temperature for hydrogen transfer was reached, and polymerization and hydrogen transfer became competitive reactions. Therefore, the temperature range between 371 and 427°C should be spanned as rapidly as

possible. Furthermore, according to [22], with rare exception, no reaction between H_2 and organic compounds occur below 480°C in the absence of metal catalysts.

Gould and Wiehe [23] showed that at thermal conversion of petroleum resid fraction in the presence of a super reactive hydrogen donor, 1,2,3,4-tetrahydroquinoline, increased yield of lighter distillable liquids and formation of polyaromatic cores also. As far the asphaltene core was found not being converted in thermal conversion, the highest hydrogen donation established was rather an unwanted feature. Besides, reactive hydrogen donors greatly reduced the thermal reaction rate by reducing the free radial concentration.

1.5. Catalytic Hydroconversion of Heavy Fractions Using Hydrogen Donor Solvents. Several hydrocracking and -purification catalysts have been investigated and used for intensification of hydrogen transfer activity. Generally heterogeneous catalysts, such as cobalt, molybdenum, or nickel sulphides supported on alumina or silica-alumina and formed into pellets or beads have been used in the upgrading of heavy fractions. One exception to this is Raney-type catalysts, composed of fine grains of an alloy of nickel and aluminum or from various rare earths intermetallic compounds, which are effectively employed in unsupported states. Unfortunately, as a rule, the surface of the catalysts is deactivated by depositing coke. Thereby, the catalysts display short service life and bad operation stability.

Hydrodesulphurization of the heavy fraction (>320°C) of Pakistan petroleum crude containing 1.12% sulfur was investigated in a micro-autoclave in the presence of 0.5–10% various hydrogen donor solvents, and 1% catalysts in the 0.98 MPa inert atmosphere of N_2 at temperature 320°C during 3 h [24]. It was found that desulphurization percentage of the fraction decreased in the row of the hydrogen donors as follows: methanol—53, propanol—47, polyethylene glycol and tetralin—30, formic acid—15, and no donors—8%. As a surprise, it was shown that with decrease of methanol concentration from 1.5 to 0.5%, the desulphurization percentage increased from 22 to 52%. Regrettably, the region below 0.5% of the coreactant was not examined. The desulphurization efficiency of the catalysts tested decreased in the row: Mo-montmorillonite, Zn-ZSM5, Ni, Co-montmorillonite (fresh prepared), montmorillonite, and kaolin.

In [25], the direct liquefaction of a green waste composed of straw, wood, and grass was carried out using Raney Ni as the catalyst and tetralin as the solvent. The experiments were carried out in a 300 mL stainless steel autoclave filled with 70 g tetralin, 5 g green waste (which corresponds to 4.2 g of organic matter), and 1 g Raney Ni. The temperature range was 330–420°C and initial hydrogen pressure 1.6 MPa. The working pressure was between 4 and 7 MPa, depending on the reaction temperature. It was found that the presence of the catalyst had practically no effect on the oil yield being about 30% but amended the oil quality decreasing the oxygen content and increasing the hydrogen content in the oil due to promoting the dehydrogenation of the solvent.

Metecan et al. [26] studied hydroliquefaction of Göynük oil shale in the presence of 2–12% pyrite catalyst and toluene as solvent under hydrogen initial pressure 2–8 MPa and temperature range 300–450°C. It was found that the pyrite catalyst increased considerably the conversion (from 35 to 58%) and extract yield (from 17 to 33%) at 350°C, however, since 400°C the effect was only some percentages.

In order to eliminate the fast poisoning of catalysts in heavy oils and residues, slurry-phase hydrocracking using water dispersed unsupported catalysts without any hydrogen donor solvent has been developed. Tian et al. [27] studied upgrading of the waxy residue from Petronas Petroleum Refinery in Malaysia in a 300 mL Parr batch reactor heated to 340°C and 7 MPa hydrogen pressure. It was found that a water dispersed Ni-Mo catalyst (prepared from a solution of Nickel chloride and ammonium molybdate in molar ratio 0.5) was effective and comparable with the presulfided supported commercial Co-Mo/alumina catalyst (each loading 0.3 %).

The latest hydrocracking technologies of heavy oil using unsupported heterogeneous solid powders or homogeneous water-soluble and oil-soluble dispersed catalysts were reviewed by Rana et al. [28], Zhang et al. [29], and Maity et al. [30].

It was noted in [28] that high conversion of complicated heavy oils and residua to high value liquids could be achieved when fine particles of hydroprocessing catalysts were slurried/dispersed in feeds. As far the fine catalysts could not be reused, only low-cost, throw-away materials possessing catalyst activity can be practical.

In [29] it was suggested that asphaltenes deactivating catalysts the most should be removed before hydroprocessing. Only after that, the feed oil, hydrogen, and a single used dispersed oil-soluble (molybdenum, cobalt, iron and nickel naphtenates or multi-carbonyl compounds) or water-soluble (phospho-molybdic acid, ammonium molybdate) catalyst should be mixed and went together through the reactor. Despite the oil-soluble catalysts are the most active, high cost greatly restricts their application. Thus, water soluble cheap inorganic compounds have become popular. Sodium molybdate, nickel nitrate, and iron nitrate were used as precursors to prepare water-soluble multimetal composite catalysts for residue hydrocracking. Their coke inhibiting behavior arranged in sequence of Mo-Ni-Fe > Mo-Fe > Ni-Fe > Mo > Fe. In the process, firstly water soluble catalysts are dissolved and then mixed with parts of the residue feed to form an emulsion. Generally, activation of the catalyst via dehydration and sulfurization is the subsequent steps, and finally the catalyst reacts with the residue feed in the reactor.

Maity et al. [30] have published a review on the use of catalytic aquathermolysis of heavy crude oils. The viscosity reduction achieved by these catalysts followed the order: mineral < water-soluble < oil-soluble < dispersed. When tetralin was used with anf Fe catalyst, the viscosity decreased more effectively, and the coke formation was reduced from 3.6 to 0.3 wt %.

Reviewing upgrading processes of a number of different feedstocks, the conclusion was drawn in [31] that there was not a general rule that can give a solution to all refineries, and the final choice should be made by comprehensive

consideration of the feed property, product demand, and economic benefit.

2. Experimental

2.1. Materials. The initial material being hydrogenated was Estonian carbonaceous kukersite oil shale consisting 40.15% of organic matter (OM^d), 48% ash (A^d), and 0.90% moisture (W). The content of mineral matter was calculated as $100 - OM^d$. According to Lille et al. [32], OM of kukersite can be characterized with empirical formula $C_{421}H_{638}O_{44}S_4NCl$. A set of structural elements comprises mainly alkylated phenolic structures particularly alkyl-1,3-benzenediols and condensed alicyclic rings. Up to 80% of methylene groups in kerogen are located in aliphatic chains and the complicated mixture of phenols in the retort oil supposed to result mainly from the thermal conversion of alkyl-1,3-benzenediol units originally present in OM.

During the process of kerogen low-temperature pyrolysis, two types of reactions might occur simultaneously before oil formation: (a) rapid release of volatiles coming primarily from the destruction of carboxyl, carbonyl, hydroxyl, phenolic hydroxyl, and other oxygen functionalities at the periphery of the aromatic and hydroaromatic components of the matrix (b) thermal cracking of the solid kerogen into high molecular semi-product, thermobitumen (TB) where the relatively less rapid release of volatile matters coming primarily from hydrogen produced during the conversion of hydroaromatic portions to aromatic building blocks and coke. The first reaction could be dominant at lower pyrolysis temperature. For stabilization of the free radicals forming in both processes additional hydrogen is required.

The commercial catalysts applied for activation of the hydrogen donation from tetralin to the oil shale decomposition products were in the form of granules. In addition, some local powdered minerals were applied. The nomenclature of the catalysts tested is given in Table 1.

The commercial catalysts were obtained from producers, and were designed as Co, Mo, and Ni supported ones with a maximum number of so-called Super Type II Active Sites (STARS) whose exact composition is confidential technical information. The original granules of the catalysts (3 mm in diameter and 8 mm in length) and presulfided for activation ones using shale oil as a spiking agent were tested.

Marine-type Estonian Dictyonema argillite (also known as dictyonema oil shale, Dictyonema shale, or alum shale) occurs in most of northern Estonia on an area of about 11,000 square kilometers (4,000 sq mi). Although reserves of the dictyonema argillite surpass those of kukersite, its quality is poor as a source for the energy production. The shale consists of 65–70% mostly silicate minerals, 10–15%, organic and 10–20% X-ray amorphous matter. The Fischer Assay oil yield is 3–5% per oil shale. The content of minerals depends on grain size fraction and gradual changes occur laterally as well as vertically. The average to whole rock composition is 37% phyllosilicates (illite, illitic illite-smectite, chlorite), 34% K-feldspar, and 29% quartz [33]. Dictyonema argillite taken from Maardu deposit was applied in this work.

Pyrite crystals, FeS_2, were obtained from the Institute of Geology at Tallinn University of Technology and were powdered in a mortar before addition.

The solvents applied in extractions, tetralin, benzene, hexane, and tetrahydrofurane, were commercial and had purity $\geq 99\%$ (GC).

2.2. Procedures. Reactions were carried out in glass test-tubes inserted into 100 mL stainless steel batch autoclaves. Mass of the initial oil shale loaded was 10 gram. The weight ratio of tetralin to oil shale OM was $1:1$, and the ratio of catalysts to OM content was $0.1:1$. The autoclaves were placed into electrical oven heated to the nominal temperature (360–420°C). After the duration prescribed (1–3 h), the autoclaves were left in room temperature and opened on the next day.

All the yields were calculated on the basis of OM.

Gas yield (G) was found from the weight loss of the closed and opened autoclaves. The content of the test-tubes was relayed into weight paper cartridge and extracted with benzene in a Soxhlet extractor. The properly washed cartridge with the insoluble in benzene residue was dried in a drying oven at 105°C and weight (G_{PA}), thereafter extracted using tetrahydrofurane, and dried and weighted again (G_{SR}).

The yield of organic solid residue (SR) was found basing on the initial mass of OM (G_{OM}), subtracting from G_{SR} the corresponding weight of the empty cartridge (G_c) processed likewise and the weight of the mineral matter (G_{MM}, estimated as the ash at 550°C) of the sample, weight of the catalyst (G_{CAT}) as follows:

$$SR = \frac{100(G_{SR} - G_C - G_{MM} - G_{CAT})}{G_{OM}}. \quad (1)$$

The yield of preasphaltenes (PA), the coke precursors, was estimated directly as the distillation residue after evaporation of tetrahydrofurane from the extract and also as the weight loss in tetrahydrofurane extraction

$$PA = \frac{100(G_{PA} - G_{SR})}{G_{OM}} \quad (2)$$

agreeing with the direct residue.

Estimation of the amount of benzene extract was somewhat problematic because it was impossible to separate the superfluous tetralin and its decomposition products from shale oil. So, the yield of benzene extract consisting of asphaltenes and maltenes ($A + M$) was estimated as the difference between the weight of initial sample (G_o) and the weights of gas (G_G), and the weight of the insoluble residue after benzene extraction

$$A + M = \frac{100[G_o - G_G - (G_{PA} - G_C)]}{G_{OM}} \quad (3)$$

presupposing that there are no changes in mineral matter in the process.

The yield of asphaltenes was estimated precipitating asphaltenes in the ratio of hexane to an aliquot of the benzene extract v/w $10:1$. At that, on the next day, characteristic to the solutions, asphaltenes formed an insoluble lacquer flake

TABLE 1: Catalysts applied.

Catalyst	Producer	Type	Positive features
DN-3100 Th	Shell, US	Universal	Effectiveness
KF-848	Akzo Nobel, Netherlands	Hydropurification	Effectiveness and selectivity
KF-1015	Akzo Nobel, Netherlands	Hydrocracking	
Dictyonema argillite	Another Estonian local shale	Hydrocracking	Cheapness, reach
Pyrite	Estonian local deposit	Hydrocracking	Cheapness, reach

on the glass surface of the beaker being easily washed and decanted. Finally, the washed residue in beakers was dried at 105°C and weighted.

The yield of maltenes was found subtracting from the yield of benzene extract estimated according to (3) the yield of asphaltenes. So, the value of M is somewhat overestimated due to inclusion of water. In some experiments, the water content in the benzene extract was estimated according to the classic distillation method of Dean and Stark [ASTM D95-05 (2010)].

In some hexane extracts the ratio of the peaks area of tetralin and naphthalene (x) was estimated using the GC-MS apparatus Shimadzu QP2010 Plus. The yield of naphthalene (N) resulted from hydrogen donation of tetralin to oil shale was calculated based on the equal quantity of OM and tetralin in the experiments. Neglecting the minor quantity of by-products in the hydrogen-donating reaction [8, 14, 17], and taking the initial content of tetralin as 100%, the sum of tetralin remained (T) and naphthalene formed should be

$$T + N = 100,$$
$$\frac{T}{N} = x, \tag{4}$$
$$N = \frac{100}{(x+1)}. \tag{5}$$

3. Results and Discussion

3.1. Effect of Heating Duration.
The effect of time on the yield of the products in "dry" pyrolysis, in the environment of tetralin without any catalyst, and adding the hydropurification catalyst Akzo Nobel KF-848 is depicted in Figure 1.

The catalyst KF 848 was chosen because it had given the highest yield of the diesel fraction 200–360°C (72.7%) and of the total fraction boiling below 360°C (78.4%) in our preliminary experiments where the shale oil boiling above 360°C, was upgraded under initial pressure of molecular hydrogen 7.0 MPa, nominal temperature 380∘C and duration 1 h without tetralin.

The results obtained in this work prove that the main advantage from the addition of tetralin (Figures 1(a) and 1(b)) occurs in an increase in the maximum yield of total extract (curves 5) from 78 to 86%, and in decrease in the minimum percentage of OM remaining in solid residue (curves 0) from 8.4 to 5.2%. At that, unfortunately, formation of the target product, maltenes is higher in the "dry" experiment than in tetralin. The results agree with Behar and Pelet [17] who found that when tetralin was present

in thermal cracking of asphaltenes, radicals, once formed, preferentially underwent H-transfer reaction and the resulting hydrocarbons were inactive to further cracking and had the same carbon number as the initial radicals from primary cracking. The same was confirmed by Gould and Wiehe [23] who explained that reactive hydrogen donors greatly reduced the thermal cracking rate of petroleum resids by reducing the free radial concentration.

Addition of the catalyst KF 848 (Figure 1(c)) in tetralin environment, surprisingly, moderates the decomposition rate of the initial shale (curve 0) and formation of the total extract (curve 5) in comparison with the results in Figures 1(a) and 1(b). Nevertheless, the catalyst evokes continuous increase in the yield of maltenes with time (curve 1), unlike a steady state in the interval 1-2 h without the catalyst (Figure 1(b)), and a maximum between 1–1.5 h without tetralin and the catalyst (Figure 1(a)).

3.2. Effect of Nominal Temperature in the Environment of Tetralin and KF 848.
The influence of nominal temperature on the thermal treatment of oil shale in tetralin without catalyst is depicted in Figure 2(a), and with the catalyst KF 848 in Figure 2(b). At that, the insufficient duration for formation of maltenes, two hours, was chosen for better revelation of the temperature effect. The results suggest again that under the conditions studied addition of the catalyst KF 848 being the best in hydrogenation of heavy shale oil with molecular hydrogen rather decreases the yield of total extract in comparison with the test without any catalyst. The maximum extract yield under two hours duration is at temperature 380°C without any catalyst, and at 400°C with the catalyst. But at that, addition of the catalyst amplifies the effect of temperature on the increase in the yield of the target product, maltenes, and decreases the yield of organic solid residue at 360°C.

It can be concluded that tetralin as a hydrogen donor improves liquefaction deepness of oil shale. At that, in the environment of tetralin the rate limiting stage is formation of thermobitumen (TB) resulted from splitting of the kerogen macromolecules, not hydrogen donation from the tetralin to the radicals formed. As far the catalyst KF 848 had unexpected low effect, the variety of catalysts was tested.

3.3. Effect of Different Catalysts.
The commercial catalysts applied (Table 1) were oxides of Mo, Co, and Ni supported on alumina or silica-alumina in the forms of granules. The representatives of three types of catalysts, hydropurification, cracking, and universal, were tested in their original forms
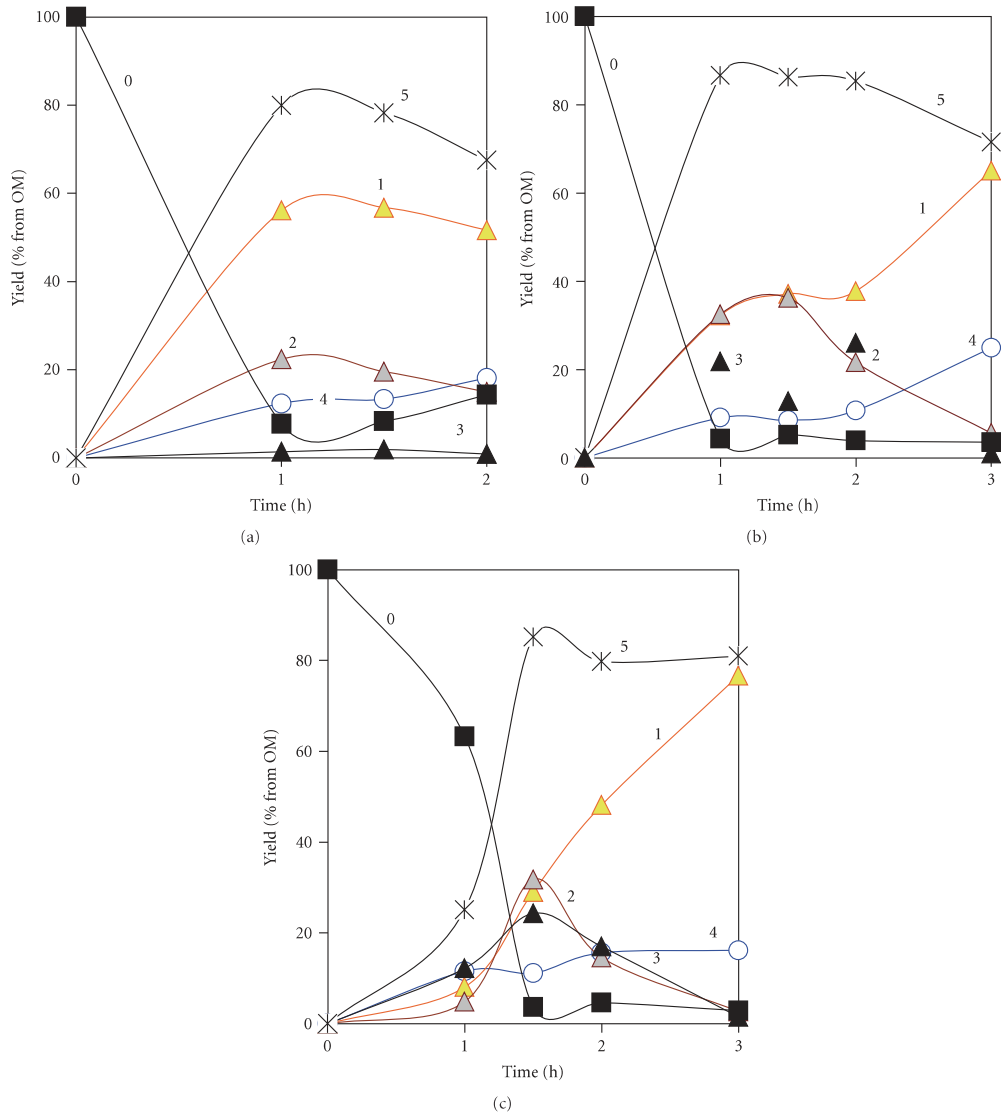
FIGURE 1: Effect of heating duration on the yield of decomposition products in the environment of (a) no tetralin and catalyst, (b) tetralin and no catalyst, (c) tetralin and KF 848. 0: organic solid residue, 1: maltenes, 2: asphaltenes, 3: pre-asphaltenes, 4: gas, 5: total extract. Nominal temperature $400°C$.

and after activation using shale oil as a presulfiding spiking agent. The natural catalysts, dictyonema argillite and pyrite, were grinded to powder size. The experimental series with catalysts varieties were conducted at temperature $400°C$. The two durations, 1.5 and 2 h, were chosen to found out whether the process is completed or not.

Comparison of the experimental results depicted in Figure 3 reveals the following.

(i) *Coke (organic solid residue)* formationis decreased in the presence of tetralin (Figures 3(b)–3(j)) in comparison with the pyrolysis without addition of tetralin and catalysts (Figure 3(a)). At that, an increase in the coke yield with time in the "dry" pyrolysis (8.4–14.4%) and a little effect of time in tetralin (below 5%) prove suppression of the secondary coke formation by hydrogen-donating behavior of tetralin.
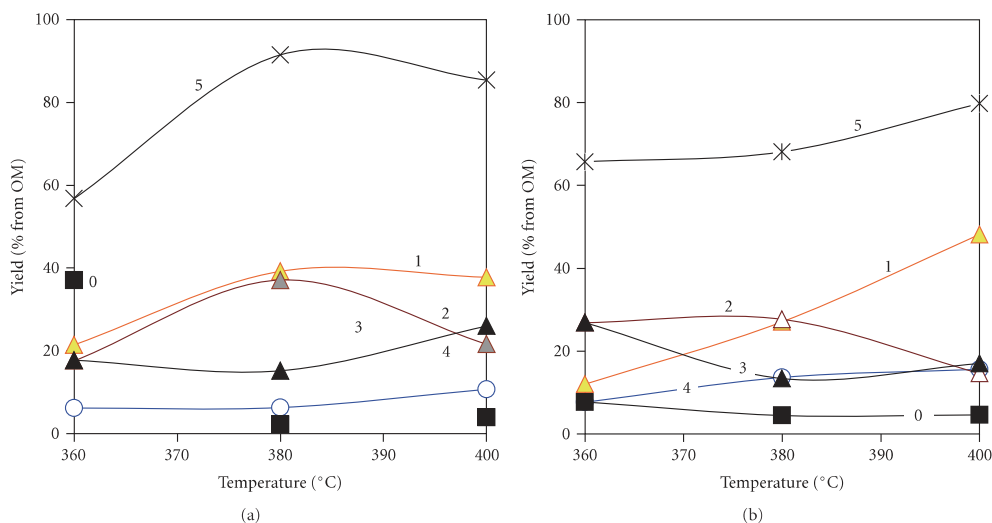
(a)

(b)

Figure 2: Effect of nominal temperature on the yield of decomposition products (see in Figure 1) in the environment of (a) tetralin without catalysts and (b) tetralin and the catalyst KF 848. Duration 2 h.

(a)

(b)

(c)
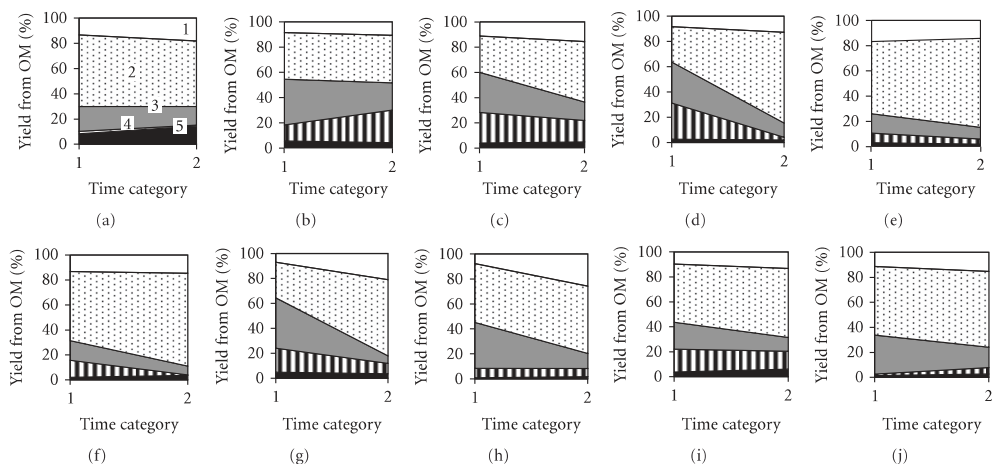
(d)

(e)

(f)

(g)

(h)

(i)

(j)

Figure 3: Effect of duration and fixings: (a) none, (b) tetralin 1 g/g OM, (c) tetralin and KF 848 pellets, (d) tetralin and activated KF 848 pellets, (e) tetralin and DN 3100 TH pellets, (f) tetralin and activated DN 3100 Th pellets, (g) tetralin and KF 1015 pellets, (h) tetralin and activated KF 1015 pellets, (i) tetralin and Dictyonema, (j) tetralin and pyrite on the yield of pyrolysis products: 1: gas, 2: maltenes (+water), 3: asphaltenes, 4: preasphaltenes, 5: solid residue. Time category: 1–1.5 h, 2–2 h. Temperature 400°C.

The lowest yields of OM in the solid residue, 0.93%, are obtained using the activated cracking catalyst KF 1015 [experiment (h), 1.5 h], 1.46% using pyrite [experiment (j), 1.5 h], and 1.50%, using the not activated universal catalyst DN 3100 TH [experiment (e), 2 h].

(ii) *Gas* formation is quite similar with and without tetralin and catalysts being 8–13% after 1.5 h, and

increasing to 14–18% after 2 h. An exception is the cracking catalyst KF 1015 [experiments (g, h)] resulting a significant increase in gas yield in time not completed during tested two hours.

(iii) *Total extract* of liquid products decreases with time increase from 1.5 to 2 h in the "dry" experiment (a) from 78 to 67%, and using the original and activated cracking catalyst KF 1015 (g, h) from 88 to

75 and from 91 (the maximum in the series) to 72% because of the secondary decomposition reactions. In the other experiments, the yield of total extract overcomes 80%. At that, noteworthy is the high extract yield, 87%, obtained using as catalysts the available local Dictyonema argillite (i) and pyrite (j).

(iv) *Preasphaltenes* yield is the lowest, 1-2%, in "dry" experiment (a) and 1–5% with pyrite (j). In tetralin without catalysts (b), the yield of preasphaltenes increases in time from 13 to 26%. In presence of any catalysts tested, inversely, the yield of preasphaltenes decreases in time, the most drastically, from 29 to 2%, in the test with the activated hydropurification catalyst KF 848 (d). The unique increase in the yield of preasphaltenes in time without catalyst in tetralin (b) is supposed to take place because of the secondary complex formation between the radicals formed, thereby catalytic splitting of the complexes is absent.

(v) *Asphaltenes* act quite analogously to preasphaltenes. Their yield in tetralin in every experiment (b–j) overcomes that in "dry" experiment (a) and thereafter decreases with time. The decrease is the sharpest, from 40 to 6%, with natural KF 848 pellets (g). The total yield of the little decomposed high molecular asphaltenes and preasphaltenes is the lowest,13.4% and 7.5%, with original and activated DN 3100 Th after 2 h.

(vi) *Maltenes*, the main target product, have in "dry" conditions (a) higher yield, 57–51%, than in the environment of tetraline without any catalyst, 37-38% (b) like it was shown in Figure 1 above and in the work of Behar and Behar and Pelet [17]. Addition of catalysts increases decomposition rate of high-molecular asphaltenes (c–j) and preasphaltenes (c–i) and hereby the yield of maltenes (c–j). So, the positive influence of the longer duration is evident only with catalysts (c–j). The highest yield of maltenes, 74%, is obtained using the activated universal catalyst DN 3100 TH (f) and 72%, using the activated hydropurification catalyst KF 848 (d) at time 2 h. The durations longer than two hours should be tested in further works.

(vii) *Water* is formed inevitably when the oxygen-rich oil shale is hydrogenated. As said above, because of the environment of tetralin and its decomposition product, naphthalene, the yield of hexane extract was evaluated as the weight loss of the initial sample during benzene extraction minus the yield of asphaltenes precipitated in hexane. So, in this work, maltenes contain also the water fraction, estimated not for all samples. It can be seen in Figure 4 that there was no clear relationship between yields of water and any other decomposition products. Yet, the lower water yield at higher yields of solid residue can take place due to the incomplete decomposition of the shale. The dependence of water formation on different
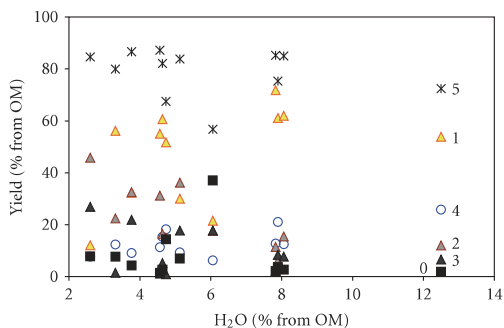

FIGURE 4: Relationship between the yields of water and pyrolysis products (see numbers in Figure 1) in the environment of tetralin.

catalysts, temperature, and duration affecting the oil shale transformation needs further systematic study.

Activation of the catalysts according to the confidential Technical Information instruction of producers increases the total extract yield at 1.5 hours duration to 3-4%. At 2 hours duration addition of the hydropurification catalysts KF 848 increases the yield of maltenes significantly, from 48 (c) to 72% (d), whereas the total extract yield increases only from 80 to 85% (d). Presumably, the changes take place mainly, due to the favored removal of heteroatoms from asphaltenes and preasphaltenes. Under the condition tested, the effect of activation of the universal catalyst DN 3100 Th (e-f) and cracking catalyst KF 1015 (g-h) on the distribution of products was substantially lower than that of KF 848.

The most efficacious conditions for liquefaction of oil shale were obtained without activation under the environment of tetralin and universal original catalyst DN 3100 Th at 400°C and 2 h (f). Under these conditions the yield of total extract was 84.3%, maltenes 70.9%, asphaltenes 9.3%, preasphaltenes 4.1%, gas 14.2%, and organic solid residue 1.5%.

Considering problems concerning cost, poisoning, and activation of the catalyst, replacement of the commercial catalysts with local natural minerals seems attractive. In this point of view, pyrite (j), just at duration 1.5 h, has promised rather good results. The extract total yield is 87%, of maltenes and asphaltenes 55 and 31%, and solid residue 1.5% only. Like in liquefaction of biomaterials [25], the presence of the catalyst had practically no effect on the extract yield in comparison with tetralin alone (b) but improved the oil quality. The quantity and conditions need for utility of pyrite as catalyst further optimization. The extract, probably, has to undergo further multistep upgrading.

3.4. Transformation of Tetralin in Upgrading of Oil Shale. Appearance of naphthalene shows that tetralin has acted as hydrogen donor. The transformation degree of tetralin into naphthalene characterizes the extent of hydrogen donation to TB. The results given in Table 2 evident that in the series tested approximately one third of tetralin have been used

TABLE 2: Yields of naphthalene (N) from tetralin (T) added, %, and maltenes (M), % from oil shale OM.

	No catalyst		KF 848					KF 1015	
	—	—	Original	Original	Original	Original	Activated	Original	Activated
T (°C)	400	400	380	400	400	400	400	400	400
t, h	1.5	2	2	1	1.5	2	1.5	1.5	1.5
M	37.14	37.76	27.08	8.09	29.06	48.16	27.96	28.55	47.01
T^*/N	3.15	2.26	1.8	3.58	2.66	1.31	2.61	2.38	2.46
N	24.10	30.67	35.71	21.83	27.32	43.29	27.70	29.59	28.90

T^*: tetralin current concentration.

for hydrogenation. Generally, the yield of naphthalene found according to (5) increases with an increase in the yield of maltenes. The relationship is not unilateral because all the variables tested: temperature, duration, type of catalysts and activation of the catalysts, and secondary decomposition of maltenes can influence on the relationship between the yields of maltenes and naphthalene. The systematic interplay of the mutual effects needs investigation in further works.

4. Conclusions

Addition of tetralin as a hydrogen-donor in thermal decomposition of oil shale increases the extract yield and suppresses coke formation. In hydrogenation of the unstable thermobitumen *in statu nascendi* about one third of tetralin per OM of oil shale, g/g, is expended and transformed into naphthalene.

Addition of tetralin avoids the secondary decomposition and condensation of hexane soluble fraction, maltenes, but without catalysts also slows down formation of maltenes in comparison with "dry" pyrolysis. Subsequent distribution of the extract between the fractions soluble in hexane, benzene (asphaltenes), and tetrahydrofurane (pre-asphaltenes) depends on temperature, duration, and type of catalysts. Formation of the target product, maltenes, increases with time and temperature.

Activation of the commercial hydrocracking and universal catalysts KF 1015 and DN 3100 Th using as a spiking agent the shale oil middle fraction has a little effect on the yield of pyrolysis products in comparison with addition of the original pellets. Activation of the hydropurification catalyst KF 848 has a little effect during the first 1.5 h and thereafter increases the formation rate of maltenes from asphaltenes and preasphaltenes.

The best catalyst among the tested ones for liquefaction of oil shale under the environment of tetralin is universal catalyst DN 3100 Th without activation at 400°C and 2 h. Under these conditions, the yield of total extract was 84.3%, maltenes 70.9%, asphaltenes 9.3%, preasphaltenes 4.1%, gas 14.2%, and organic solid residue 1.5%.

Quite promising catalytic effect gives addition of 1% of an available local mineral, pyrite. In the environment of tetralin at duration 1.5 h, the extract total yield was 87%, of maltenes 55%, asphaltenes 31%, gas 11%, and solid residue 1.5%. Here, the second-step upgrading of asphaltenes should be followed.

References

[1] B. Lipták, http://www.sustainableplant.com/2012/01/safely-scraping-the-bottom-of-the-barrel-part-1.

[2] I. Johannes and L. Tiikma, "Thermobituminization of baltic oil shale," in *Advances in Energy Research*, M. I. Acosta, Ed., vol. 2, chapter 9, pp. 267–282, Nova Science, New York, NY, USA, 2011.

[3] H. Luik, "Supercritical extraction of the Estonian kukersite oil shale," in *Advances in Energy Research*, M. I. Acosta, Ed., vol. 2, chapter 10, pp. 283–298, Nova Science, New York, NY, USA, 2011.

[4] L. Luik, H. Luik, V. Palu, K. Kruusement, and H. Tamvelius, "Conversion of the Estonian fossil and renewable feedstocks in the medium of supercritical water," *Journal of Analytical and Applied Pyrolysis*, vol. 85, no. 1-2, pp. 492–496, 2009.

[5] I. Johannes, L. Tiikma, A. Zaidentsal, and L. Luik, "Kinetics of kukersite low-temperature pyrolysis in autoclaves," *Journal of Analytical and Applied Pyrolysis*, vol. 85, no. 1-2, pp. 508–513, 2009.

[6] J. Sokolova, L. Tiikma, M. Bityukov, and I. Johannes, "Ageing of kukersite thermobitumen," *Oil Shale*, vol. 28, no. 1, pp. 4–18, 2011.

[7] R. J. Hooper, H. A. J. Battaerd, and D. G. Evans, "Thermal dissociation of tetralin between 300 and 450°C," *Fuel*, vol. 58, no. 2, pp. 132–138, 1979.

[8] B. M. Benjamin, E. W. Hagaman, V. F. Raaen, and C. J. Collins, "Pyrolysis of tetralin," *Fuel*, vol. 58, no. 5, pp. 386–390, 1979.

[9] J. A. Franz, "13C, 2H, 1H n.m.r. and gpc study of structural evolution of a subbituminous coal during treatment with tetralin at 427°C," *Fuel*, vol. 58, no. 6, pp. 405–412, 1979.

[10] J. Pajak and L. Socha, "Effects of pressure on the rate of hydrogen transfer from tetralin to different rank coals," *Fuel Processing Technology*, vol. 77-78, pp. 131–136, 2002.

[11] W. E. Robinson and J. J. Cummins, "Composition of low-temperature thermal extracts from colorado oil shale," *Journal of Chemical and Engineering Data*, vol. 5, no. 1, pp. 74–80, 1960.

[12] R. Bacaud, "Influence of catalysts upon hydrogen transfer pathways during hydroliquefaction of coal," *Applied Catalysis*, vol. 75, no. 1, pp. 105–117, 1991.

[13] K. Hirano, M. Kouzu, T. Okada, M. Kobayashi, N. Ikenaga, and T. Suzuki, "Catalytic activity of iron compounds for coal liquefaction," *Fuel*, vol. 78, no. 15, pp. 1867–1873, 1999.

[14] A. S. Kafesjian, *Studies of thermal solution of Utah oil shale kerogen [Ph.D. dissertation]*, Department of Chemical Engineering, University of Utah, 1983.

[15] R. M. Baldwin, W. L. Frank, G. L. Baughman, and C. S. Minden, "Hydroprocessing of stuart a (Australian) oil shale," *Fuel Processing Technology*, vol. 9, no. 2, pp. 109–116, 1984.

[16] A. M. Abu-Khalaf and D. Al-Harbi, "Hydrogen transfer cracking of Arabian residua in tetralin-I," *Journal of King Saud University*, vol. 14, pp. 235–250, 2002.

[17] F. Behar and R. Pelet, "Hydrogen-transfer reactions in the thermal cracking of asphaltenes," *Energy and Fuels*, vol. 2, no. 3, pp. 259–264, 1988.

[18] S. Rahmani, W. McCaffrey, and M. R. Gray, "Kinetics of solvent interactions with asphaltenes during coke formation," *Energy and Fuels*, vol. 16, no. 1, pp. 148–154, 2002.

[19] C. Ovalles, P. Rengel-Unda, J. Bruzual, and A. Salazar, "Upgrading of extra-heavy crude using hydrogen donor under steam injection conditions. Characterization by pyrolysis GC-MS of the asphaltenes and effects of a radical initiator," *Fuel Chemistry*, vol. 48, pp. 59–60, 2003.

[20] E. A. Cotte and I. C. Machin, "Additives for improving thermal conversion of heavy crude oil," U.S. Patent 7067053, 2006.

[21] A. W. Langer, J. Stewart, C. E. Thompson, H. T. White, and R. M. Hill, "Hydrogen donor diluent visbreaking of residua," *IandEC Process Design and Development*, vol. 1, no. 4, pp. 309–312, 1962.

[22] S. Nishimura, *Handbook of Heterogeneous Catalytic Hydrogenation for Organic Synthesis*, John Wiley & Sons, New York, NY, USA, 2001.

[23] K. A. Gould and I. A. Wiehe, "Natural hydrogen donors in petroleum resids," *Energy and Fuels*, vol. 21, no. 3, pp. 1199–1204, 2007.

[24] M. Shakirullah, I. Ahmad, M. Ishaq, and W. Ahmad, "Catalytic hydro desulphurization study of heavy petroleum residue through in situ generated hydrogen," *Energy Conversion and Management*, vol. 51, no. 5, pp. 998–1003, 2010.

[25] R. Beauchet, L. Pinard, D. Kpogbemabou et al., "Hydroliquefaction of green wastes to produce fuels," *Bioresource Technology*, vol. 102, no. 10, pp. 6200–6207, 2011.

[26] I. H. Metecan, M. Saglam, J. Yanik, L. Ballice, and M. Yüksel, "Effect of pyrite catalyst on the hydroliquefaction of Goynuk (Turkey) oil shale in the presence of toluene," *Fuel*, vol. 78, no. 5, pp. 619–622, 1999.

[27] K. P. Tian, A. R. Mohamed, and S. Bhatia, "Catalytic upgrading of petroleum residual oil by hydrotreating catalysts: a comparison between dispersed and supported catalysts," *Fuel*, vol. 77, no. 11, pp. 1221–1227, 1998.

[28] M. S. Rana, V. Sámano, J. Ancheyta, and J. A. I. Diaz, "A review of recent advances on process technologies for upgrading of heavy oils and residua," *Fuel*, vol. 86, no. 9, pp. 1216–1231, 2007.

[29] S. Zhang, D. Liu, W. Deng, and G. Que, "A review of slurry-phase hydrocracking heavy oil technology," *Energy and Fuels*, vol. 21, no. 6, pp. 3057–3062, 2007.

[30] S. K. Maity, J. Ancheyta, and G. Marroquín, "Catalytic aquathermolysis used for viscosity reduction of heavy crude oils: a review," *Energy and Fuels*, vol. 24, no. 5, pp. 2809–2816, 2010.

[31] Y. Liu, L. Gao, L. Wen, and B. Zong, "Recent advances in heavy oil hydroprocessing technologies," *Recent Patents on Chemical Engineering*, vol. 2, no. 1, pp. 22–36, 2009.

[32] Ü. Lille, I. Heinmaa, and T. Pehk, "Molecular model of Estonian kukersite kerogen evaluated by ^{13}C MAS NMR spectra," *Fuel*, vol. 82, no. 7, pp. 799–804, 2003.

[33] A. Loog, T. Kurvits, J. Aruväli, and V. Petersell, "Grain size analysis and mineralogy of the Tremadocian Dictyonema shale in Estonia," *Oil Shale*, vol. 18, no. 4, pp. 281–297, 2001.

APPENDIX C: CURRICULUM VITAE

ELULOOKIRJELDUS

1. Isikuandmed
   Ees- ja perekonnanimi   Julia Krasulina
   Sünniaeg ja -koht   05.12.1982 Venemaa
   Kodakondsus   Eesti

2. Kontaktandmed
   Aadress   Mahtra 2-27, 13811, Tallinn
   Telefon   +372 5536762
   E-posti aadress   julia.krasulina@ttu.ee

3. Hariduskäik

Õppeasutus (nimetus lõpetamise ajal)	Lõpetamise aeg	Haridus (eriala/kraad)
Tallinna Tehnikaülikool	2008–...	Keemia- ja materjalitehnoloogia, doktoriõpe
Tallinna Tehnikaülikool	2007	Tehnikateaduste magistrikraad
Tallinna Tehnikaülikool	2005	Tehnikateaduste bakalaureusekraad
Narva Humanitaargümnaasium	2002	Keskharidus

4. Keelteoskus (alg-, kesk- või kõrgtase)

Keel	Tase
Eesti keel	Kõrgtase
Vene keel	Kõrgtase (emakeel)
Inglise keel	Kõrgtase

5. Täiendusõpe

Õppimise aeg	Täiendusõppe läbiviija nimetus
2009–2012	Doktorikool „Funktsionaalsed materjalid ja tehnoloogiad" (Tartu Ülikool ja Tallinna Tehnikaülikool)
2008	Energeetikateaduskonna Üliõpilasnõukogu sügiskool

6. Teenistuskäik

Töötamise aeg	Tööandja nimetus	Ametikoht
01.03.2009–…	Tallinna Tehnikaülikool, Keemia ja materjalitehnoloogia teaduskond, Polümeermaterjalide instituut, Põlevkivi ja taastuvkütuste teaduslaboratoorium	insener
01.01.2008– 28.02.2009	Tallinna Tehnikaülikool, Keemia ja materjalitehnoloogia teaduskond, Põlevkivi instituut	keemiainsener

7. Kaitstud lõputööd

Magistritöö: Biomassi ja põlevkivi termokeemiline koostöötlemine, Tallinna Tehnikaülikool, 2007. Juhendaja: H. Luik

8. Uurimisprojektid

„Energiatehnoloogia teadus- ja arendustegevuse toetamine" raames projekt „Põlevkivi maksimaalse vääristamise alused"
ETF9331 Diktüoneema põlevkivi orgaanilise aine vedeldamine superkriitiliste lahustite ja reagentidega (2012-2015)
SF0142722s06 Fossiil- ja taastuvkütuste ning orgaaniliste jäätmete termokeemilise koostöötlemise alused (2006-2008)
SF0140028s09 Põlevkivi ja kütuste segude termokeemilise töötlemise uued tehnoloogiad (2009-2014)
ETF5673 Põlevkivijäätmete kahjutustamine ja vääristamine fluiid- ja gaasifaasilisel ekstraktsioonil keemiliselt aktiivses keskkonnas (2004-2007)
ETF7292 Termobituumeni moodustumine ja vääristamine vedelkütuseks (2008-2011)

CURRICULUM VITAE

1. Personal data

    Name   Julia Krasulina
    Date and place of birth   05.12.1982 Russia

2. Contact information

    Address   Mahtra 2-27, 13811, Tallinn
    Phone   +372 5536762
    E-mail   julia.krasulina@ttu.ee

3. Education

Educational institution	Graduation year	Education (field of study/degree)
Tallinn University of Technology	2008–...	Chemical and Materials Technology, doctoral studies
Tallinn University of Technology	2007	M. Sc. in Engineering
Tallinn University of Technology	2005	B. Sc. in Engineering
Narva Humanitarian Gymnasium	2002	Secondary education

4. Language competence/skills (fluent; average, basic skills)

Language	Level
Estonian	fluent
Russian	Fluent (native language)
English	fluent

5. Special Courses

Period	Educational or other organisation
2009–...	Graduate school „Functional Materials and Processes" (University of Tartu and Tallinn University of Technology)
2008	Engineering faculty student council school

6. Professional Employment

Period	Organisation	Position
2009–…	Tallinn University of Technology, Faculty of Chemical and Materials Technology, Department of Polymer Materials, Laboratory of Oil Shale and Renewables Research	Engineer
2008–2009	Tallinn University of Technology, Faculty of chemical and materials technology, Department of oil shale technology	Chemistry Engineer

7. Defended theses

M. Sc. thesis: Thermocemical co-processing of biomass and oil shale. Tallinn University of Technology, 2007. Supervisor: H. Luik

8. Research projects

EU Structural funds National R&D program „Energy Technology" „Fundamentals to oil shale maximum upgrading"
ETF5673 Disposal and upgrading of the oil shale wastes by fluid- and gas-phase extraction in chemically active media (2004-2007)
ETF7292 Formation of thermobitumen and its upgrading to liquid fuel (2008-2011)
SF0142722s06 Fundamentals of thermochemical co-processing of fossil and renewable fuels and organic wastes (2006-2008)
ETF9331 Liquefaction of the organic matter of dictyonema oil shale with supercritical solvents and reagents (2012-2015)
SF0140028s09 New technologies of thermochemical processing of oil shale and blended fuels (2009-2014)

DISSERTATIONS DEFENDED AT
TALLINN UNIVERSITY OF TECHNOLOGY ON
CHEMISTRY AND CHEMICAL ENGINEERING

1. **Endel Piiroja**. Oxidation and Destruction of Polyethylene. 1993.

2. **Meili Rei**. Lihatehnoloogia teaduslikud alused. Fundamentals of Food Technology. 1995.

3. **Meeme Põldme**. Phase Transformations in Hydrothermal Sintering Processing of Phosphate Rock. 1995.

4. **Kaia Tõnsuaadu**. Thermophosphates from Kovdor and Siilinjärvi Apatites. 1995.

5. **Anu Hamburg**. The Influence of Food Processing and Storage on the N-Nitrosamines Formation and Content in Some Estonian Foodstuffs. 1995.

6. **Ruth Kuldvee**. Computerized Sampling in Ion Chromatography and in Capillary Electrophoresis. 1999.

7. **Külliki Varvas**. Enzymatic Oxidation of Arachidonic Acid in the Coral *Gersemia fruticosa*. 1999.

8. **Marina Kudrjašova**. Application of Factor Analysis to Thermochromatography and Promotion Studies. 2000.

9. **Viia Lepane**. Characterization of Aquatic Humic Substances by Size Exclusion Chromatography and Capillary Electrophoresis. 2001.

10. **Andres Trikkel**. Estonian Calcareous Rocks and Oil Shale Ash as Sorbents for SO_2. 2001.

11. **Marina Kritševskaja**. Photocatalytic Oxidation of Organic Pollutants in Aqueous and Gaseous Phases. 2003.

12. **Inna Kamenev**. Aerobic Bio-Oxidation with Ozonation in Recalcitrant Wastewater Treatment. 2003.

13. **Janek Reinik**. Methods for Purification of Xylidine-Polluted Water. 2003.

14. **Andres Krumme**. Crystallisation Behaviour of High Density Polyethylene Blends with Bimodal Molar Mass Distribution. 2003.

15. **Anna Goi**. Advanced Oxidation Processes for Water Purification and Soil Remediation. 2005.

16. **Pille Meier**. Influence of Aqueous Solutions of Organic Substances on Structure and Properties of Pinewood (*Pinus sylvestris*). 2007.

17. **Kristjan Kruusement**. Water Conversion of Oil Shales and Biomass. 2007.

18. **Niina Kulik**. The Application of Fenton-Based Processes for Wastewater and Soil Treatment. 2008.

19. **Raul Järviste**. The Study of the Changes of Diesel Fuel Properties a its Long Term Storage. 2008.

20. **Mai Uibu**. Abatement of CO_2 Emissions in Estonian Oil Shale-Based Power Production. 2008.

21. **Valeri Gorkunov**. Calcium-Aluminothermal Production of Niobium and Utilization of Wastes. 2008.

22. **Elina Portjanskaja**. Photocatalytic Oxidation of Natural Polymers in Aqueous Solutions. 2009.

23. **Karin Reinhold**. Workplace Assessment: Determination of Hazards Profile using a Flexible Risk Assessment Method. 2009.

24. **Natalja Savest**. Solvent Swelling of Estonian Oil Shales: Low Temperature Thermochemical Conversion Caused Changes in Swelling. 2010.

25. **Triin Märtson**. Methodology and Equipment for Optical Studies of Fast Crystallizing Polymers. 2010.

26. **Deniss Klauson**. Aqueous Photocatalytic Oxidation of Non-Biodegradable Pollutants. 2010.

27. **Oliver Järvik**. Intensification of Activated Sludge Process – the Impact of Ozone and Activated Carbon. 2011.

28. **Triinu Poltimäe**. Thermal Analysis of Crystallization Behaviour of Polyethylene Copolymers and Their Blends. 2011.

29. **Mariliis Sihtmäe**. (Eco)toxicological Information on REACH-Relevant Chemicals: Contribution of Alternative Methods to *in vivo* Approaches. 2011.

30. **Olga Velts**. Oil Shale Ash as a Source of Calcium for Calcium Carbonate: Process Feasibility, Mechanism and Modeling. 2011.

31. **Svetlana Jõks**. Gas-Phase Photocatalytic Oxidation of Organic Air Pollutants. 2012.

32. **Aleksandr Dulov**. Advanced Oxidation Processes for the Treatment of Water and Wastewater Contaminated with Refractory Organic Compounds. 2012.

33. **Aleksei Zaidentsal**. Investigation of Estonian Oil Shale Thermo-bituminization in Open and Closed System. 2012.

34. **Dmitri Šumigin**. Composites of Low-Density Polyethylene and Poly(Lactic Acid) With Cellulose and Its Derivatives. 2014.

35. **Aleksandr Käkinen**. The Role of Physico-chemical Properties and Test Environment on Biological Effects of Copper and Silver Nanoparticles. 2014.

36. **Ada Traumann**. Improvement of Work Environment through Modelling the Prevention of Health Risks Focusing on Indoor Pollutants. 2014.

37. **Marika Viisimaa**. Peroxygen Compounds and New Integrated Processes for Chlorinated Hydrocarbons Degradation in Contaminated Soil. 2014.

38. **Olga Budarnaja**. Visible-light-sensitive Photocatalysts for Oxidation of Organic Pollutants and Hydrogen Generation. 2014.

39. **Jelena Hruljova**. Role of Specifically Interacting Solvents in Solvent Swelling of Kukersite Oil Shale Kerogen. 2014.

40. **Irina Klimova**. Modification of Ammonium Nitrate Fertilizer. 2014.